Device-Free Visible Light Sensing: A Survey

Morteza Alijani, Cedric De Cock, Wout Joseph, *Senior Member, IEEE*, and David Plets, *Member, IEEE*

***Abstract*—The latest advancements in visible light communication (VLC) technology have greatly facilitated the evolution of wireless sensing based on visible light, commonly referred to as visible light sensing (VLS) systems. Similar to other wireless sensing technologies, these systems can be categorized into two primary types: device-based (or active) and device-free (or passive), depending on whether targets, such as people or objects of interest, are equipped with an optical receiver (e.g., a photodiode or camera). By reusing the existing Light-emitting diode (LED) lighting infrastructure as transmitters in indoor environments, device-free VLS (DF-VLS) systems can help address the growing energy demands of ubiquitous sensing and communication in Sixth-Generation Wireless Networks (6G). This survey meticulously explores the landscape of DF-VLS technology, proposing a redefinition of the classification of VLS systems and delving into the existing literature in this domain. We conduct a comprehensive analysis of various DF-VLS sensing techniques, focusing on their diverse applications in the Internet of Things (IoT). By closely examining the integration and utility of DF-VLS in IoT environments, we highlight the potential of this technology. Furthermore, we underscore critical open challenges that demand attention for the effective development of efficient DF-VLS systems. Finally, the paper outlines a future roadmap for DF-VLS systems, shedding light on potential directions this field may embark upon.**

***Index Terms*—Sensing, visible light sensing (VLS), device-free wireless sensing (DFWS), device-free, DF-VLS.**

I. INTRODUCTION

WIRELESS sensing, an umbrella term including detection, tracking, identification, and localization, is a key feature within sixth-generation wireless networks (6G) [1], [2], [3]. It manifests in two distinct forms: on the one hand, device-based (DB) (or active) sensing, illustrated in Fig. 1 (a), where an optical receiver (e.g., a photodiode (PD)) is attached to the user for functionality (e.g., localization); and on the other hand, device-free (or passive) wireless sensing (DFWS), as shown in Fig. 1 (b) [2], [3], [4], [5], [6], [7], [8], [9], [10]. The main principle underlying device-free wireless sensing (DFWS) is the utilization of wireless signals for unobtrusive sensing and communication, without requiring objects of interest (e.g., individuals) to carry specialized wireless devices (e.g., tags) [2], [3], [4], [5], [6], [7], [8], [9], [10]. DFWS has become a well-established area of investigation, receiving attention from both academia and industry in recent years [1], [2], [3], [4], [5], [6], [7], [8], [9], [10]. It leverages a range of existing wireless signals, including both

Received 27 June 2024; revised 3 December 2024 and 24 January 2025; accepted 24 February 2025. Date of publication 25 February 2025; date of current version 2 January 2026. *(Corresponding author: Morteza Alijani.)*

The authors are with the Research Group imec-WAVES, Department of Information Technology, Ghent University, 9052 Ghent, Belgium (e-mail: Morteza.Alijani@UGent.be).

Digital Object Identifier 10.1109/COMST.2025.3546166

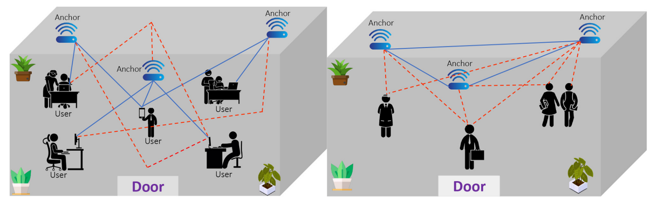

(a) (b)

Fig. 1. Visualizing DB (or active) (a) and DF (or passive) (b) wireless sensing/localization: A comparative example with anchor as a sensing modalities. In both figures, blue lines shows LoS, and dashed red lines represent multipath components from the surroundings.

radio frequency (RF) signals (e.g., wireless fidelity (WiFi), bluetooth low energy (BLE), etc.) and non-RF signals (e.g., magnetic, acoustic, visible light (VL), etc.) [2], [3], [4], [5], [6], [7], [8], [9], [10], [11], [12]. These signals are employed to detect modifications to the environment resulting from the presence or movement of objects [2], [7]. DFWS boasts diverse applications, optimizing building systems (e.g., smart buildings and home automation [13], [14], [15]), enhancing healthcare monitoring (e.g., fall detection) [16], [17], [18], improving autonomous driving safety [19], [20], and aiding agriculture in wildlife and livestock management [21], [22].

To date, achieving seamless connectivity for the Internet of Things (IoT) through the integration of RF communication and sensing technologies faces scalability issues and has been the subject of numerous studies in recent years, leading to a flooded area of study without a unanimous solution [7], [24], [25], [26]. These obstacles stem from limitations in energy resources, interference, privacy concerns, and the pervasive problem of RF spectrum congestion, commonly known as the spectrum crunch [7], [24], [25], [26]. Additionally, there is a necessity to regulate or completely avoid the utilization of RF technology in specific scenarios, including aircraft or spacecraft cabins, hospitals (e.g., medical devices [27]), and hazardous environments like underground mining, chemical or nuclear facilities, and oil industries [7], [24]. Several non-RF-based technologies have been introduced alongside RF-based DFWS to overcome the potential challenges associated with RF-based systems. By offering complementary capabilities, they enhance the overall localization/sensing performance [7], [24]. In this regard, as an alternative approach, researchers have delved into solutions that can support robust sensing and passive localization using emerging technologies centered around VL signals rather than RF [7], [9], [10]. VL, spanning a frequency range from 430 to 790 TeraHertz (THz) and a wavelength range of 380 to 750 nanometers (nm) [28], [29], [30], serves as a versatile entity in the electromagnetic spectrum [23], [29]. Beyond its role in

TABLE I
A COMPARATIVE ANALYSIS OF OUR SURVEY ON DF-VISIBLE LIGHT SENSING (VLS) WITH EXISTING RELATED STUDIES

Publication Year	Ref.	Features / Taxonomy Method				
		DF-VLS Hardware	Mathematical & Technical Insights for DF-VLS	DF-VLS Sensing Techniques	DF-VLS Challenges	DF-VLS IoT Applications
2015	[23]*	Yes	Limited	Limited	No	No
2017	[9]	Limited	No	Limited	In-depth	Yes
2020	[10]	Limited	No	Limited	Yes	Limited
2021	[7]*	No	No	No	Limited	Limited
2023	[24]*	Limited	Limited	No	Yes	Yes
Our Survey		In-depth	Yes	In-depth	In-depth	In-depth

The symbol * indicates a partial coverage of the DF-VLS topic.

illumination, VL finds applications in communication, sensing, and positioning [23], [29], [31]. visible light communication (VLC), leveraging light emitting diodes (LEDs), enables data transmission through modulation of the light intensity, which is invisible to the human eye [23], [29]. This innovation facilitates rapid and secure wireless communication [23], [29]. The VLC market, valued at USD 2.5 billion in 2022, is anticipated to grow at a Compound Annual Growth Rate (CAGR) of over 35% from 2023 to 2032 [32]. In this evolving scenario, VLC is expected to function either in conjunction with traditional RF-based wireless technologies or as a viable alternative [23], [29], [31], [33], [34], [35], [36]. Specifically, VLC techniques designed for positioning are commonly referred to as visible light positioning (visible light positioning (VLP)) [29], [30], while those tailored for sensing applications are usually referred to as VLS, DFWS based on VL, or passive VLP [9], [10], [24], [25], [37], [38], [39], [40], [41].

VLS offers certain advantages over RF and other non-RF methodologies. Thanks to VL propagation being confined to the room itself, it can provide enhanced privacy compared to RF-based sensing systems where signals penetrate through walls [42]. Unlike camera-based VLS (excluded from this paper; see Section II-A), the VLS approaches in this paper do not capture detailed photos or videos of individuals, significantly reducing privacy concerns [43], [44]. Besides, VLS can alleviate the spectrum crunch issue associated with RF-based systems due to the wide bandwidth and unlicensed frequency channels afforded by light waves [10], [29], [30], [43], [44]. Furthermore, VL signals are considered safe for human exposure under typical lighting conditions, unlike RF signals or lasers, which may pose safety risks when power levels exceed allowable limits [43]. Finally, the widespread availability of LEDs and ambient light in various environments means that implementing VLS requires minimal infrastructure investment, making this technology more cost-effective than RF and other non-RF-based systems [9], [10], [29], [33], [45]. Unlike RF-based systems, which require dedicated transmitters (Txs) and receivers (Rxs), VLS systems provide a more energy-efficient solution to the growing demands of ubiquitous sensing and communication in 6G, by reusing the existing lighting as Tx. In addition, in case the receiver sensors are collocated with the transmitter (i.e., reflection-based VLS), they can also be mains-powered, eliminating the need for battery-powered Rxs and reducing e-waste. VLS, however, also faces some limitations and challenges (e.g., the requirement of an adequate lighting level, VL interference, sensing range, light blockage issues, etc.), which will be discussed later in this work.

A. Survey Focus and Key Contributions

In recent years, several prominent survey and review articles on sensing and positioning systems using VL have been published. However, most of these works focus primarily on DB (or active) VL positioning approaches (e.g., VLP) [29], [30], [46], [47], [48], [49], [50], [51], while only a few studies address DFWS methods based on VL (see Table I). For example, Pathak et al. [23] provide an in-depth discussion of VLC modulation and medium access mechanisms, but only briefly touch on VLS‘s mathematical background and sensing techniques. Singh and Raza [10] presented a study that provides an overview of VLS and includes an comparative analysis. Furthermore, Alam et al. [7] conducted a survey of non-RF techniques for indoor positioning, providing a general perspective on positioning and sensing techniques based on VL. More recently, Ullah et al. [24] conducted a review focusing on visible light backscattering (VLB) as an innovative optical transmission concept. They classified VLB-based systems into two categories: visible light backscatter communication (VLBC) systems, which are designed for data communication, and visible light backscatter positioning (VLBP) systems, which are aimed at localization purposes. Finally, Wang and Zuniga [9] proposed a classification framework for the VLS systems, organizing it according to the active and passive characteristics of both light sources and objects as a user. Furthermore, their study provided an examination of various challenges and outlines research trajectories within the realm of the VLS systems. However, these studies do not thoroughly address the hardware, sensing techniques, mathematical and technical insights for VLS, or the challenges associated with VLS. More importantly, they lack a broad investigation into the potential and the use of DF-VLS for IoT applications. This highlights the need for a more comprehensive survey to address these gaps. Motivated by this, our study makes several key contributions, as outlined in the

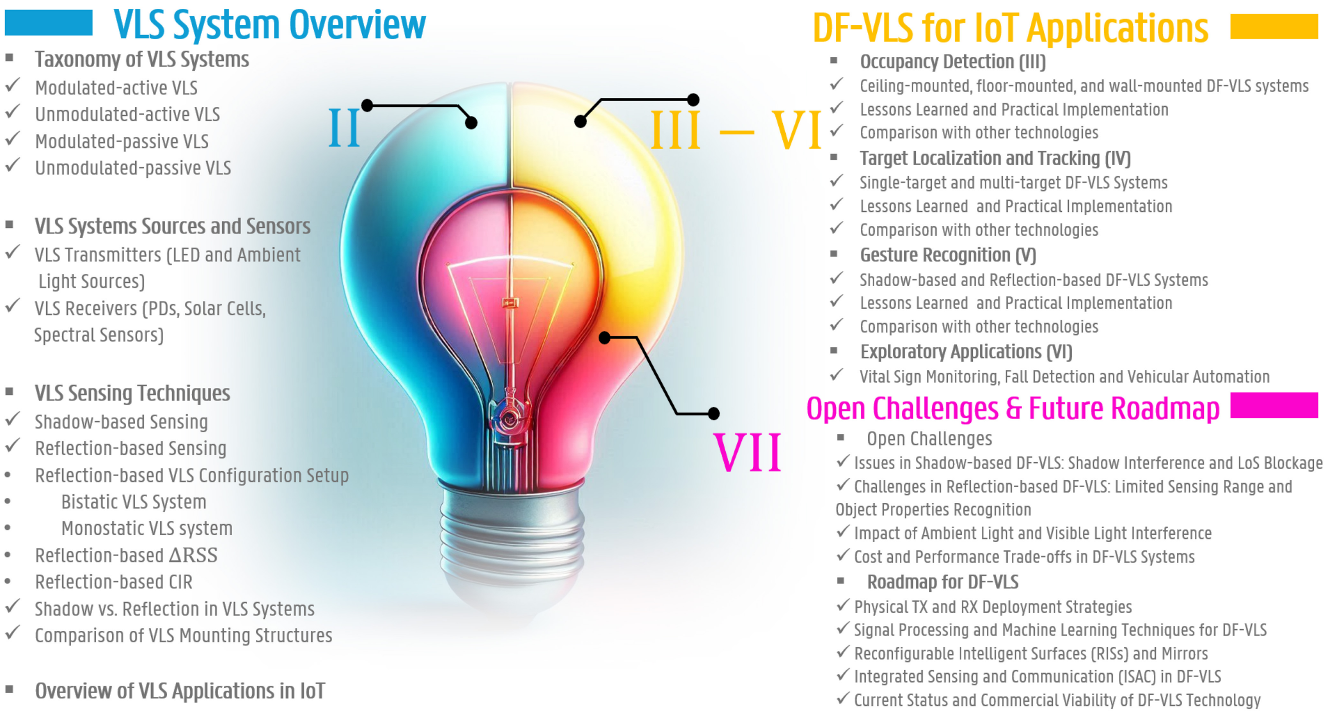

Fig. 2. Survey Structure Overview.

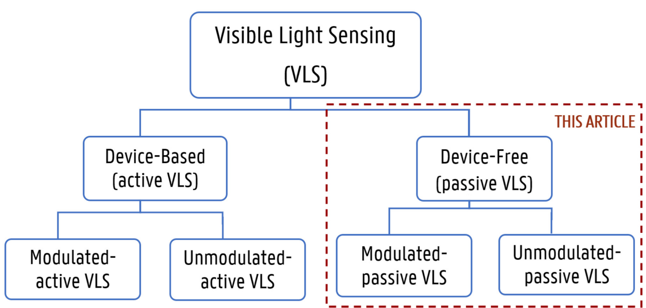

Fig. 3. Classification of VLS systems.

survey structure in Fig. 2. First, we redefine the taxonomy of VLS systems, building on the definitions in [9] and [10]. We unambiguously define a VLS taxonomy based on DF (or passive) VLS (the focus of this paper) and DB (or active) (see Fig. 3). We then provide an overview of the sensing techniques used in DF-VLS, including their mathematical foundations (Section II). Next, in Section II-D, we present an extensive review of the DF-VLS literature, categorized by targeted use cases. In particular, we offer greater depth and insight into DF-VLS compared to other surveys listed in Table I, which only partially cover DFWS based on VL systems. Section VII discusses current challenges in DF-VLS and proposes potential research pathways, offering readers a robust foundation to understand and engage with the evolution of DF-VLS systems. Finally, Section VIII provides a summary of our study.

II. VLS System Overview

A. Taxonomy of VLS Systems

Before delving into the technical aspects of DFWS systems based on VL, it is important to understand their categorization as it provides an organized framework for comprehending, evaluating, selecting, designing, investigating, and collaborating on various aspects of VLS technology. Both studies reported in [9] and [10] are the main existing high-level overviews in the domain of VLS, presenting similar classifications for VLS systems. Their classification is based on the concept that a light source (i.e., the Tx side) is designated as ***active*** when it is modulated, and ***passive*** when it is not [9], [10]. Likewise, a user (on the Rx side) who carries a light sensitive device (e.g., a PD) is characterized as ***active***, whereas the absence of such a device denotes a ***passive*** user [9], [10]. In line with this perspective, they classified VLS systems into distinct categories: ***fully active VLP*** (involving both an active source and an active user), ***passive-src*** (passive source, active user), ***passive-usr*** (active source, passive user), and ***fully passive*** (passive source, passive user) scenarios [9], [10]. In their classification, all classes except fully active VLP were categorized as either passive VLP or VLS [9], [10].

Nevertheless, within this particular classification framework, the term ***passive-src*** deviates from the prevalent understanding found in existing literature, where passive localization and sensing usually pertain to device-free localization (DFL) and DFWS, respectively, implying that no receiving devices should be attached to the user [2], [3], [4], [5], [6], [7], [11], [12]. Hence, this paper proposes a redefinition of VLS classification introduced in [9], [10]. This refined framework is grounded in the concepts of ***device-based*** and ***device-free*** sensing/positioning from the receiver's perspective, aligning it more closely with terminology commonly employed in the literature [2], [3], [4], [5], [6], [7], [8]. Additionally, from the transmitter's perspective, we consider two scenarios for light sources: one involving modulated light sources and another with unmodulated light sources. Accordingly, as shown in Fig. 3, we categorize the VLS system into DB (receiver attached to sensing target) and DF (receiver not attached to sensing target), each with the subcategories of "modulated" (involving modulated light) and "unmodulated" (using unmodulated light):

1) Modulated DB-VLS: In modulated-active VLS, the light source is actively modulated, and the photodetector is attached to the object of interest for sensing or positioning. VLP is its most common application.
2) Unmodulated DB-VLS: In the unmodulated-active VLS class, the source light remains unmodulated, but light-sensitive devices are attached to the object of interest. Prominent examples within this class are unmodulated visible light positioning (uVLP)[1] [29] and photoplethysmography (PPG) [53], [54], an optical technique widely used in healthcare to measure blood volume changes [53], [54].
3) Modulated DF-VLS: In modulated-passive VLS, the object of interest is entirely DF, meaning it has no light-sensitive device attached to it, e.g., light detection and ranging (LiDAR).
4) Unmodulated DF-VLS: Unmodulated-passive VLS systems, rely on existing light (e.g., ambient or unmodulated artificial sources) to sense the environment or a specific target that is not attached to the photo-sensitive receiver. Smartphone ambient light sensors (ALSs), but also cameras can be classified in this category.

Note that laser-based VLS approaches (e.g., LiDAR) and camera-based VLS are specifically excluded from this study, due to the rich literature already available on these topics [55], [56], [57], [58], [59]. While we will only consider incoherent light sources, lasers emit coherent light, resulting in highly directional, monochromatic, and intense beams [60], [61], used for e.g., environmental mapping and obstacle detection [62], gesture recognition [63], and precise distance measurement in monitoring systems [64]. They are expensive and their use requires strict power regulation to ensure safety for human eyes and skin [65], [66].

The receiver in both "modulated-passive VLS" and "unmodulated-passive VLS" can be placed within the environment itself, such as on walls [67], [68], floors [39], [47], [69], or ceilings [70], [71]. These are frequently referred to in the literature as wall-mounted, floor-mounted, and ceiling-mounted VLS systems, respectively [9], [10]. The main challenge in DF-VLS systems stems from the fact that direct information from the target cannot be obtained, necessitating reliance on environmental cues [9], [10]. Indeed, none line of sight (NLoS) components, such as lighting condition interference caused by the presence of targets in the environment, can be utilized for sensing and positioning purposes [9], [10]. These components primarily include reflected signals, where the signal bounces off the target's surface or the environment, and shadowed signals occur when the light signal is partially obstructed and occlusion when the light transmission is completely blocked [72], which happens when objects positioned in various locations block the direct LoS between the Tx and Rx (e.g., in floor-mounted VLS [39], [69]).

Our paper exclusively focuses on DF-VLS, covering both ***modulated-passive*** and ***unmodulated-passive*** VLS systems. Therefore, readers interested in modulated-active VLS are encouraged to consult [29], [30], [73]. For uVLP systems, we recommend exploring [52], [74], [75], [76]. Additionally, this paper does not cover VLBP and VLBC, which require a device (e.g., tag) equipped with a retroreflector for passive uplink transmission [24], [77], [78], [79]. This method involves modulating light and reflecting it back from the target toward the receiver, falling under the DB approach, and is therefore beyond the scope of our discussion. Further details about VLBP and VLBC can be found in [24].

1) Modulated vs. Unmodulated-Passive VLS: Typically, in modulated-passive VLS systems, thanks to the use of modulators, it is possible to achieve a clearer signal (e.g., a better signal-to-noise ratio (SNR)) and the ability to distinguish between the received signals from each light source [29]. This makes modulated-passive VLS systems generally more flexible than unmodulated-passive VLS systems, as they provide more detailed data, albeit with increased complexity and cost due to the additional (de)modulation hardware and processing required [9], [10], [52].

There are three main approaches to using unmodulated-passive VLS systemstotal light intensity, spectrum-based analysis, and demultiplexing by characteristic frequency (CF) each with different trade-offs in terms of complexity, cost, and implementation. The most straightforward method leverages the total light intensity received [25], [80], [81]. It is a low-cost approach, but is sensitive to external factors and has a limited accuracy, as the total light intensity is influenced by all light sources, and usually has a low gradient. Spectrum-based analysis improves upon this by using intensity information per wavelength bin (e.g., 18 bins [72], [82], [83]), slightly enhancing discriminative power (1D intensity value becomes 18D intensity value [72], [82], [83]) but requires more expensive sensors, which increases both cost and complexity [72], [82], [83]. The third approach, demultiplexing based on a LED‘s CF [52], allows for the separation of contributions from individual LEDs. Despite having a lower SNR compared to a dedicated modulated signal and an increased complexity due to the required signal processing, it retains all the advantages of a modulated approach. Finally, fingerprinting often complements the total intensity approach in unmodulated-passive VLS systems [9], [10]. However, it can be challenging since it often requires manual labor [9], [10], [80], [81]. In addition, these systems must be adjusted if the weather changes, such as during rain, fog, or sunshine [9], [10], [80], [81]. One approach is to use training models like those examined in FieldLight [80]. For more details on VLP, we refer to [29].

Unmodulated-passive VLS systems have spurred a more extensive body of research in the literature than modulated-passive VLS systems [39], [81], [84], [85], [86], [87]. This is mainly because they can make use of widely available

[1]Note that in characteristic frequency-based uVLP [52], despite the sources not being purposefully modulated, it is still possible to demultiplex the LEDs' contributions, using Fast Fourier transform (FFT)-based methods [52].

unmodulated sources in indoor (and outdoor) environments, such as lights and natural sunlight pouring through windows, which serve as transmitters for sensing and positioning in this classification [9], [10], [37], [72], [80], [81], [86], [87].

B. VLS System Sources and Sensors

A VLS system builds on the use detection (or not) of light sources, using optical sensors. Two frequently used sources of light in VLS are LEDs and ambient light [23], [29], [88], [89]. The primary purpose of the LED is to convert an electrical signal into an optical signal, which then propagates through the free space medium [23], [89], [90], [91]. LEDs are distinctive semiconductor components capable of emitting light when subjected to a forward voltage [23], [71], [89], [92]. They are widely employed as transmitters in VLS systems [23], [29], [88], [89]. In addition to LEDs, ambient light (also known as available light or background light) can also be considered a VLS source [9], [10], [72], [80], [81], [93] (see Fig. 4). Ambient light includes natural sunlight through windows or skylights, artificial light, and even the biasing contributions and unintended modulation by-products from VLP-enabled transmitters [29], [94]. Several unmodulated-passive VLS systems utilize ambient light as light sources [80], [81], [86], [93], [95], [96], [97]. The details of mentioned studies will be presented in Section II-D.

VLS receivers are used to capture (or not) VL signals either directly from light sources, or via reflections from objects or their surroundings [9], [10]. Receivers in VLS systems encompass photodetectors (e.g., PDs) [97], [98], solar cells [87], [95], and spectral sensors [72], [82], [99] (see Fig. 4). A PD functions as a reversely biased P-N junction semiconductor device, converting incoming optical photons (e.g., light) into electrical current [29], [90], [100]. PDs are used in optical communication systems (e.g., VLC, VLP, and VLS) due to their compact size, rapid detecting speed, high detection efficiency, and ability to sample VL at rates up to tens of megahertz (MHz) [23], [29], [90], [100], [101]. Solar cells, unlike typical PDs, are engineered for optimal power production, eliminating the requirement for energy-intensive amplification components like transimpedance amplifier (TIA) to provide a strong signal output [87], [95], [102]. Solar cells, when exposed to VL, generate voltage or current [29], [101], [103], [104]. This dual-purpose functionality detects and converts light into usable electrical energy, which makes it valuable for energy-efficient and sustainable applications such as IoT devices and sensor networks powered by ambient light, also within VLS systems [29], [87], [95]. Successful studies have already demonstrated the viability of conducting DF-VLS using a solar cell receiver, which will be detailed in Section II-D [87], [95], [102], [105].

Unlike PDs, which generate a continuous output signal (e.g., voltage signals) to represent the intensity of incident light without distinguishing between different wavelengths, light spectral sensors, also known as spectrometers or spectrophotometers, can provide information on the distribution of light intensity across different wavelengths of the electromagnetic spectrum [72], [99], [106] (see Fig. 4). These sensors

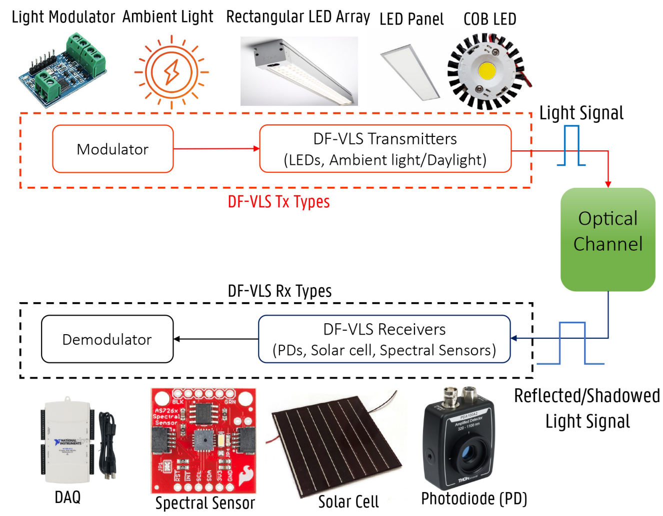

Fig. 4. Illustration of the DF-VLS transmitter and receiver types, featuring Tx components such as LEDs (e.g., COB LED or other types) and ambient light (e.g., sunlight or daylight), and Rx components including a DAQ [109] system for data collection, spectral sensors (e.g., AS7265x (Qwiic) [107]), solar cells, and PD (e.g., PDA100A2 [110]). The (de)modulation modules are optional (see also Fig. 3).

cover specific sections of the spectrum, including ultraviolet (UV), VL, near-infrared (NIR), and infrared [72], [82], [99], [106]. In DF-VLS, the AS7265x (Qwiic) spectral sensor [107] is commonly used, combining three spectral sensors with six channels each for green, red, and blue wavelengths [72], [99], [108]. This sensor enables measurement across 18 wavelength channels from 410 nm (UV) to 940 nm (infrared), providing data in μW/centimeters (cm)^2 units with a 20nm bandwidth for each channel [108]. We refer to [29] for a more elaborate discussion of VLS‘s architectural components.

C. VLS Sensing Techniques

VLS systems commonly employ two primary channel sensing techniques: ***shadow-based*** and ***reflection-based*** methods [9], [10], [37], [45]. These classifications are based on how the target influences the light signals reaching the light-sensitive sensor (e.g., PDs) (see Fig. 5) [9], [10], [37], [45].

1) Shadow-Based Sensing: Obstructing a light beam with an opaque object (e.g., human body) casts a silhouette (see Fig. 5) [47], [111], [112], [113], [114], [115]. A DF-VLS system (e.g., floor- or wall-mounted) employing shadow-based sensing relies on the characteristics of shadows cast by objects and operates by detecting variations in brightness or the presence or absence of light (occlusion) when light is blocked [39], [80], [81]. Several investigations monitor indoor activities of objects by sensing changes in ambient or indoor light brightness when objects block the light reaching the sensor [39], [80], [81]. However, this method typically exhibits limited precision in targeting and is vulnerable to changes in brightness caused by external interference, as it can only approximate the shape and characteristics of shadows [40].

2) Reflection-Based Sensing: VLS systems (e.g., ceiling-mounted) employ reflection-based sensing techniques to detect light reflected off surfaces, including diffuse [37], [45], specular [40], spread [40], [116] and multiple reflections [37], [45],

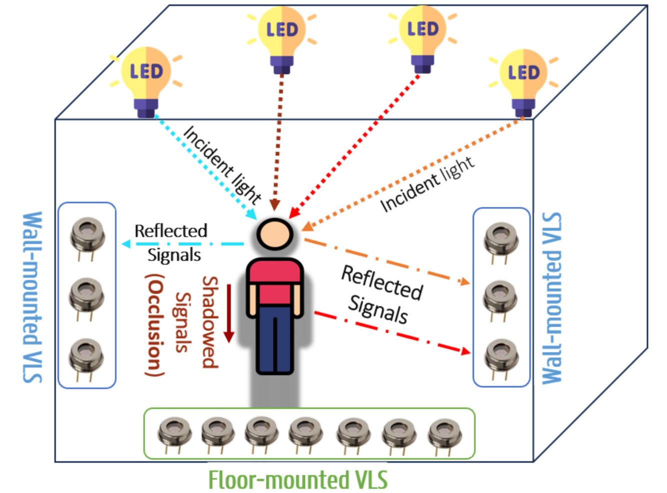

Fig. 5. Visual representation of shadow-based (e.g., occlusion) and reflection-based DF-VLS sensing. Typically, a floor-mounted DF-VLS system demands more PDs on the floor [10].

[71], [87]. These approaches analyze reflected light characteristics, such as intensity, polarization, or spectral composition, using PDs or image sensors [37], [45], [71], [87]. They capture and analyze reflected light from sources and surroundings, measuring metrics like received signal strength (RSS) [37], [45], [71], [87] or based on channel impulse response (CIR) simulation [38], [117], [118], [119].

a) Reflection-based VLS configuration setup: Two configurations, monostatic [68] and bi/multistatic VLS [120], [121], [122], [123], have been used in the literature. Given that the bistatic VLS system depicted in Fig. 6 (and monostatic VLS system) only receives reflected components, the received photocurrent signal due to the presence of a target (e.g., a human), can be calculated as follows [29], [90], [100]:

$$I_R = \sum_{k=1}^{N} P_{t,k} \cdot \left(M \sum_{A} R_P(\psi', \gamma') \cdot h_{c,NLoS}^{(k,\, dA_i)} \right), \quad (1)$$

where M (e.g., device-type dependent parameter) represents the gain factor introduced to account for the wavelength mismatch between the transmitter and receiver [29], [94], [124]. ψ and ψ' represent the elevation component of the incident angle from the LED at the PD for the LoS and NLoS components, respectively. Similarly, γ, and γ' characterize the azimuthal counterparts of ψ and ψ', respectively [29], [94], [124]. In eq. (1), the responsivity $R_P(\psi,\gamma)$ models the PD receiver's angular dependency, i.e., its acceptance function [29], [94], [124]. Note that, $R_P(\psi,\gamma)$ is only nonzero within the receiver field of view (FoV) (ψ_C) [29], [94], [124]. Finally, A represents the total reflective surface area, consisting of small surface elements dA_i [29], [94].

Bistatic VLS system: Fig. 6 illustrates the bi/multistatic (e.g., spaced Tx-Rx) DF-VLS system, with transmitters and receivers located at reasonably separated locations [86]. The target is assumed to be located far from the transmitter in an ideal environment (e.g., an empty room with zero reflectivity from walls, ceiling, floor, etc.) [90], [100]. Thus, the received reflected signal is solely due to the target's presence and properties (e.g., shape, color, etc.) and effective cross-section (e.g., reflective area) and is corrupted by noise [90], [100]. By neglecting the specular reflection component and focusing only on the diffuse NLoS components due to the two reflective areas dA_i $(i = 1{,}2)$, the calculation for $h_{c,\,BS,\,NLoS}^{(k,dA_i)}$ (BS refers to the bistatic configuration) can be performed as follows [29], [90], [94], [100]:

$$h_{c,\,BS,\,NLoS}^{(k,\,dA_i)} = \begin{cases} \dfrac{(m_k+1)(m_d+1)A_R}{4\pi^2 d_{k,i,in}^2 d_{k,i,refl}^2} \rho r_d \, dA_i \cos^{m_k}(\phi'_k) \\ \cos\left(\theta'_{i,k}\right) \cos^{m_d}(\theta_{i,k}) \cos(\psi'_k)\, T_s(\psi_k)\tau(\psi_k), \\ \qquad\qquad 0 \le \psi_k \le \psi_c \\ 0, \qquad\qquad 0 \ge \psi_c, \end{cases} \quad (2)$$

where $d_{k,2,in}$ represents the distance between the transmitter and the target, while $d_{k,1,refl}$ denotes the distance between the target and the receiver. As depicted in Fig. 6, the maximum horizontal detection range of VLS, denoted by R_M^{FoV}, can be determined based on the receiver's photodetector FoV as [90], [100]:

$$R_M^{FoV} = \tan(\psi_c)(d_0 - H), \quad (3)$$

where ψ_c represents the semi-angle of the photodetector's concentrator, d_0 is the perpendicular distance between the k-th receiver location $L_R^{(k)} = (x_{R,k}, y_{R,k}, d_0)$ (ground is set at $z = 0$) and the ground reference point $G_R = (x_{R,k}, y_{R,k}, 0)$, and H is the height of the target to be sensed [90], [100].

Monostatic VLS system: In the monostatic DF VLS scenario, both the PD and the LED$_k$ are ceiling-mounted very close to each other or can be co-located [37], [45], [100], [125]. This configuration is commonly employed in point-to-point VLBC systems [24]. Given that the Tx and Rx are co-located, the angles ψ'_k in Fig. 6 are equal to ϕ'_k. Additionally, due to the consistent direction of light and reflection, and the equal distances $d_{k,1,in} = d_{k,1,refl}$ from reflective area dA_1 and $d_{k,2,in} = d_{k,2,refl}$ from reflective area dA_2, the angles $\theta'_{1,k}$ are equal to $\theta_{1,k}$, and $\theta'_{2,k}$ are equal to $\theta_{2,k}$. Based on these considerations, the NLoS component from two reflective areas dA_i $(i = 1{,}2)$ (see eq. (2)) simplifies to [29], [90], [94], [100] (MS refers to the monostatic configuration):

$$h_{c,\,MS,\,NLoS}^{(k,\,dA_i)} = \begin{cases} \dfrac{(m_k+1)(m_d+1)A_R}{4\pi^2 d_{k,i,in}^4} \rho r_d \, dA_i \\ \qquad \cos^{m_k+3}(\psi'_k)\, T_s(\psi_k)\tau(\psi_k), \\ \qquad\qquad 0 \le \psi_k \le \psi_c \\ 0, \qquad\qquad 0 \ge \psi_c, \end{cases} \quad (4)$$

For a linear response receiver chain, the obtained total received photocurrent for both monostatic and bistatic configurations can be simply converted using the transimpedance gain of the PD (e.g., G_{PD}) to voltage [29], [94], which corresponds to the RSS in volts or millivolts [37], [45].

b) Reflection-based ΔRSS: Consider the bistatic VLS setup illustrated in Fig. 6. The detection and sensing of targets (e.g., human) become feasible by analyzing changes in the reflection patterns through the relative RSS approach, denoted as ΔRSS [37], [45], [126]. This method hinges on two sets of measurements: RSS for an empty room (e.g., RSS$_e$), representing a humanless area, and RSS for the study

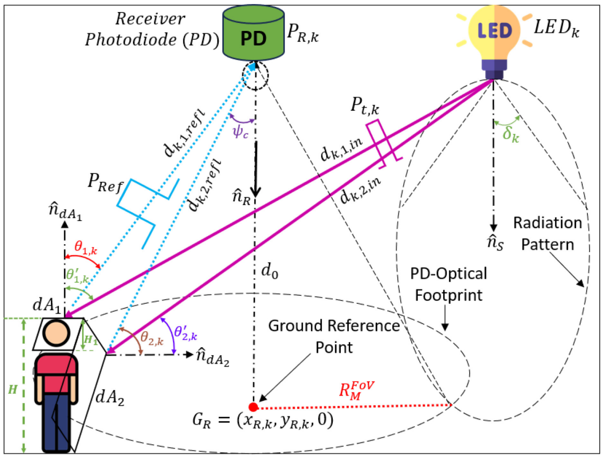

Fig. 6. Visualizing the bistatic ceiling-mounted VLS system with a target (e.g., a human) placed away from the transmitter (Tx). Inspired by studies in [90], [100].

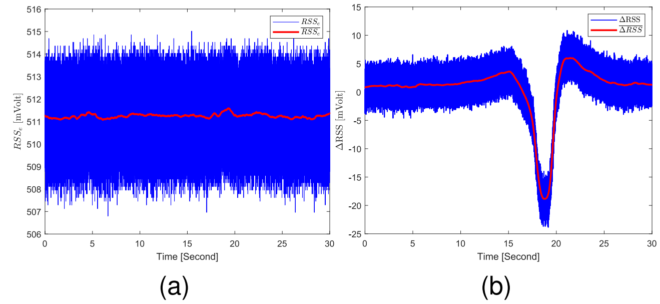

Fig. 7. An illustration of RSS values for (a) an empty study area and (b) the ΔRSS signal. In both figures, blue shows the raw signal and red represents the averaged signal using a moving average filter for noise removal.

area with a human present (e.g., RSS_{wo}) [37], [45], [126]. By considering the constant emitted power by the LED in the study area, the measured and recorded RSS_e serves as a baseline; a single measurement in a specific time frame providing temporal information about a location [37], [45]. This baseline encompasses reflections from walls, the floor, and static objects [37], [45], [126]. Refering to Fig. 6, the ceiling-mounted arrangement ensures that only NLoS light, specifically reflections, reaches the PD [37]. This setup introduces challenges due to the low power of incident light resulting from an extended path and light absorption at reflectors [37], [45], [126]. The presence of a human near the LED-PD setup significantly influences RSS values [37]. Therefore, RSS_{wo} contains both reflections from an object and the surrounding environment [37], [45]. By computing the difference between the two sets of values, including RSS_{wo} and RSS_e, the relative values of ΔRSS can be obtained as follows [37], [45], [126]:

$$\Delta RSS = RSS_{wo} - RSS_e. \tag{5}$$

Fig. 7 presents an example plot of RSS_e and ΔRSS over 30 seconds, demonstrating the response to a moving object in the study area [45]. RSS_e remains constant across the area (Fig. 7 (a)), while ΔRSS shows a drop when the object enters the FoV of the PD (Fig. 7 (b)), allowing object detection [37], [45]. Coarse localization becomes feasible with temporal data and knowledge of the object's walking direction [37], [45], [126]. The study [37] identifies that positioning an individual below or between the PD-LED setup, or within the PD's FoV, scatters reflections on the person, obstructing first-order reflections from the floor which normally contributes to higher received power and influences the relative RSS pattern significantly [37]. Human presence introduces diffuse first-order reflections due to the rounded shape compared to the floor, causing a minimum in relative RSS indicative of a drop [37], [45]. Positive relative RSS values are plausible, particularly with reflective surfaces like white-colored objects that reflect more light compared to black-colored ones, which absorb light, reducing reflected light reaching the PD [37], [45]. The study highlights VLS sensitivity to factors such as object size, shape, clothing and object color, walking direction, and LED-PD configuration (e.g., height) [7], [37], [45], [127]. Adjustments in ceiling height affecting LED and PD positions impact irradiance and incidence angles in VLS [37]. Despite variations, RSS patterns consistently demonstrate VLS reproducibility [37], [45], [126]. However, there's a discernible maximum room height threshold for optimal human sensing accuracy in VLS [37]. Beyond this, VLS implementation becomes impractical, though adjusting receiver gain or transmitted light power may extend this threshold [37], [45], [126].

c) Reflection-based CIR: According to [38], [117], [118], [119], it is possible to conduct sensing and localization tasks based on CIRs. The process of determining an object's position involves simulating the set of impulse responses (IRs) between all sources and receivers and utilizing the established database [117], [118]. When calculating IRs for the empty study area, each light source is activated individually, and the corresponding simulations are recorded and stored in a pre-existing database [118]. These IRs demonstrate minimal temporal changes and can be accurately estimated through repetitive simulations conducted within the room [117], [118]. The next step involves computing IRs when the object (e.g., a human) is present in the study area, which relies on both the object's location and the background. The resulting matrix represents the assortment of IRs when the object is positioned at specific coordinates. Typically, the notable peak or drop in the IR amplitude aids in object detection [117], [118]. Fig. 8 shows a typical simulated IR plot for a room sized $4\ m \times 4\ m \times 3\ m$, comparing the scenarios with and without the presence of a user. The plot illustrates the difference in the IR due to the user's impact on the reflected signals [38], [117], [118], [119].

As outlined in the simulation study presented in [118], the effectiveness of this technique relies on the densities of both luminaires and grid points, with an increase in either component resulting in a larger database [118]. Thus, there exists a trade-off between the precision of the method and the associated deployment workload [118]. It is important to note that the research solely relies on simulations, without any prototype development or physical system implementation. Obtaining IR measurements in practical optical wireless channels (OWCs) (e.g., VLS), is challenging. The main reason

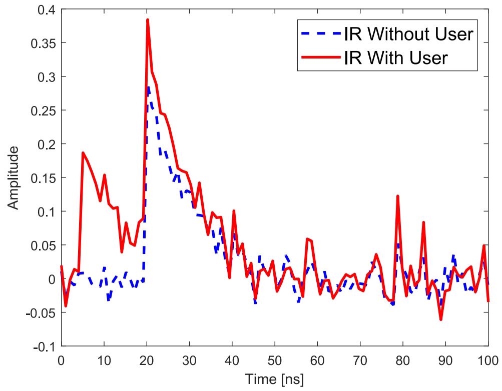

Fig. 8. IR plot comparing scenarios when a user is not present and when a user is present in a room.

is the limited bandwidth of LEDs (order of MHz), which does not allow the transmission of pulses that are sufficiently short to separate multipath components. Currently, IRs are investigated via simulations, including recursive models, ray tracing, etc [128], [129], [130], [131]. The most realistic indoor VLC channel modelling is detailed in [132], using Zemax® ray tracing to simulate IRs across various environments [133], which allow estimating the contribution of reflections on the observed light intensity.

3) Shadow vs. Reflection in VLS Systems: In Table II, we compare the shadow-based and reflection-based techniques used in VLS, illustrating that the advantages and challenges may vary depending on the specific application. Shadow-based VLS systems generally achieve higher accuracy compared to reflection-based systems [10]. However, this superiority depends on the practicality of deploying a large number of light sensors (e.g., PDs) on the floor to obtain LoS links with the Tx [10], [125]. On the other hand, reflection-based VLS systems are adaptable to various surroundings and conditions, operating independently of specific lighting or shadow presence [10], [37], [45], [125]. While reflection-based approaches offer versatility, they are more complex and sensitive to surface features compared to shadow-based methods [9], [10], [125]. They find applications in diverse indoor settings such as retail stores, museums, and warehouses for item or individual identification and tracking [10], [125], [127], [127], [134], [135], [136]. Moreover, reflection-based methods enhance gesture detection for human-computer interaction (HCI), enabling users to interact with electronic devices through hand gestures [135]. They also contribute to surface inspection and quality control in manufacturing, effectively identifying surface faults or abnormalities [137].

4) Comparison of VLS Mounting Structures: In the context of VLS mounting arrangements, ceiling-based VLS systems are usually reflection-based and frequently employ RSS or CIR techniques [37], [45], [118]. In contrast, wall-mounted [70], [81], [86] and floor-mounted [39], [47] VLS systems operate using both shadow-based and reflection-based techniques [67], [68]. The configuration of ceiling-mounted VLS, whether in monostatic setups [37], [118], [125], [138] or bi/multistatic structures [25], [39], [75], [80], [81], has experienced abundant investigation. Its performance is intricately

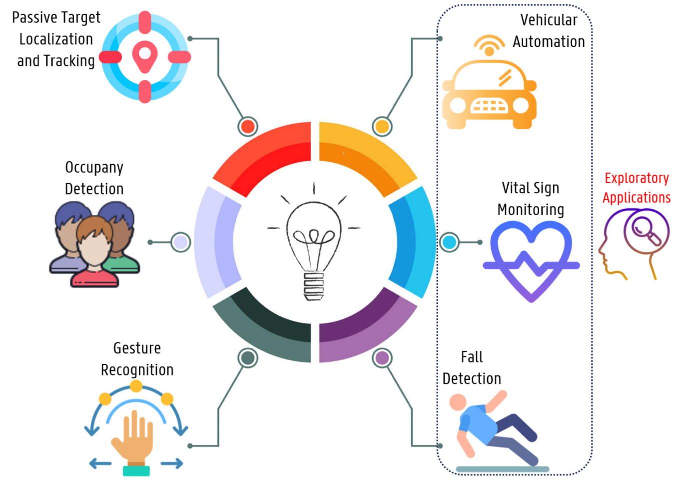

Fig. 9. Overview of DF-VLS IoT applications across six categories: Occupancy Detection, Gesture Recognition, Fall Detection, Vital Sign Monitoring, Passive Target Localization, and Vehicular Automation. It should be highlighted that DF-VLS research has largely focused on gesture recognition, occupancy detection, and passive target localization and tracking. The remaining applications (on the right) are exploratory use cases for DF-VLS, requiring additional investigation and development.

influenced by different factors such as clothing color, walking direction, hair color, and the spacing between LEDs and PDs have been identified as vital in human passive localization studies [9], [37], [37], [45].

In terms of ease of installation and freedom of movement for users, ceiling-mounted and wall-mounted VLS systems are more attractive options compared to floor-mounted VLS systems (e.g., for occupancy detection) [9], [10]. This is mostly because floor-mounted VLS systems require a denser deployment of PDs, making it challenging to move past the sensors [9], [10], [47]. Additionally, floor-mounted VLS systems, which can also be configured in bistatic setups, face challenges in achieving consistent coverage across diverse floor layouts [39], [47], [111]. Environmental changes, particularly furniture movements, greatly impact the calibration and operational performance of these systems [39], [47], [111]. Finally, floor-mounted VLS systems are more vulnerable to shadows and obstructions caused by furniture and users [9], [10]. To mitigate this, approaches like FieldLight [80] opt for wall-mounted PDs, minimizing shadowing effects by receiving dispersed light components from multiple sources.

D. Overview of VLS Applications in IoT

VLS systems demonstrate broad applicability across various domains. Fig. 9 illustrates the utilization of DF-VLS systems based on existing literature. These IoT applications include **occupancy detection, target (e.g., human) localization and tracking, gesture recognition, vital sign monitoring, fall detection, and vehicular automation**. In the following sections, we describe these IoT applications for DF-VLS systems in detail, along with related research efforts.

III. DF-VLS FOR OCCUPANCY DETECTION

At the heart of smart building technology is the seamless integration of diverse devices and technologies to enhance

TABLE II
COMPARISON OF BENEFITS AND LIMITATIONS OF REFLECTION-BASED AND SHADOW-BASED SENSING IN DF-VLS IoT APPLICATIONS

	Method	**Reflection-Based Sensing (RBS)**	**Shadow-Based Sensing (SBS)**
	Key Principle	Measuring the intensity of reflected light from surfaces or objects [9], [10], [37], [45], [125]	Detecting changes in light intensity caused by objects obstructing a light source [9], [10], [37], [45], [125]
	Typical Mounting	Ceiling-mounted [37], [45]	Both Floor [39], [47] & Wall-mounted [81], [86]
	System Design	Simple setup, full integration, compact system with co-located Tx and Rx [125], [127], [139], [140]	Low-cost, relatively simple, and non-intrusive method. Distributed Tx-Rx system for occupancy & localization makes deployment more difficult than reflection-based sensing (RBS) [96], [135], [139], [141]
DF-VLS IoT Applications	**Occupancy Detection**	★ pro RBS: • shadow-based sensing (SBS) requires an unobstructed path between Tx and Rx for detection, while RBS does not need LoS [125] • Due to PD placement, SBS has a higher likeliness of being affected by ambient light (e.g., sunlight) than RBS, particularly complex as mostly not all PDs will be affected equally [47] • RBS is cost-wise more scalable than SBS [125], [127], [140] • RBS has an easier detection of individuals due to shorter detection range [125], [127], [140] • RBS has quite homogeneous coverage by nature, SBS needs careful PD planning to make the LED-PD links cover the entire area [125], [127], [140] • RBS expected to perform better with unmodulated light, as SBS is more sensitive to interference from other light sources [47] ★ pro SBS: • SBS should perform better at person counting with modulated (demultiplexable) light sources, as it has a larger number of detection links within range (i.e., $M \times N$ with M number of LEDs, N number of PDs), vs RBS having one detection zone per PD, in which it is difficult to exactly relate RSS changes to the number of people in that zone • RBS has a shorter detection range than SBS [37], [45], [47], [127] • RBS expected to perform worse at low illuminance levels as reflected signals might be too weak [37], [45], [47], [127] • RBS performance is more impacted by target characteristics (color, material, etc.) than SBS [37], [45], [47], [127]	
	Passive Target Localization and Tracking	★ pro RBS: • Positioning is easier in RBS due to the shorter detection range, while SBS position detections correspond to a line (see Fig. 11 (b)) • RBS is cost-wise more scalable than SBS [125], [127], [140] • RBS potentially more accurate due to ability to capture and combine subtle RSS variations from different LEDs along the trajectory, in particular for 1D tracking (e.g., corridors) • Due to PD placement, SBS has a higher likeliness of being affected by ambient light (e.g., sunlight) than RBS, particularly complex as mostly not all PDs will be affected equally [47] ★ pro SBS: • RBS performs worse when the baseline reflecting material (i.e., floor) and/or the target are less reflective • RBS performance is more impacted by target characteristics than SBS [37], [45] • RBS is very vulnerable to confusion of individuals in multi-target tracking, as the area of the separable target detection zones (i.e., the area where confusion might happen) is larger in RBS (i.e., the detection area around a PD) than in SBS (i.e., an LED-PD link) • Moving/moved clutter below the SBS PD height has limited influence on SBS compared to RBS, as it barely impacts the LED-PD links in SBS	
	Gesture Recognition	★ pro RBS: • SBS is impacted in case of obstacles between the body (e.g., hand) and the receiver [96], [135], [139], [141] • SBS integration somewhat more complex due to separate Txs and Rxs and usually requires more light sensors than RBS [96], [135], [139], [141] ★ pro SBS: • RBS has an extremely limited sensing range, while SBS performs better [96], [135], [139], [141] • RBS is more sensitive to illuminance, reflective surfaces and users (e.g., people) [96], [135], [139], [141]	

the efficiency, comfort, and security of residential living spaces [134]. These buildings commonly incorporate features such as home automation, smart lighting, heating control, and occupancy detection [142], [143], [144], [145], [146], [147]. For instance, optimizing heating and cooling systems based on the number of occupants in a room effectively reduces power consumption [10], [148]. According to research, deploying occupancy detection systems may end up resulting in energy savings of 10% to 40% [148], [149]. In environments like shopping malls and large retail stores, integrating occupancy measurement techniques enhances the ability to predict areas with the highest footfall, facilitating spatial layout optimization and targeted announcements to attract customer attention [9], [10], [148], [149]. Furthermore, occupancy estimation is critical in airports for crowd management and staff direction, bolstering security measures by detecting anomalous activities [146], [149]. Several occupancy detection and estimation systems based on DF-VLS have been developed to date, and these are comprehensively summarized in Table III. We categorize these investigations into

TABLE III
A SUMMARY OF EXISTING DF-VLS SYSTEMS FOR OCCUPANCY DETECTION

	Scheme	DF-VLS Type & Configuration	VLS Hardwares (Tx vs. Rx)	Design Goal(s)	VLS Sensing Technique & Feature	Key Contributions	Limitations
Ceiling-mounted	**CeilingSee [127], [150]**	Ceiling-mounted Monostatic VLS Modulated-passive VLS	Tx-Rx: 16 LED lighting units mounted on the ceiling, with considering reverse biased LED luminaries as receivers	Indoor static and dynamic occupancy estimation	Reflection-based RSS (Light Intensity)	Over 90% accuracy for static and dynamic occupancy estimation with four VLS units using the SVR algorithm, though 12 VLS units outperform (static: 100% and dynamic: 97%)	It yields inadequate accuracy in dynamic occupancy scenarios, requiring additional changes in lighting fixtures
	Ibrahim et al. [138]	Ceiling-mounted Monostatic VLS Modulated-passive VLS	Tx-Rx: LEDs co-located with the receiver on the ceiling, modulated using ON-OFF and TDMA	Human presence detection and motion sensing (e.g., open doors)	Reflection-based ΔRSS (Light Intensity)	Validated for indoor human presence detection; 12% error rate for open door detection	It does not track or localize the target
	EyeLight [125]	Ceiling-mounted Monostatic VLS Modulated-passive VLS	Tx-Rx: 6 light units, (ON-OFF keyed luminaries, TDM), each co-located (e.g., surrounded) with four PDs on the ceiling	Occupant localization, estimation and activity classification	Reflection-based RSS (Light Intensity)	0.89 m median localization error, with 93.7% and 93.78% accuracy for occupancy estimation and activity classification, respectively	It functions effectively only under controlled conditions
	Ouahabi et al. [151]	Ceiling-mounted Monostatic VLS Unmodulated-passive VLS	Tx-Rx: Three LED-PD units on the ceiling	Occupancy, movement direction, and walking speed determination	Reflection-based ΔRSS (Light Intensity)	Over 95% accuracy for occupancy, movement direction, and walking speed under varying ambient lighting	The designed system is vulnerable to failure due to miscounting in close proximity (less than 1 meter apart)
	Hao et al. [152]	Ceiling-mounted Monostatic VLS Modulated-passive VLS	Tx-Rx: 16 LED lighting units mounted on the ceiling, with considering reverse biased LED luminaries as receivers	Indoor static and dynamic occupancy estimation	Reflection-based RSS (Light Intensity)	Improved the results of work [127] by using ensemble learning, achieving 88% accuracy with 0.13 MSE for dynamic occupancy, and 93% accuracy with 0.088 MSE for static occupancy	The study needs validation in large areas with varying occupancy patterns
	Deprez et. al [37]	Ceiling-mounted Bistatic VLS Unmodulated-passive VLS	Tx: Ambient lights & Rx: One PD on the ceiling	Single human detection	Reflection-based ΔRSS (Light Intensity)	100% accuracy in both controlled lab and real-world tests	The system's performance may be influenced by multiple individuals
	ChickSense [45]	Ceiling-mounted Bistatic VLS Unmodulated-passive VLS	Tx: One DLS & Rx: Two PDs on the ceiling	Chicken counting	Reflection-based ΔRSS (Light Intensity)	Over 90% accuracy in chicken counting during real farm tests	Further research is needed to investigate overlapping zones in real farms and the impact of soil type
Floor-mounted	**LocaLight [39]**	Floor-mounted Multistatic VLS Unmodulated-passive VLS	Tx: Three LEDs on the ceiling, Rx: Five PDs on the floor	Detecting a person at different walking speeds (e.g., slow and fast)	Shadow-based RSS (Light Intensity)	Person detection accuracy of 93.3% for fast speed and 100% for slow speed	It does not prioritize precise localization or tracking
	Mestiraihi et al. [69]	Floor-mounted Bistatic VLS Unmodulated-passive VLS	Tx: One LED on the ceiling, Rx: One PD on the floor	Occupancy estimation (1 to 7 people)	Shadow-based RSS (Light Intensity)	Occupancy estimation using KL-divergence with MSE of 1.6, outperformed Euclidean distance with MSE of 1.8. An increasing trend in KL was reported, ranging from 0.1 to 0.5, as occupancy changed from 2 to 5 people	It needs to be investigated further by analyzing light scattering in the proposed algorithm
Wall-mounted	**Iris [72]**	Wall-mounted Multistatic VLS Unmodulated-passive VLS	Tx: Ambient lights & Rx: LSI sensors on the wall	Localizing individuals	Shadow- & Reflection-based LSI (Light Spectrum)	LSI-based DF-VLS outperforms RSS-based DF-VLS for localizing individuals, achieving 0.71 m 90^{th} error with 0.68 sensor/m^2 in a 25 m^2 apartment and 0.88 m 90^{th} error with 0.24 sensor/m^2 in a 111.7 m^2 office	Challenges: Multi-occupant limitations, fingerprinting efficiency, and sensor deployment optimization
	Wang et al. [67]	Wall-mounted Multistatic VLS Modulated-passive VLS	Tx: Twelve RGB-LED on the ceiling & Rx: twelve Colorbug wireless optical light sensors on the wall	Estimate the occupancy distribution in an indoor space	Shadow- & Reflection-based RSS (Light Spectrum)	Average correlation coefficients of 0.498 for the light blockage model and 0.326 for the light reflection model, between ground truth and the estimated occupancy distribution	Costly, slow, and non-customizable, Colorbug sensors hinder real-time occupancy-sensitive lighting
	LASSO [68]	Wall-mounted Multistatic VLS Modulated-passive VLS	Tx: Twelve RGB-LED on the ceiling & Rx: Twelve Colorbug wireless optical light sensors on the wall	Localizing objects with different sizes	Reflection-based RSS (Light Spectrum)	Ridge regression algorithm achieves an average localization error between 0.24 inch and 1.39 inch for object sizes ranging in width and length from 1 inch to 80 inch	Further research is required to evaluate the proposed algorithm for estimating object height

ceiling-mounted, floor-mounted, and wall-mounted VLS systems, respectively.

A. Ceiling-Mounted VLS

Fig. 10 shows a typical ceiling-mounted VLS configuration for occupancy detection, in this case with two PDs mounted at either side of the (linear) LED, and a person walking parallel along that line, at different lateral separations from it. It shows that as the lateral separation from the LED-PD system increases, the detection performance decreases.

CeilingSee estimates room occupancy (e.g., determining the number of people inside a particular region) using ceiling luminaires that also serve as receivers [127], [150]. Their system consists of two primary parts: a customizedLED driver that uses the photoelectric effect of LEDs to turn them from light emitters to light sensors, enabling the capture of ambient reflections on demand [127], [150]. Then, they employed support vector regression (SVR) algorithm to analyze real-time snapshots of ambient reflection fluctuations, inferring indoor occupancy based on these inputs. Using monostatic reflection-based VLS sensing techniques, this modulated-passive VLS system showcased an occupancy inference performance surpassing 90% [127], [150]. The algorithm performs well with static occupancy but faces challenges with moving occupants, as individual snapshots can be unstable, particularly during peak times like mornings and afternoons. Accuracy ranges from 65% to 94%, decreasing with higher occupancy levels, and may dip to around 50% due to disturbances from furniture movement [127], [150].

Ibrahim et al. [138] explored the implementation of a smart building concept using a monostatic ceiling-mounted VLS system. They integrated photosensors with LED light sources and utilized a time-division flickering scheme to multiplex the light from the LED luminaires [138]. This allowed them to identify the source of incoming light at each PD for tracking human motion and activities, employing a reflection-based sensing approach [138]. Their evaluation showcased the system's ability to detect basic activities like door openings, achieving a 12% Equal Error Rate by employing a sensitive standard difference measurement technique (e.g., ΔRSS) to detect subtle voltage changes [138].

The comprehensive investigation conducted in [138] has led to the development of EyeLight, as detailed in [125]. EyeLight is a DF-VLS system utilizing a reflection-based sensing approach, was proposed to estimate occupancy, recognize activities and positioning. It assesses the fluctuations in the average received power from the base light level (e.g., established when the room is empty) to achieve a precise occupancy count of 93.7% and a median positioning error of 0.89 meters. EyeLight employed a ceiling-mounted monostatic VLS, using ON-OFF signaling and implementing

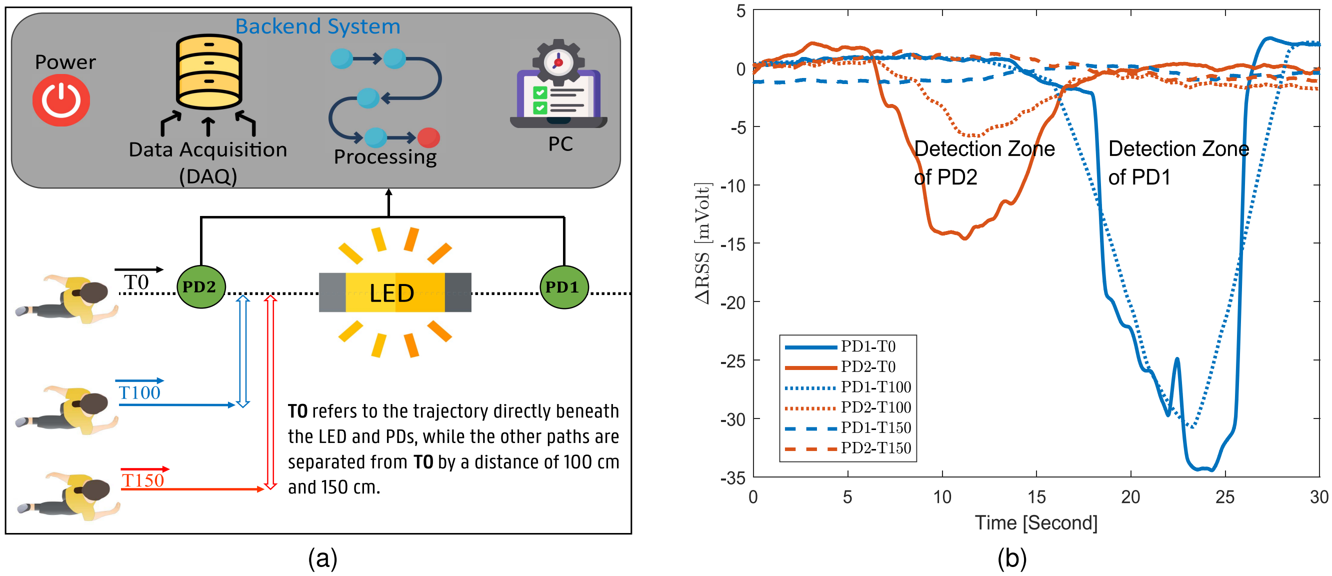

Fig. 10. Overall framework of ceiling-mounted reflection-based DF-VLS occupancy detection system. The left side (a) provides practical insights into the system's implementation, while the right side (b) showcases example results of occupancy detection for one person across various trajectories, highlighting its ability to effectively monitor occupancy within the FoV (i.e., detection zone) of the PDs (e.g., PD1 and PD2).

time-division multiplexing (TDM) methods in each of their transmitter nodes [125]. They positioned four PDs around each LED bulb, directed in different directions and tilted at an angle of 10° compared to the vertical line [125]. The research was conducted solely under controlled lighting conditions, such as in a windowless conference room with a floor illuminance measurement below 5 lux [125]. However, there is a need for additional investigation in environments where natural light enters through windows, as this could lead to receiver saturation issues [125].

Ouahabi et al. [151] developed a monostatic ceiling-mounted VLS system by integrating PDs into a luminaire. This setup determines occupancy, movement direction, and walking speed using reflection-based sensing and backscatter VLS technology. They observed that when an individual enters the FoV of a PD, it triggers a distinct change in the RSS compared to when no one is present (e.g., ΔRSS approach) [151]. This change intensifies as the person moves beneath the PD and diminishes afterward. By employing multiple PDs, they could distinguish the sequence of RSS changes, enabling the estimation of walking speed based on the known distance between PDs and the time gap between detected changes [151]. The study posits that additional ambient light affects all PDs similarly, and assumes uniformity in floor material across the luminaire's length. Experimental assessments validated the system's robustness across various scenarios, including different lighting conditions and individuals, yielding consistent and accurate outcomes [151].

Hao et al. [152] emphasize that while existing inference algorithms utilizing DF-VLS datasets can achieve high accuracy for occupancy detection, their performance tends to degrade when occupants are in motion [152]. To address this issue, they focus on occupancy inference and introduce an ensemble learning algorithm to enhance accuracy. Heterogeneous learning algorithms are employed to generate diverse learners [152]. The researchers adopt forward sequential pruning to refine the ensemble, aiming to minimize inference errors. They evaluated the algorithm using a daily dataset from [127], which is known for its relatively minor fluctuations in occupancy. The results indicate that the algorithm achieves an accuracy of up to 88% and an mean squared error (MSE) of 0.13, with the unit of MSE being the square of the number of occupants, for dynamic occupancy datasets. Additionally, for daily occupancy datasets, the algorithm achieves an accuracy of 93% with an MSE of 0.088 [152].

Finally, in [45], the author proposed a machine learning (ML)-enhanced VLS system (called ChickSense) that leverages a dynamic lighting system (DLS) to improve poultry welfare by accurately sensing and counting chickens [45]. This low-cost, unmodulated-passive VLS system uses reflected signals from the chickens' bodies as they move within the study area, aiming to identify underutilized zones, track preferences, and monitor changes in farm density [45]. ChickSense processes smoothed ΔRSS signals to extract time and frequency domain features, which are then fed into multiple ML classification models (e.g., support vector machine (SVM), K-nearest neighbor (KNN), etc). Experimental results with both large and small white chickens demonstrated that ChickSense, through ensemble learning, outperforms other ML models, achieving over 90% accuracy in chicken counting [45]. However, further research is needed to explore overlapping zones in real farm environments and assess the impact of soil reflections on DF-VLS measurements [45].

B. Floor-Mounted VLS

Di Lascio et al. [39] explored tracking by strategically positioning floor receivers to capture shadows cast by individuals, employing a shadow-based sensing approach. Their system, LocaLight [39], is a multistatic DF-VLS setup featuring three ceiling-mounted commercial off-the-shelf luminaires and five PDs on the floor to detect passing shadows [39]. However, it is important to note that while the system effectively detects the presence of people, whether stationary or walking in a straight line, its main focus is on this aspect rather than providing detailed target-level localization or tracking [39].

Mestiraihi et al. [69] highlight that fluctuations in the number of individuals crossing the LoS between the light source and the PD directly impact the received power at the receiver. Hence, changes occur in both the probability density function (PDF) and cumulative distribution function of the received power [69], [146]. Building upon this idea, they have developed a bistatic floor-mounted DF-VLS system, utilizing the shadow-based sensing approach. This method detects alterations in the LoS between the Tx and Rx as occupants move across their path [69], [146]. They employed Kullback-leibler (KL) divergence and Euclidean distance algorithms to estimate the total number of occupants. The estimation method minimizing the discrepancy between the database PDFs and measured data PDF is considered the estimated number of occupants. Simulation and theoretical results for PDFs and cumulative distribution functions (CDFs) demonstrate consistency [69], [146]. Notably, KL divergence proves more accurate than Euclidean distance, particularly with fewer than 1,000 samples in occupancy estimation. Experimental validation demonstrated that variance and standard deviation features are viable for occupancy estimation. Specifically, as the number of individuals crossing the LoS increased, the variance of the data also increased [69], [146].

C. Wall-Mounted VLS

Hu et al. [72] proposed Iris, an unmodulated-passive VLS system developed for indoor occupancy localization (refer to Table III). Iris uses ambient light as a transmitter (e.g., diffused light) and light spectral information (LSI) (Light Spectral Information) sensors (e.g., AS7265x spectral sensor) on walls to collect both light intensities and different colorfeatures (e.g., light spectrum) in a multistaticDF-VLS setup. By exploiting the occlusion (e.g., Shadow sensing) and reflection effects of indoor light sources by human bodies, Iris estimates occupant locations. The offline phase involves recording LSI fingerprinting of occupant positions in the study area, while in the online phase, occupants move freely. To address ambient light fluctuations, a mixture of gaussian approach is employed, distinguishing ambient light as background and occupant-induced light changes as foreground. Signal processing and convolutional neural networks-based classification enable Iris to predict occupant locations accurately [72]. Iris achieved a 0.71 m 90$^{\text{th}}$ percentile error using 0.68 sensor/m^2 density in a 25m^2 apartment space and a 0.88 m 90$^{\text{th}}$ percentile error with 0.24 sensor/m^2 density in a 111.7 m^2 office space [72]. However, while this research shows promise, addressing three critical issues are essential for real-world applications. First, the system's performance limitations in environments with multiple occupants need to be addressed. Second, although fingerprinting efforts are reduced compared to RSS-based passive VLS, fingerprinting remains necessary for new environments. Lastly, optimizing sensor deployment beyond simple even distribution in the study area is crucial to reduce costs and enhance the overall applicability of the system [72].

Wang et al. [67] proposed a method for estimating room occupancy utilizing perturbation-modulated red, green and blue (RGB)-LEDs. Their setup comprised twelve color-controllable LED fixtures mounted in the ceiling, each with independent adjustment capabilities for the red, green, and blue channels. Additionally, they deployed twelve Colorbug wireless optical light sensors on the walls [67]. Central to their research was a light reflection model customized for two-dimensional (2D) floor-plane occupancy assessment. They introduced randomly generated perturbation patterns onto the LED drive signals, observed changes in the color sensor responses, and reconstructed a comprehensive light transport model for the room (e.g., confidence map). Their methodology encompassed two approaches for estimating occupancy spatial distribution: a light blockage model and a light reflection model. These methods could be amalgamated to unveil occupancy scenarios within indoor spaces while upholding occupants' privacy [67]. Finally, although the commercially available Colorbug sensors are easy to install but come with significant drawbacks: they are expensive, slow, and lack customization. Each color measurement takes several seconds, presenting challenges for real-time implementation of an occupancy-sensitive lighting system due to the limited performance of the current fixtures and sensors [67].

Drawing from Wang et al. [67]'s light reflection model and testbed, Zhao et al. [68] introduced two enhanced methods for object localization: one employing LASSO and the other localized ridge regression. In simulated experiments, both approaches surpassed Wang et al. [67]'s confidence map-based localization. The localized ridge regression algorithm achieved an average localization error between 0.24 in and 1.39 in for objects ranging from 1in to 80 in width and length. In a real-world scenario with two individuals and a chair in a room, the localized ridge regression algorithm accurately located all three objects. Furthermore, their system, utilizing LED fixtures and light sensors, proved cost-effective to build and respected user privacy. However, further research is needed to explore extensions such as multiple-object localization, object size estimation, and integration of object height into the system [68].

D. Lessons Learned and Practical Implementation

The review of existing investigations on DF-VLS-based occupancy detection, as discussed in earlier sections (see Table III), shows that high accuracy in static occupancy detection is achievable using either shadow-based sensing (e.g., LiSense [47]) or reflection-based sensing (e.g., CeilingSee [127], [150] or EyeLight [125]), which consistently achieves over 90%. These methods preserve user privacy as they do not rely on cameras or wearable devices. However, their accuracy diminishes in dynamic situations with increased traffic. For instance, in CeilingSee [127], [150], the accuracy decreases from 97% for static occupants to between

60% and 90% for dynamic occupants [152]. This reduction in performance is mainly due to continuous fluctuations in occupancy, especially during high-traffic periods such as early mornings and late afternoons, which result in lower accuracy under dynamic conditions [150], [152]. To address this, ML approaches could be explored, such as using SVR with a Gaussian kernel, as in CeilingSee [127], [150], or applying ensemble learning techniques, as suggested in [152], to improve accuracy. Another challenge is ambient light interference, which can be mitigated through techniques like light modulation and signal filtering, using optical filters such as interference filters, dichroic filters, Bayes filters combined with neural networks [140], and liquid crystal filters to reduce noise and enhance the SNR [153]. Additionally, adaptive algorithms are necessary to maintain accurate detection, taking into account factors like room layout, furniture placement, user diversity, clothing, and fluctuating occupancy levels [7], [37], [47], [127], [138], [150].

The implementation of DF-VLS for occupancy detection has progressed from theoretical research to practical applications validated in relevant environments (e.g., office buildings), as summarized in Table III. To create a fully operational system, the PD modules must be connected to a backend system, such as a DAQ device linked to a PC (see Fig. 10 (a)) either through wired connections (e.g., directly wiring PDs to a central controller), or through wireless RF (e.g., hybrid VLS/RF [154], [155]). In reflection-based systems, the PD can often be wired (and powered) more easily because it is integrated within or located close to the LED fixture [37], [45]. In shadow-based systems (e.g., PDs positioned on the floor or walls), it is often more complex to wire the receiver devices. Possible solutions include the use of batteries or solar-based receivers. In these cases, the trade-offs between the amount of on-device local signal processing (vs. backend processing), the amount of wirelessly transmitted data, and the detection latency becomes a very relevant research topic.

E. Comparison With Other Technologies

Based on the study reported in [156], there is no one globally defined technology for occupancy estimates. While recent advances in camera technology provide accurate and detailed occupancy prediction [157], they have several drawbacks, including expensive installation costs, being power-hungry, LoS constraints, and serious privacy issues [156], [158], [159]. To address these problems, researchers have looked at other technologies like infrared (e.g., passive infrared sensors (PIRs) [160]) and ultrasonic sensors [161], which are cheaper and better suited for real-time applications [156]. Nonetheless, infrared sensors (e.g., Break-Beam sensors [162]) may fail to provide reliable results in scenarios where multiple individuals enter or exit simultaneously, such as in crowded buildings (e.g., shopping malls) [149]. Moreover, PIR sensors are susceptible to false-off errors [148], [158]. Ultrasonic technology may mitigate false-off errors, but it demands a clear LoS between the sensor and the occupants, leading tomore installation labor [148], [163]. Furthermore, the accuracy of ultrasonic-based methods can be greatly affected by the room's characteristics (e.g., size and materials used) [149]. radio-frequency identification (RFID)-based systems offer another option forminimizingfalse-off errors, although they, like cameras, present privacy problems since occupants have to wear RFID tags [148]. Other solutions such as pressure-[164] and capacitance-based [165] sensing, rely on placing sensors on the floor, which can be impractical for installation in many scenarios [125].

Alternative RF technologies, such as ultraWide band (UWB) and millimeter wave (mmWave) technologies can be impacted by various environmental factors, such as multipath reflections, obstructions, and electromagnetic interference from other devices, restricting their effectiveness for accurate occupancy detection [148]. However, UWB radio detection and rangings (RADARs), with their wide bandwidth, offer high precision in detecting small changes in distance, motion, and velocity, making them ideal for in-car occupancy detection [166]. Furthermore, mmWave frequency modulated continuous wave (FMCW) (frequency modulated continuous wave) RADAR could be employed for detecting occupants in vehicles at low cost and power [167]. In addition, systems that use occupancy data from various sensors, such as CO_2 and other environmental sensors, have constraints. These include expensive costs, slow reaction times (usually about 20 minutes), and sensitivity to environmental conditions [168], [169].

VLS, on the other hand, appears to be a viable choice for occupancy detection, eliminating the privacy concerns associated with cameras and without needing a LoS link, as cameras or ultrasonic sensors demand [67], [68], [72], [127]. By employing RGB color sensors, VLS can detect both moving and stationary occupants, thus overcoming the limitations typically associated with PIR sensors in this domain [125], [158]. PIR sensors primarily function as motion sensors, making them unsuitable for scenarios involving stationary individuals and hence unfit for the particular applications (e.g., occupancy detection) [125], which is required for detecting the presence of individuals, whether stationary or moving [170], [171]. Compared to the other methods outlined above for occupancy detection, VLS has important advantages. For instance, it is a cost-effective option due to its low installation costs [29], [52], [149]. Second, its power usage is considerably less (similar to UWB and RFID) frequently at the milliwatt level, allowing for accurate real-time monitoring [23], [29], [30]. However, it should be noted that the limited modulation bandwidth of traditional LEDs [125] prevents them from being used in traditional timing-based ranging approaches. Traditional LEDs have intrinsic modulation bandwidth restrictions due to physical characteristics such as carrier recombination lifetimes and internal RC time constants. Typically, their modulation bandwidth spans from a few MHz to about 20 MHz, which refers to how rapidly an LED can be switched on and off—a vital factor for transferring data or pulses in communication and ranging systems [29], [89], [172], [173], [174]. Traditional timing-based ranging methods, such as those typically used in UWB-based positioning, have a bandwidth of at least 500 MHz, allowing the emission of short pulses [175], [176]. This allows determining the time it takes for the pulses to travel between objects and -to a certain extent- separating multipath components [175], [176]. Given a LED‘s limited bandwidth, the rising edge of a LED pulse is too slow to allow for accurate timing estimations or multipath component separation.

IV. DF-VLS for Target Localization and Tracking

This section explores DF-VLS systems developed for passive target localization and tracking, commonly referred to as DFL in the literature. The investigations are categorized into single-target and multiple-target passive VLS systems, as summarized in Table IV.

A. Single-Target DF-VLS Systems

Alizadeh Jarchlo et al. [70] developed the Li-Tect algorithm, a multistatic wall-mounted system, for passive three-dimensional (3D) shape estimation of objects (e.g., single human) utilizing VLS units (e.g., separated Txs and Rxs) placed on the sides of the room. These VLS units, which include LEDs and PDs, are aware of the environment and communicate mainly via LoS transmission. The technique detects shadowing effects generated by objects by inferring the existence of objects based on the lack of transmitted light [70]. Based on a ray-tracing approach, the system determines the geometry of objects by comparing the missing links (e.g., blocked paths) to the remaining active paths [70]. In the simulation, Li-Tect utilizes a shadow-based technique to detect cubic and spherical objects within a $5 \times 5 \times 5m^3$ room equipped with 96 evenly distributed VLS units [70]. Realistic validation using 9 VLS units resulted in a MSE of 5.50 m, while simulation yielded an MSE of 0.05 m due to differences in Tx and Rx placements. This highlights a trade-off between the number of VLS units and the accuracy of object size estimation [70].

Liu et al. [71] developed the PASAL system, an indoor passive VLS and localization prototype. This modulated-passive VLP system comprises a single RGB-LED unit with a grid of 6 × 6 RGB-LEDs mounted on the ceiling in a monostatic configuration [71]. PASAL utilizes the spectral selectivity of RGB-LEDs to improve the spectral response of the LED receiver, thus extending sensing range of the received signal. Its primary function is to sense variations in diffuse reflection caused by objects [71]. The study reported a localization accuracy of approximately 0.25 m for object sensing based on extensive experiments [71]. They conducted tests during both daytime and nighttime, including sunlight and fluorescent lamps. However, the system's performance is heavily dependent on the number of RGB-LEDs [71]. Furthermore, PASAL performs better in diffuse reflection scenarios than in specular reflection situations [71]. Additionally, it shows reduced sensing range when objects are in a seated position due to the increased vertical distance between the RGB-LED unit and the object [71].

In another investigation, FieldLight [80] utilizes a multistatic shadow-based RSS approach for 2D passive human localization, employing PDs mounted on the wall in typical indoor environments such as corridors, foyers, and laboratories. Custom boards integrate ISL29023 digital ambient light sensors with microcontrollers (e.g., ESP8266) to sample PD output [80]. The ISL29023 sensor offers built-in 50/60Hz flicker and UV rejection, and is cost-effective for smart home applications (each sensor node costs less than 5$) [80], [81]. Median errors of 0.68 m, 1.20 m, and 0.84 m were achieved in various environments, with a 0.63 m lower median error compared to wireless RSS-based localization methods [80].

In line with the approach proposed in [80], Faulkner et al. [81] introduced the Smart Wall, an unmodulated-passive VLS system utilizing multistatic shadow-based RSS for 2D passive target localization in indoor environments. Deploying seven light sensors (e.g., ISL29023) positioned on a wall, the system relies solely on ambient light for target localization. Experimental studies demonstrated a median error of 7.9 cm in a corridor setting, slightly increasing to 11.4 cm in an open-room scenario. However, the system's reliance on extensive fingerprinting makes it less appealing for real-world implementation. Also, experiments were conducted under nighttime conditions, overlooking the impact of varying ambient light levels [81]. This highlights the need for future research to quantify and address its influence, with proposed solutions including exploring modulated light from LED ceiling luminaires to mitigate ambient light effects [81].

Another wall-mounted multistatic unmodulated-passive VLS system, named watchers on the wall (WoW), is proposed in [86], for 2D target localization and tracking. The study analyzes changes induced in ambient light's RSS by the target. Experimental results showed median and 90$^{\text{th}}$ percentile localization errors of 7 cm and 13 cm for stationary and mobile targets, respectively, within a 2 m × 3.6 m testbed [86]. The study found that even with four sensors, a median accuracy of 16 cm was achieved for stationary targets. The system successfully tracked mobile targets with a median error of 12 cm [86]. Challenges regarding ambient light variability were addressed, suggesting VLC-enabled luminaires for stable RSS and employing two RSS metrics to measure ambient light levels. These strategies offer promising solutions to enhance the reliability and accuracy of passive VLP systems [86].

Zhou et al. [177] investigated the performance limits of an unmodulated-passive VLS system that utilizes shadowing effects with a single LED and multiple PDs (e.g., 784) evenly placed on the floor in a room measuring 9 m × 9 m × 4 m [177]. The system is designed to localize a single object by exploring the closed-form Cramer-Rao Lower Bound (CRLB) for object positioning and receiver orientation error estimation [177]. Through simulations obtaining shadowed RSS signals and using the maximum likelihood estimation (MLE) approach, they evaluated various critical physical factors affecting DF-VLS measurements. The study highlights that positioning error in DF-VLS increases with a reduced number of positioning receivers, with around 15 positioning receivers generally achieving better VLS performance at a lower cost [177]. Additionally, the VLS error decreases as the receiver orientation becomes more perpendicular to the ground, while a nearly parallel orientation leads to a sharp decline in DF-VLS performance [177].

Finally, Rizk et al. [87] proposed PVDeepLoc, a battery-free multistatic unmodulated-passive VLS system designed for user localization. This system utilized four solar cells positioned

TABLE IV
A SUMMARY OF EXISTING DF-VLS SYSTEMS FOR PASSIVE TARGET LOCALIZATION AND TRACKING

	Scheme	DF-VLS Type & Configuration	VLS Hardwares (Tx vs. Rx)	Design Goal(s)	VLS Sensing Technique & Feature	Key Contributions	Limitations
Single-Target DF-VLS Systems	**Li-Tect [70]**	Wall-mounted Multistatic VLS Modulated-passive VLS (e.g., identity number & assigned frequency)	Tx-Rx: 9 VLS units on the wall (Practical Test) Tx-Rx: 96 VLS units on the wall (Simulation)	3D object shape detection	Reflection-based ΔRSS (Light intensity)	MSE of 5.50 m in real-world tests and 0.05 m in simulations for 3D object shape detection	High accuracy requires a large number of VLS units
	PASAL [71]	Ceiling-mounted Monostatic VLS Modulated-passive VLS (e.g., FPGA Controller)	Tx-Rx: The LED array consists of 3×3 RGB-LED	2D object localization	Reflection-based (Light spectrum)	0.25 m accuracy in object localization using 36 RGB-LED units	Performance depends on RGB-LED quantity, with better results only in diffuse reflection
	FieldLight [80]	Wall-mounted Multistatic VLS Unmodulated-passive VLS	Tx: Ambient lights on the ceiling, Rx: 14 PDs on the wall	Indoor (2D) human localization	Shadow-based (Light intensity)	Median errors of 0.68 m, 1.20 m, and 0.84 m for 2D human localization in a corridor, foyer, and laboratory, respectively, and median error of 0.63 m lower than wireless RSS-based DFL methods	Overhead PDs are assumed under constant ambient light
	Smart Wall [81]	Wall-mounted Multistatic VLS Unmodulated-passive VLS	Tx: Ambient lights on the ceiling, Rx: Seven PDs on the wall	2D target localization	Shadow-based (Light intensity)	2D target localization median errors of 7.9 cm in corridors and 11.4 cm in open rooms	Relied on labor-intensive fingerprinting and overlooked ambient light effects
	WoW [86]	Wall-mounted Multistatic VLS Unmodulated-passive VLS	Tx: Ambient lights on the ceiling, Rx: 14 PDs on the wall	2D stationary target localization and tracking	Shadow-based (Light intensity)	Localization accuracy of 7 cm for stationary targets and 13 cm for tracking mobile targets	Relied heavily on extensive fingerprinting efforts and requires further development to function effectively in changing ambient light conditions
	Zhou et al. [177]	Floor-mounted Multistatic VLS Unmodulated-passive VLS	Tx: One LED on the ceiling, Rx: Multiple PDs on the floor	Performance limits of DF-VLS for 2D object localization	Shadow-based RSS (Light intensity)	Demonstrated the impact of various physical factors on VLS measurements for 2D object localization within a DFL framework, with location error decreasing from 0.03 m to nearly zero as SNR increased from 40 to 60 dB	Real-world validation is required
	PVDeepLoc [87]	Wall-mounted Multistatic VLS Unmodulated-passive VLS	Tx: 8 lamps of 40 watt on the ceiling, Rx: four solar cells on the wall	3D object (human) localization	Reflection-based (Light intensity)	Median localization accuracy of 0.63 m for 3D human localization	Further research is needed for multi-target scenarios
Multi-Target DF-VLS Systems	**iLight [178]**	Wall-mounted Multistatic VLS Unmodulated-passive VLS	Tx: 10 general light sources on the wall & Rx: Ten light sensors on the wall	2D single and multi-target tracking	Shadow-based RSS (Light intensity)	DF tracking of both single and multi-target (up to five) with cm-level accuracy	Requires high memory and computing resources
	Zhang et. al [44]	Floor-mounted Multistatic VLS Unmodulated-passive VLS	Tx: Four LEDs on the ceiling & Rx: PD nodes on the floor	2D multi-target counting and positioning	Shadow-based ΔRSS (Light intensity)	Mean positioning error of 0.10 m and a counting error of 0.02 using the geometrical localization (GL) algorithm for multi-target	The proposed GL method is sensitive to changes in node density
	VLS-RCNN [179]	Floor-mounted Multistatic VLS Unmodulated-passive VLS	Tx: Four LEDs on the ceiling & Rx: PD arrays on the floor	3D multi-target recognition and positioning	Shadow-based ΔRSS (Light intensity)	Mean positioning error of 0.077 m (one-class, 100% recognition) and 0.075 m (two-class, 97.3% recognition)	System evaluation lacks tracking, range, and speed measurement tasks, highlighting the need for real-world validation
	Inti [102]	Wall-mounted Multistatic VLS Unmodulated-passive VLS	Tx: Ambient light & Rx: Six tags compose of a solar cell, a microprocessor and BLE transmitter	3D multi-target detection and tracking	Shadow & Reflection based (Light intensity)	100% tracking accuracy during the day, reduced accuracy at night under artificial lighting (1 out of 5 misdetections after filtering), frequent misdetections in case of light fluctuations while tracking two people	The prototype requires an external power source; further analysis is needed to enable operation using solar cells alone. Accuracy is reduced in the presence of light fluctuations

vertically on the walls, along with an LED light source on the ceiling. Operating in a real room testbed spanning 2 m × 3 m [87]. They measured photocurrent values from the solar cells during offline and online phases, and subsequently trained a deep neural network to estimate user location with fine-grained accuracy [87]. To ensure robustness, the system employed various regularization techniques, enhancing its ability to generalize and avoid overfitting. The study demonstrated median localization accuracy surpassing 0.63 meters. The research emphasized the significance of solar panel density in achieving accurate localization, with even just two cells enabling acceptable room-level localization with a median error of under 2 meters [87].

B. Multi-Target DF-VLS Systems

Recent research has focused on using passive VLS systems to localize and track multiple targets [44], [102], [179]. However, existing multi-target DFL algorithms are primarily designed for scenarios with two or three widely spread targets, leading to problems when dealing with closely spaced targets [180]. This may give rise to crossing shadowed connections and incorrect pseudotarget positioning [44], [181]. Moreover, many DFL algorithms assume prior knowledge of the number of targets, which can often be unavailable in real-life situations [40], [44], [179], [181].

In this context, Mao et al. [178] presented the iLight system, a wall-mounted multistatic unmodulated-passive VLS system designed for DF passive tracking of multiple targets (e.g., five humans with varied heights) utilizingVL. The iLight system leverages a standard geometrical localization (GL) approach to identify target locations based on the intersection points of shadowed links (e.g., shadow-based sensing) [178]. When three light sensors are positioned 30 cm apart, the maximum error is around 8 cm [178]. However, increasing the number of sensor nodes to six lowers the average error to about 2 cm. In addition, the analysis found that toavoid the impact of a target's movement speed on the proposed setup, the sampling rate of a wireless node should be sufficient to capture any passing target (e.g., individuals). Finally, iLight system requires significant memory and computer resources to generate intersection points, resulting in pseudo-target positions [44].

Zhang et al. [44] proposed a floor-mounted multistatic DF-VLS system utilizing the shadow-based ΔRSS sensing approach for multi-target DFL, capable of tracking up to ten targets. Their proposed GL technique, consists of a weight computing phase and an adaptive multi-target positioning (AMTP) algorithm phase. In the weight computing step, the method clusters shadowed nodes to identify potential target areas using a sector ring model. Thereafter, by constructing a weight map for the monitored area and employing the AMTP algorithm, they compared the performance of the proposed GL method with traditional GL presented in [178] and fingerprinting methods during simulations. When considering targets as cubes randomly positioned within the monitored area, they reported a mean positioning error of 0.102 m and a counting error of 0.02 [44]. The evaluation of all three methods as the number of targets increased from 1 to 10 revealed a degradation in performance, with a reported counting percentage of around 95% and a positioning error of 0.1 m for the proposed GL approach. Also, the study demonstrated that the localization errors of the three DFL methods decrease as the distance between targets increases [44]. With a localization error less than 0.3 m when the distance between targets set to 3.5 m. Furthermore, the study reported that the localization errors of the three DFL methods increase as the light sensor spacing increases [44]. Finally, the study reported that a change in target height from 1 m to 2 m has a slight effect on the localization error and counting percentage of the proposed GL method [44]. Finally, as mentioned in this study, a primary limitation of this system lies in the proposed GL method's sensitivity to changes in node density (e.g., PDs on the floor) [44].

In multi-target DFL, integrating recognition and positioning functionalities while minimizing overhead [40], [179] is necessary. A proposed solution, termed as the Multi-Scale VLS-Region Convolutional Neural Network (VLS-RCNN) outlined in [179], involves constructing shadow models for objects of various shapes (e.g., cube and sphere). Traditional image processing methods struggle with feature discrimination due to shadow features varying with object positioning and shape [179]. To address this, convolutional neural networkss (CNNs) offer improved accuracy by integrating with classifiers [179]. In this context, VLS-RCNN operates by using a shadow-based ΔRSS sensing approach and based on the simulation results, it shows a mean positioning error of 0.077 m and achieved a recognition rate of 100% in one-class object testing. In the two-class object test, the positioning error reduced to 0.075 m with a recognition performance of 97.3%. However, the system evaluation falls short as it lacks tracking, range, and speed measurement tasks, highlighting the need for real-world validation [179].

Lastly, Xu [102] developed Inti, an unmodulated-passive VLS 3D multi-target indoor detection and tracking system using solar cells in a wall-mounted and multistatic configuration. This system is comprised of three main parts. First, they utilize a ray-tracing model to optimize solar cell location inside the tracking environment, to maximize SNR [102]. They then employed changepoint detection methods to turn the chaotic solar cell output into a binary detection signal, with a Bayesian approach for flexibility in different lighting situations [102]. Finally, they integrated the binary signals from multiple solar cells to track multiple targets using a particle filter implementation. This approach facilitated tracking without requiring prior knowledge of the exact number of targets present. Evaluation in a small apartment demonstrated that Inti tracked humans under several lighting settings, including uncontrolled daylight and controlled night-time illumination [102].

C. Lessons Learned and Practical Implementation

DF-VLS for passive indoor positioning and tracking has been explored in wall-mounted setups (e.g., Smart Wall [80], WoW [86]), ceiling-mounted setups (e.g., PASAL [71]), and floor-mounted setups (e.g., VLS-RCNN [179]), supporting single- [70], [71], [80] and multi-target DFL [102], [178], [179] (see Table IV). These studies achieved cm-level accuracy at relatively low cost by reusing existing lighting infrastructure and affordable sensors (e.g., PDs or solar cells) [71], [80], [86], [87]. However, some systems rely on labor-intensive fingerprinting, as seen in Smart Wall [80], and Wow [86], which impacts performance under changing lighting conditions [80], [236]. This issue can potentially be managed by using background light subtraction [37], [45], or by using GL, a training-free method that reduces fingerprinting needs and improves DFL efficiency [236]. Other systems, like Li-Tect [70] and iLight [178], require dense deployment of VLS units, increasing the cost. For example, Li-Tect's accuracy improves from 5.50 m to 0.05 m as the number of units increases from 9 to 96 [70], and iLight's accuracy improves from 8 cm to 2 cm when the number of sensors increases from 3 to 6 [178]. Additionally, most multi-target DFL studies assume widely spaced targets, which is impractical when targets are close together, leading to overlapping shadows and pseudo-target errors [178], [180], [181]. Many VLS-based DFL algorithms also assume prior knowledge of the number of targets, which is often unrealistic [178], [180], [181]. Probabilistic classification methods, such as those in [237], show high accuracy with few targets but struggle at larger scales. To address these limitations, a hierarchical framework combining data-driven and knowledge-driven techniques, like K-means clustering and broad learning-based DFL models, offers a scalable alternative [236], [238].

VLS for DFL purposes can be practically implemented using either modulated light sources (e.g., specially designed, controlled light sources [78]) or unmodulated sources (e.g., ambient light [86]), with light sensors (e.g., PDs) positioned on walls, floors, or ceilings. The RSS values, channel model, and known LED locations are then used as inputs to the localization engine, which estimates the absolute target location [29]. Fig. 11 illustrates an experiment how a single PD allows detecting a target passage, but it is clear that a sufficient number of LED-PD links is required to perform area-wide positioning. In an environment with N LEDs and M PDs, up to $N \times M$ links are available for positioning, on the condition that the N LED contributions can be demultiplexed. This can be realized either by modulating the LEDs or by relying on CF-based unmodulated VLS [52], which was the case for the results shown in Fig. 11 (with $N = 2$, $M = 1$).

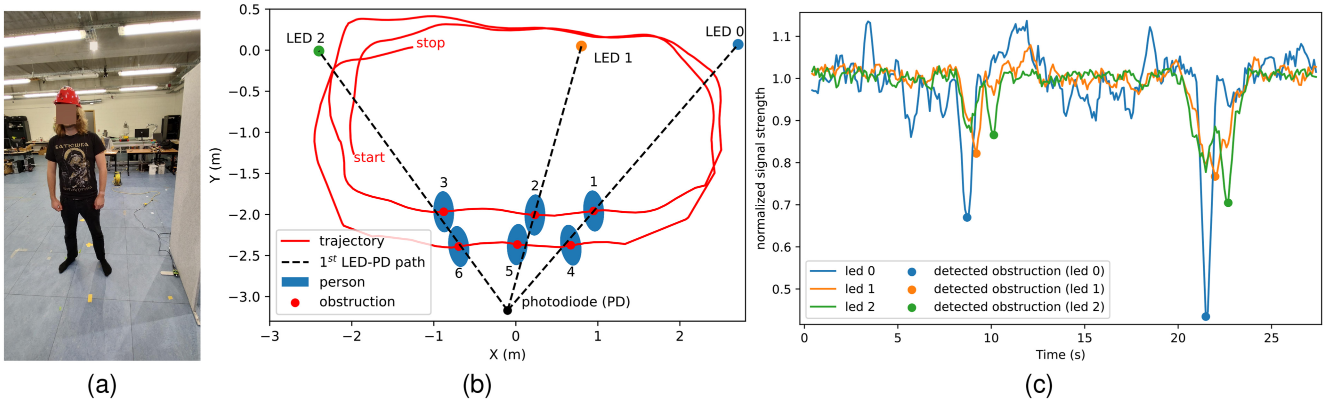

Fig. 11. Visualization of experimental DFL using a shadow-based sensing technique in a floor-mounted DF-VLS system with a single PD (e.g., PDA36A2). (a) Shows a picture of a person standing next to the PD, wearing a hat with infrared markers for recording the ground truth with motion capture (mocap). (b) The pedestrian's movement trajectory is illustrated, showcasing the shadow-based sensing mechanism in the DF-VLS system. (c) The RSS variations are presented as the pedestrian progresses along the trajectory.

Depending on the requirements for complexity, latency, and accuracy, a suitable localization algorithm (e.g., MLE [177], etc) from the literature can be selected for positioning [29], possibly fused with dead reckoning in postprocessing filters. Finally, as discussed in [86], [177], practical considerations include the number and placement of receivers, as well as other deployment factors [86], [177], similar to the occupancy detection case.

D. Comparison With Other Technologies

DFL techniques can be generally classified as RF and non-RF-based technologies [7]. Each of these different technologies has its own set of benefits and disadvantages. Table V compares VLS and other methods for DFL. While vision-based DFL methods (e.g., cameras) provide rich object information and excellent spatial resolution, they may pose privacy concerns when used in private settings (e.g., home, offices) [72]. Ultrasonic DFL can achieve good accuracy, especially for methods using time-of-arrival (ToA) [220], but it is affected by body interactions, background noise, echoes, and multiple sound sources [5], [239]. DFL techniques using mechanical devices (e.g., pressure sensors) or electric fields (e.g., floor tiles), although they can provide high-resolution occupant tracking, demand significant infrastructure investment [5], [214].

In the RF-based DFL solutions category, the most researched DFL approach is WiFi-based indoor localization [5], [7], [240], [241], [242]. WiFi-based DFL primarily relies on channel state information (CSI) to capture physical layer metrics, demonstrating the superiority of CSI profiles over RSS profiles in multi-person monitoring due to their richer feature set (e.g., amplitude, phase) and heightened sensitivity to crowd size [241]. However, WiFi equipment (e.g., routers and access points) requires continuous power for operation and coverage provision, leading to significant energy consumption [240]. Additionally, CSI's limitation to WiFi excludes other wireless technologies like BLE and Zigbee [7].

VLS is less susceptible to interference from other devices, making it excellent for seamless integration with parallel technologies [23], [29], [30]. Several advantages make VLS as a potential candidate for passive target localization and tracking. For instance, passive VLP systems can provide cm-level accuracy similar to other RF-based approaches (e.g., UWB, RADAR) and non-RF-based approaches (e.g., sound, camera, etc.), but at a lower cost [29], [74]. This is mainly because LEDs and ambient lights are widespread in our environments, and for localization and sensing, we only need low-cost receivers (e.g., PDs) [23], [29], [30]. Also, the intrinsic and distinguishable characteristic frequencies of LEDs present an opportunity to bypass even the need for costly modulation drivers in VLP systems (e.g., unmodulated-passive VLS systems) [52], [74]. In contrast, both RF-based and non-RF-based approaches typically require significant investments in specialized infrastructure. For example, since RFID has a limited coverage distance, deploying several RFID readers or anchor nodes for tracking incurs considerable expenses [8], [240]. Similarly, technologies like cameras, UWB, mmWave, and radar-based DFL approaches require large upfront investments.

Finally, when comparing VLS with RF technologies like UWB or mmWave for DFL applications, each has its own unique benefits and limitations, making them suitable for different use cases [4], [8], [12], [243]. UWB and (especially) mmWave excel in high-precision ranging and angular measurements, thanks to their large available modulation bandwidths and phased array capabilities [4], [8], [12], [243]. UWB has the potential to sense objects through walls, while mmWave and VLS cannot [12], [243]. VLS is also less suited for outdoor usage compared to RF-based sensing; however, VL suffers less than RF from multipath interference in highly reflective environments. Furthermore, VLS-based sensing systems are typically less complex, expensive, and power-hungry [12], [37], [45], [74], [176], [244] than their RF counterparts. VLS stands out for its simpler integration, leveraging existing LED infrastructure, and its vast, interference-free spectrum [23], [29], [30], [74]. In conclusion, depending on

TABLE V
COMPARISON OF PASSIVE TARGET LOCALIZATION AND TRACKING TECHNOLOGIES

Category	DFL Technology [Ref.]	Benefits	Drawbacks	DF Sensing Range	Power Consumption	DFL Accuracy	Resolution	Privacy Concern
RF-Based / *RADAR*	UWB [182]–[188]	✓ High accuracy and bandwidth ✓ Efficiency ✓ Phone integration	× Relatively expensive × Low update rate × Scalability issue	A few cm to meters	**Low** mW-range (e.g., 8 GHz UWB Radar Chips below 1mW)	cm-level	**High** (e.g., high ranging, high level of multipath resolution)	**Low**
RF-Based / *RADAR*	mmWave [12], [189]–[193]	✓ Ultra-high-speed data transfer ✓ Small-size receiver ✓ Low latency ✓ Wide bandwidths	× Hardware complexity × Energy consumption and Range considerationg	A few cm to meters	**High** W-range (e.g., TI MMWCAS-RF-EVM >20W)	cm-level	**High** (e.g., 60 GHz band)	**High**
RF-Based	RFID [194]–[198]	✓ Small and cost-effective ✓ Battery-free (passive) tags ✓ Scalable	× Huge cost RFID reader × Costly maintenance, installation and software × (Tag) detuning, collisions and interference	A few cm to meters	**Medium** μW to W-range (e.g. TRF7960: 200mW, UHF 8dbi RS232: 1W)	cm-level	**Low** (e.g., RFID Signal Collision)	**High** (e.g., inventorying)
RF-Based	BLE [199]–[204]	✓ Low energy ✓ Cheap ✓ Widespread ✓ IC integrated in phones	× Scalability issue × Low update rate × prone to interference	up to few meters	**Low** mW-range (e.g., CC2674R10)	m-level	**Low** (e.g., poor time resolution)	**Low** (e.g., Smart privacy feature)
RF-Based	WiFi [205]–[210]	✓ Widespread adaptation ✓ Scalability ✓ Non-intrusive sensing capabilities	× Prone to environmental interference × Privacy and security issues × Impacted by network performance	up to few meters	**High** W-range (e.g., TI CC3200 WiFi Module)	m-level	**Low** (e.g., Signal Fading and Shadowing)	**High**
RF-Based	wireless sensor network (WSN) [211]–[213]	✓ Flexibility ✓ Network scalability ✓ Efficient sensing capabilities	× High cost × Vulnerability to hacking × Limited speed	up to few meters	**Low** mW-rang (e.g., STM32L4 Series)	m-level	**Low** (e.g., Binary output, communication bandwidth issues)	**High** (e.g., Data leakage)
Non-RF-Based	Camera [214]–[218]	✓ Rich locating data ✓ Ubiquitous ✓ IC integrated in phones	× Requires sufficient light levels × Easily spoofed and attacked	up to few meters	**High** W-range (e.g., Mobotix M26)	m-level, or cm-level (when dense)	**High** (e.g., Detailed imaging)	**High**
Non-RF-Based	Ultrasonic [7], [149], [219]–[221]	✓ Low cost ✓ Widely available ✓ High recording capability (e.g., 192 kHz) in many mobile devices	× Not low energy × Interference from environmental noises × Impact of multi-user in the sensing area	up to few meters	**Low** mW-range (e.g., MaxBotix MB1242)	cm-level	**High**	**Medium**
Non-RF-Based	Electrical Field [7], [222]–[226]	✓ Low power consumption ✓ Non-Invasive ✓ Real-Time Monitoring ✓ High Sensitivity	× Complex Calibration × Interference from strong electrical fields × Hard to detect static objects × short sensing range	up to few meters	**Low** mW-range (e.g., FDC1004)	cm-level	**High**	**Low**
Non-RF-Based	Mechanical [7], [227]–[230]	✓ Simplicity ✓ Cost-effective ✓ Robustness ✓ Low power consumption	× Calibration challenges × Sensitivity to the ambient temperature	up to few meters	**Low** mW-range (e.g., ADXL362)	cm-level	**High** (e.g., Synthetic Aperture Radar Integration)	**Medium**
Non-RF-Based	Infrared [231]–[235]	✓ Ease of installation ✓ Wide bandwidths ✓ Non-licensed channels ✓ Minimum electromagnetic interference	× Impacted by noise and interference from ambient visible and infrared light × limited sensing range	up to few meters	**Low** μW to mW-range (e.g., HCSR501)	cm-level	**Medium**	**Low**
Non-RF-Based	VLS [10], [37], [45], [47]	✓ Less infrastructure change ✓ Low-cost receivers (e.g., PDs) ✓ Wide bandwidths ✓ Non-licensed channels ✓ Minimum electromagnetic interference	× Impacted by noise and interference from ambient VL × limited sensing range	A few cm to meters	**Low** μW-range (e.g., PDA100A2)	m-level	**Medium**	**Low**

the use case, VLS and RF technologies like UWB and mmWave can complement each other to enhance sensing capabilities.

V. DF-VLS FOR GESTURE RECOGNITION

Gesture recognition streamlines interaction within smart buildings by enabling users to effortlessly manage devices such as lighting and heating, ventilation, and air conditioning (HVAC) systems without the need for physical contact [95], [96], [135]. This progress not only improves user comfort but also saves energy and reinforces security measures, ultimately optimizing building functions and creating a harmonious living space. Furthermore, gesture recognition is widely applicable across diverse HCI applications, spanning from household to commercial and office environments [95], [96], [135].

Fig. 12 illustrates a general framework of the DF-VLS-based gesture recognition systems encountered in literature, leveraging both shadow-based and reflection-based sensing techniques, utilizing PDs or solar cells as receivers [95], [96], [135], [245], [246]. Following the initial measurements (e.g., data collection), the raw signals undergo essential processing steps to enhance their quality, including signal denoising (e.g., discrete wavelet transformation), thresholding, and normalization (e.g., min-max normalization, Z-score normalization, etc.). Thereafter, these processed signals serve as inputs for feature extraction, where various techniques are employed to capture relevant gesture characteristics [95], [96], [135]. The extracted features are then fed into various ML classification algorithms (e.g., KNN, SVM, etc.), facilitating gesture detection [95], [96], [135], [245], [246]. Several studies exploring gesture recognition via DF-VLS have been conducted by

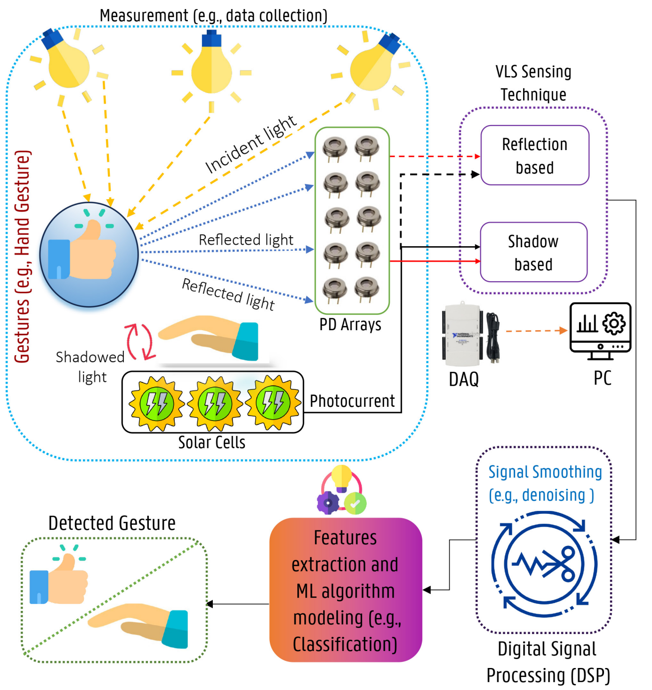

Fig. 12. Overall framework and components of a DF-VLS-based gesture recognition system encompasses both shadow-based with solar cells and reflection-based with PD arrays. This includes the key stages of measurements, sensing, signal processing, and machine learning classification algorithms modeling. Additionally, the integration of red and black dashed lines illustrates the potential to develop a DF-VLS-based gesture recognition system utilizing reflection-based sensing with PD arrays and solar cells, respectively.

researchers, as outlined in Table VI, and will be discussed in subsequent sections. This investigation categorizes into shadow-based and reflection-based methods, each of which can be further classified based on the type of receiver, either PDs or solar cells (e.g., Shadow/Reflection & PDs and Shadow/Reflection & Solar Cells).

A. Shadow-Based Using PD

Li et al. [245] developed a proof-of-concept prototype called Aili, functioning as a table lamp to reconstruct a 3D hand skeleton by assessing how the hand obstructs light rays emitted by LED chips within the lamp. This modulated-passive VLS system consists of 24 $\times$ 12 white LEDs and a lamp base embedded with 16 low-cost PDs arranged in a 4 $\times$ 4 grid in a multistatic VLS configuration. Aili captures blockage data using an array of PDs within the lamp base when the user performs hand gestures under the light [245]. By combining blockage maps from different PDs and utilizing high flashing frequency techniques to differentiate shadows, Aili identifies the 3D hand pose that best matches the observed blockage maps. The prototype demonstrates an average reconstruction time of 7.2 ms with a 10.2° angular deviation and a 2.5 mm translation deviation compared to Leap Motion [245].

In another study discussed by Li et al. [47], LiSense was introduced as a modulated-passive VLS system. By employing a shadow-based RSS approach, LiSense constructs a shadow map to reconstruct 3D human skeleton postures [47]. The system consists of 324 floor-mounted PDs arranged on a 3m$\times$3m testbed and five modulated LEDs on the ceiling, forming a multistatic DF-VLS system. frequency division multiplexing (FDM) distinguishes shadows from each light source [47]. Experimental results indicate reasonable accuracy of reconstruction of five main body joints, with a mean angular error of 10 degrees [47]. However, LiSense's focus on large-scale skeleton reconstruction limits its ability to accurately detect hand and finger gestures [246]. Additionally, the system requires full control of the lighting environment for optimal performance, which may not be practical in most commercial buildings [246]. In their subsequent research, the same group introduced StarLight [111], which utilizes 20 PDs on the floor and 16 ceiling-mounted LEDs. It achieves a marginally higher error of 13.6 degrees for 3D reconstruction of five key body joints compared to the previous design [47]. However, this study requires attaching a laser pen on object for calibration, rendering it unsuitable for DF-VLS [111].

Furthermore, An et al. [247], motivated by the observation that shadows cast by users with diverse body types exhibit distinct characteristics, developed a modulated-passive VLS system for 3D human skeleton recognition (e.g., user identification) using a similar testbed as proposed in the LiSense study [47]. They emphasized that shadow maps captured from various angles aid in localizing key points on the human body, allowing for the extraction of vital body parameters such as shoulder width and arm length, which are then utilized as features for 3D human skeleton recognition. Their preliminary experiments with 10 participants achieved an 80% success rate, accurately identifying 8 out of 10 participants [247]. The mean error in estimating body parameters was reported to be 0.03 meters [247]. However, the performance of this system may face challenges with a greater variety of user movements, as the participants in this study were restricted in their movement, particularly for the legs, being asked to only move their arms freely. Additionally, the system was tested within a limited age range (e.g., 20 to 31 years old), height range (e.g., 1.55 m to 1.90 m) and weight range (e.g., 45 kg to 87 kg), necessitating investigation across broader demographics. Furthermore, variations in factors such as hair color, shirt color, and movement style could also impact performance [247].

Another study akin to LiSense [47] was presented in [246], introducing GestureLite which is an unmodulated-passive VLS system, tailored for hand gesture recognition using ambient light exclusively. It functions by thoroughly monitoring fluctuations in light levels caused by hand movements across a wide FoV (e.g., 90°) array, comprising nine PDs arranged in a multistatic configuration. For GestureLite training, they measured around 10 samples of each gesture users may want to employ [246]. Then, these samples undergo logging and analysis using ML algorithms to facilitate real-time gesture identification. During real-world testing, GestureLite attains a 98% classification rate for user gestures when trained with ample samples collected throughout the day. However, GestureLite faces difficulties in bright lights due to PD saturation and in darkness where shadows are poorly defined [246]. Shadow interference from users or objects further hampers GestureLite's functionality, especially in environments with

TABLE VI
A SUMMARY OF EXISTING DF-VLS SYSTEMS FOR GESTURE RECOGNITION

	Scheme	VLS Type & Configuration	VLS Hardwares (Tx vs. Rx)	Design Goal(s)	VLS Sensing Technique & Feature	Key Contributions	Limitations
Shadow & PDs	**Aili [245]**	Multistatic VLS Modulated-passive VLS (e.g., high flashing frequency modulation)	Tx: 24×12 LEDs & Rx: 16 PDs as lamp table	3D hand skeleton recognition	Shadow-based RSS (Light Intensity)	Reconstructed a 3D hand pose within 7.2 ms on average, with a 10.2° mean angular deviation and a 2.5 mm translation deviation compared to Leap Motion	Aili prototype has portability limitations and struggles with transparent objects
Shadow & PDs	**LiSense [47]**	Multistatic VLS Modulated-passive VLS (e.g. FDM Modulation)	Tx: Five LEDs on the ceiling & Rx: 324 PDs on the floor	3D human skeleton construction (five body joints)	Shadow-based RSS (Light Intensity)	Accurate reconstruction of five main body joints with a mean angular error of 10°	It struggles with hand and finger gesture recognition and requires full lighting control, posing challenges for commercial use
Shadow & PDs	**An et al. [247]**	Multistatic VLS Modulated-passive VLS (e.g. FDM Modulation)	Tx: Five LEDs on the ceiling & Rx: 324 PDs on the floor	Recognizing the user based on estimated body parameters (e.g., shoulder width, arm length)	Shadow-based RSS (Light Intensity)	80% accuracy in user identification (correctly identifying 8 out of 10 participants), with a mean error of 0.03 m in body parameter (e.g., shoulder width, arm length) estimation	The performance may face challenges with a greater variety of user movements
Shadow & PDs	**GestureLite [246]**	Multistatic VLS Unmodulated-passive VLS	Tx: Ambient light & Rx: nine PDs	Recognizing 10 hand gestures (up, down, etc.)	Shadow-based RSS (Light Intensity)	98% classification accuracy with the KNN algorithm	It suffers from shadow interference from users or objects
Shadow & PDs	**LiGest [96]**	Multistatic VLS Unmodulated-passive VLS	Tx: Ambient light & Rx: 36 PDs on the floor	Recognizing five types of human gestures (hug, clap, etc.)	Shadow-based RSS (Light Intensity)	96.3% accuracy for all gestures, except the clap gesture, which had 92% accuracy due to hand shadows being blocked by the body	Vulnerability may arises due to fluctuations in ambient light
Shadow & PDs	**LiGeR [248]**	Multistatic VLS Unmodulated-passive VLS	Tx: Ambient light & Rx: 10 TSL237 on the wall or 4 TSL237 on the four corners	Detecting and recognizing eight different hand gestures (left, right, etc.)	Shadow-based RSS (Light Intensity)	Detection accuracy of 99.6% and 97.8%, and recognition accuracy of 97.3% and 95.5% in office and apartment environments, respectively	Limited to LoS performance and degrades in NLoS scenarios
Shadow & PDs	**ViHand [249]**	Multistatic VLS Unmodulated-passive VLS	Tx: Ambient light & Rx: A platform consist of 3 × 4 array PDs	Recognizing 17 different hand gestures (8 sliding gestures and 9 digital gestures)	Shadow-based RSS (Light Intensity)	100% accuracy for sliding gestures and 82.3% for digital gestures using KNN and dynamic time warping (DTW) algorithms	The proposed system is sensitive to ambient light interference and changes in illumination levels
Shadow & PDs	**FingerLite [97], [250]**	Multistatic VLS Unmodulated-passive VLS	Tx: Ambient light & Rx: 8 PDs on the board	Recognizing seven hand gestures (hand fist, open hand, etc.)	Shadow-based RSS (Light Intensity)	Used ambient light with RNN and FPGA, finding that GRU (Gated Recurrent Unit) provides the best balance with 99.31% accuracy and 0.06s latency	The system is limited to recognizing static motions and can be influenced by illumination and light source location
Shadow & Solar	**Varshney et al. [95]**	Bistatic VLS Unmodulated-passive VLS	Tx: Ambient light & Rx: One solar cell on the floor	Detecting three hand gestures (swipe, two taps, etc.)	Shadow-based RSS (Light Intensity)	Demonstrated the feasibility of solar-based DF-VLS, achieving 100% accuracy in detecting three hand gestures, even under bright light conditions	Further refinement needed for detecting complex gestures and improving efficiency in low-end devices
Reflection & PDs	**Yu et al. [135]**	Monostatic VLS Unmodulated-passive VLS	Tx: One LED & Rx: One PD	Recognizing eight hand gestures (circle, palm hold, etc.)	Reflection-based RSS (Light Intensity)	Achieved 96% accuracy at a 20 cm distance using both VL and infrared sources	The system's performance may vary under different lighting conditions
Reflection & PDs	**Okuli [25]**	Bistatic VLS Modulated-passive VLS (e.g. OOK Modulation)	Tx: One LED & Rx: Two PDs	Finger gestures detection and localization on a 2D plane	Reflection-based RSS (Light Intensity)	1.43 cm error rate in 90% of cases and a median error of 0.7 cm for detecting and positioning random finger gestures	Interference from ambient lighting or reflective surfaces in the environment can cause instability in Okuli
Reflection & PDs	**Webber et al. [253]**	Bistatic VLS Modulated-passive VLS (e.g., arbitrary waveform generator)	Tx: One LED & Rx: One PD	Finger motion classification for five movements	Reflection-based (Light Intensity)	The proposed long short-term memory (LSTM) algorithm achieved an average accuracy of 88% in classifying finger motions	Challenges include off-center hand focus, oversimplified gesture recognition, and neglect of environmental factors
Reflection & PDs	**SemiGest [139]**	Multistatic VLS Modulated-passive VLS	Tx: LED strips with 48 LED chips & Rx: 1 PD co-located with Tx	Recognizing 10 hand gestures (up, down, etc.)	Reflection-based RSS (Light Intensity)	97.5% classification rate	Low accuracy (60%) and reduced reliability with 4 labeled samples per class in SSL approach
Reflection & PDs	**Liang et al. [155]**	Monostatic VLS Modulated-passive VLS	Tx-Rx: VLC-based transceiver	Recognizing 12 hand gestures (up, down, etc.)	Reflection-based (Light Intensity)	95.7% accuracy with SVM, outperforming DT (86.7%) and Random Forest (92.5%)	It requires evaluation under varying ambient light conditions and for multiple gestures by different users
Reflection & PDs	**Liu et al. [259]**	Multistatic VLS Unmodulated-passive VLS	Tx: ambient light Rx:PD arrays	Air-writing digit recognition from fingers of one hand	Reflection-based (Light Intensity)	91% accuracy for air-writing digit recognition	Reducing the size of ConvRNN could degrade the accuracy and performance of the proposed system
Reflection & Solar Cell	**Ma et al. [260]**	Bistatic VLS Unmodulated-passive VLS	Tx: Ambient light & Rx: Transparent solar cells	Recognizing five hand gestures (CloseOpen, LeftRight etc.)	Reflection-based (Light Intensity)	Mean accuracy of 95%	Low light and sudden movements may disrupt system performance
Reflection & Solar Cell	**SolarGest [105], [261]**	Bistatic VLS Unmodulated-passive VLS	Tx: Ambient light & Rx: Three conventional opaque solar cells, alongside two transparent solar cells	Recognizing six hand gestures (up, down, etc.)	Reflection-based (Light Intensity)	96% accuracy, consuming 44% less power than a light sensor-based approach	Its sensing range is limited to only a few centimeters
Reflection & Solar Cell	**SolarSense [154]**	Multistatic VLS Unmodulated-passive VLS	Tx: Ambient light & Rx: Solar cells array	Recognizing 12 activity control gestures (up, down, etc.) and 10 numeric gestures (numbers 1 to 10)	Reflection-based (Light Intensity)	The SVM algorithm achieved 97.4% accuracy for activity control gestures and 98.9% for numeric gestures, outperforming other ML models (e.g., KNN and Random Forest)	It requires evaluation under varying ambient light conditions and for multiple gestures by different users

fluctuating light intensities [246]. Also, enhancing GestureLite to recognize gestures from multiple users simultaneously is imperative, requiring advancements in gesture granularity and hand tracking [246]. Moreover, optimizing PD arrangement is vital for improving GestureLite's performance and accuracy in ambient light-based recognition systems [246].

LiGest (see Table VI), proposed by Venkatnarayan and Shahzad [96], utilizes ambient light for gesture recognition, employing an unmodulated-passive VLS system equipped with 36 light sensors arranged in a square grid on the floor as a multistatic DF-VLS system. LiGest automatically detects gesture start and end times based on threshold crossings in the denoised lighter sensor streams. Upon gesture detection, the system standardizes the streams using a Z-score transform operation [96]. Subsequently, it applies stationary wavelet transform (SWT) and discrete wavelet transform to extract features from the standardized streams for classification using SVM approaches. A prototype of LiGest, developed with commercially available light sensors, underwent extensive evaluation with 20 volunteers, demonstrating an average accuracy of 96.36% [96].

The primary weakness of LiGest [96] is that it demands the entire floor to be equipped with PDs, which not only leads to high deployment costs but also hampers the regular movements of occupants and raises the risk of falls due to tripping over the light sensors [248]. In [248], the authors managed this issue by developing LiGeR, a shadow-based unmodulated-passive VLS system that uses a Hidden Markov

Model-based classification approach for gesture recognition, particularly decreasing the number of light sensors required [248]. LiGeR operates with four light sensors (e.g., TSL237) in office environments and ten in apartment settings for gesture detection, achieving an average gesture recognition accuracy of over 95%. However, it is limited to fixed sensor locations (e.g., LoS) required between Tx and Rx) in a given indoor environment, and its performance can be impacted in NLoS scenarios [248].

ViHand, proposed in [249], is an unmodulated-passive VLS system that uses a shadow-based sensing technique with ambient light to identify movements, such as sliding and digital gestures [249]. This system collects raw gesture signals using a sensing platform consisting of 12 PDs, which then undergo preprocessing (e.g., low-pass filtering, normalization, etc) before being input to the classification stage (e.g., KNN and dynamic time warping) [249]. According to experimental results, ViHand achieved 100% classification accuracy for sliding gestures and 82.3% accuracy for digital gestures [249].

Finally, in [97], [250], the authors proposed FingerLite, an unmodulated-passive VLS system using shadow-based sensing recognizing hand gestures using ambient light. The system consists of an field-programmable gate array (FPGA) development board and uses eight PDs that detect changes in light intensity caused by hand motions [97], [250]. By employing a recurrent neural network (RNN) for different sampling rates and training intensities, FingerLite demonstrated that a gated recurrent unit-based deep learning model can yield an effective balance between an accuracy of more than 99% and a limited latency of 6.22 ms [97], [250]. However, the system is limited to recognizing static motions and can be influenced by illumination and light source location [97], [250].

B. Shadow-Based Using Solar Cells

Varshney et al. [95] proposed an approach for hand gesture recognition utilizing a shadow-based sensing technique [95]. This system utilized one solar panel on the floor and employed an unmodulated light source (e.g., ambient light), for sensing and communication. Functioning as a bistatic DF-VLS system, it enabled unmodulated-passive VLS operation. Through the implementation of a thresholding circuit, the authors successfully detected three distinct hand gestures and senses human presence even in bright light conditions. This circuit, triggered by a hand approaching very close to the solar panel and causing a drop in solar energy below the threshold, facilitated gesture recognition by tallying instances of hand proximity to the panel [95]. The system demonstrated effective operation across diverse light conditions, from 100 lux to 80 kilolux, where traditional VLS designs often encounter issues due to TIA saturation [95]. Overall, this system offers efficient detection of shadow events with sub-μW power consumption and delegates sensor readings to end devices at 20 μW, ensuring energy efficiency. However, limitations include its current focus on simple gestures, the need for enhanced gesture detection at the end-device, challenges in leveraging ambient wireless signals for gesture recognition, and the loss of analog information with digital thresholding circuits, necessitating further optimization for improved performance [95].

C. Reflection-Based Using PD

In the gesture recognition systems discussed above, which utilize shadow-based sensing approaches and either ambient light or LEDs for functioning, there are potential challenges in environments where ambient light fluctuates due to weather changes (e.g., day and nighttime) [72]. The variability in ambient light color and intensity across different weather conditions and times of the day creates diverse lighting scenarios [72]. One potential solution to address this issue is the use of fingerprinting-based passive algorithms, which are expected to offer reliable performance across various conditions [80], [86], [125]. However, implementing such algorithms entails labor-intensive efforts, and lacking data in the fingerprint library for specific lighting conditions may diminish localization accuracy [72], [80], [86], [125]. Moreover, in gesture recognition VLS systems utilizing shadow-based sensing, interference from obstacles between the body and the receiver poses a significant challenge [135]. This interference disrupts captured shadow patterns, affecting accurate gesture detection and interpretation [135]. As a result, incomplete or distorted shadow data may lead to errors in gesture recognition. Hence, the utilization of reflection-based sensing techniques in gesture recognition systems for short distances presents a potential solution to address these issues. As indicated by [251], [252], examining reflected signals is more suitable for tasks requiring short-range interactions, such as gesture recognition [135].

In this context, Yu et al. [135] developed an unmodulated-passive VLS hand gesture recognition system comprising a single PD as the receiver and light sources organized in a monostatic configuration within a limited range of 20–35 cm [135]. As the hand performs different gestures, the PD captures distinct light intensity waves corresponding to variations in hand distance, shape, and scattering characteristics. Following the acquisition of reflected signals during hand gestures, discrete wavelet denoising is employed. A basic thresholding method identifies the start and end points of a gesture [135]. The processed data are then classified into specific gestures using a repository of available gestures selected based on common HCI tasks. For classification KNN exhibited superior performance over SVM in recognizing eight gestures owing to small variations in feature vectors and significant waveform overlap [135]. Assessments involving eight gestures, five subjects, diverse distances, and lighting scenarios utilizing both visible and infrared sources indicated peak performance at a distance of 20 cm, achieving an accuracy of 96% [135]. However, as discussed in the study, the system's accuracy declines as the distance increases due to the reduced intensity of reflected light [135]. Moreover, when ambient lighting is turned off, there is a slight improvement in the system's performance when VL is used for recognition. This enhancement occurs because weaker reflected signals are more susceptible to environmental noise compared to stronger ones. Additionally, factors such as the age, gender, and skin complexion of subjects should also be considered [135].

Zhang et al. [25] proposed the Okuli system for gesture recognition, utilizing VL signals for finger tracking. Okuli operates as a modulated-passive VLS system, employing modulated LED signals through on–off keying (OOK) for interaction with mobile devices. The system comprises a low-power LED and two PDs strategically positioned to detect finger movements, forming a bistatic DF-VLS setup. It incorporates four signal processing modules for channel modeling, ambient light cancellation, finger detection and background removal, and finger localization [25]. Okuli captures reflected RSS samples during the ON period and subtracts them from the OFF period to eliminate ambient light interference. Subsequently, the finger detection module identifies the user's finger presence, triggering the finger localization process. Experimental validation demonstrated Okuli's accuracy, with a 1.43 cm error rate in 90% of cases and a median error of 0.7 cm for random finger positioning [25].

Webber et al. [253], [254], [255] proposed a gesture recognition system designed for VLC infrastructure. They utilized a single LED and PD setup as a modulated-passive VLS system in a bistatic configuration, focusing on tracking the sequence of direct light blockages caused by finger movements. The system was trained to recognize five movements involving an increasing number of fingers [253], [254], [255]. A high sampling rate was necessary to capture the brief duration of light interruption caused by each finger. Modulation was eliminated by sampling the sign maxima, resulting in signals corresponding to the presence of 1–4 fingers [253], [254], [255]. Data processing involved with an LSTM (Long Short-Term Memory) algorithm featuring 50 hidden units, the system achieved an average accuracy of 88% in categorizing finger motions [253], [254], [255]. However, this study requires precise alignment and overlooks the complexity of gestures in sign language and relies on a simplified approach for pattern recognition. Furthermore, environmental factors like sunlight direction and testbed location are not thoroughly explored, leaving gaps in understanding their impact on system performance [253], [254], [255].

Zhu et al. [139] proposed SemiGest, a modulated-passive VLS system using a ring-shaped LED table, consisting of co-located transmitters (e.g., LED strips with 48 LED chips) and one PD, sharing an FPGA-integrated controller detect hand gestures through reflected signals caused by hand motion [139]. To address the large amount of labeled data required for supervised learning [135], [256], SemiGest proposed a semi-supervised learning (SSL) approach, promoting its industrial application [139]. It achieved gesture identification accuracies of 90% and 60%, for 10 and 4 labeled samples per class respectively [139].

In [155], the authors contributed by developing a VLC-based sensing system for hand gesture detection (e.g., 12 distinct categories). This system incorporated a low-cost VLC transceiver setup based on the OpenVLC platform [257] for transmitting and receiving VLC signals, utilizing OOK and Manchester encoding [155]. After obtaining raw reflected signals, Butterworth (BW) filtering was applied for preprocessing, followed by input to ML classification models such as SVM, Random Forest, and decision tree (DT) [155]. Experimental evaluation demonstrated that the SVM model achieved the highest performance, with an accuracy of 95.7%, surpassing DT (86.7%) and random forest (92.5%) performance [155]. However, it should be assessed under varying ambient light conditions and with multiple gestures performed by various users.

Finally, deep learning could automate pattern recognition through neural networks, using specialized architectures like convolutional and recurrent networks for enhanced representation learning [9], [10]. Inspired by the LightDigit study [258], Liu et al. [259] explored air-writing digit recognition using VL [258]. They proposed ViLiT (Visible Light Transformer) and a customized ConvRNN model with attention pooling to analyze spatial and temporal patterns in dynamic shadows for digit recognition [258]. The evaluation of this through-screen fingertip air-writing system showed it could achieve an accuracy of up to 91% [259]. Additionally, the size of the customized ConvRNN model could be reduced by 94% with less than a 10% drop in performance [259]. This investigation underscores the potential of deep learning to enhance VL systems, opening avenues for further exploration [97], [258], [259].

D. Reflection-Based Using Solar Cells

Ma et al. [260] explored the use of transparent solar cells for gesture recognition, aiming to integrate solar energy harvesting into device screens. They developed an unmodulated-passive VLS sensing platform. During testing, a subject performed five different hand gestures repeated 100 times [260], collected data consisted of time series voltage samples, split into individual gesture instances using 1-second windows with 50% overlap. Subsequently, statistical features such as mean, standard deviation, kurtosis, etc, were extracted from each instance to feed the ML classification models such as SVM, KNN, DT, and random forest with parameters optimized for maximum performance. Experimental results demonstrated an average accuracy of 95% in detecting the five hand gestures through 10-fold cross-validation [260]. This study served as a preliminary investigation of the feasibility of using solar cells for VLS gesture recognition [260]. Hence, it is essential to investigate whether solar cells can effectively perform gesture recognition in extremely dark environments, such as dimly lit living rooms or cinemas. Furthermore, given that the output current of solar cells is responsive to incident light intensity, it is imperative to assess and analyze any potential disruptions from nearby movements or abrupt alterations in light intensity during the gesture recognition process [260].

The same researchers, inspired by their prior work [260], developed SolarGest in [105], [261] by employing solar cells for recognizing various hand gestures in a controlled environment under a lamp. SolarGest capitalizes on the unique disruption of incident light rays by each gesture on the solar panel, resulting in a distinct signature in the harvested photocurrent. This unmodulated-passive VLS system consists of three conventional opaque solar cells, alongside two transparent solar cells made from the same organic material but with varying transparencies and thicknesses in a bistatic

DF-VLS setup. When a hand gesture occurs nearby, a solar-powered device captures the photocurrent time-series, precise gesture segmentation is achieved from the signal time-series [105], [261]. Similar to other gesture recognition systems, SolarGest requires users to briefly pause before and after a gesture, facilitated by sliding a temporal window on the denoised signal. After signal processing, SolarGest extracts 22 time and frequency domain features from each detected gesture window for classification. These features are employed for training the KNN and SVM classification model [105]. Through experimental evaluation involving both conventional opaque solar cells and see-through transparent cells, SolarGest successfully detects 96% of gestures from 6,960 samples across 6 different gestures. Interestingly, even with transparent cells, SolarGest consumes 44% less power compared to light sensor-based systems. However, while this work shows promise, it is imperative to investigate the impact of backlight on gesture recognition when employing this system for real-world application [105], [261]. Moreover, its range is limited to only a few centimeters.

Finally, Li et al. [154] proposed SolarSense, a self-powered unmodulated-passive VLS gesture recognition system employing solar cell arrays (e.g., 25 solar cells on a single board). It was designed for sustainable HCI in industrial contexts under everyday lighting conditions (e.g., ambient lighting) [154]. ML models such as KNN, Random Forest, and SVM were used to analyze reflected signals generated by gestures [154]. All models achieved over 96% in accuracy, precision, recall, and F-score for activity control gestures, with SVM reaching 97.4%, and 98.9% accuracy for numeric gestures [154]. [154]. However, the system still needs to be evaluated under varying ambient light conditions and for multiple gestures performed by multiple users.

E. Lessons Learned and Practical Implementation

The review of existing research on DF-VLS-based gesture recognition (summarized in Table VI) highlights that both shadow-based sensing (e.g., GestureLite [246], ViHand [249]) and reflection-based sensing (e.g., SolarGest [105], [261], Okuli [25]) can achieve high accuracy. These systems offer certain advantages over other technologies (e.g., vision-based recognition), such as lower complexity, cost, and energy consumption. However, most studies have been conducted in controlled environments that do not fully reflect real-world conditions, such as fixed ambient lighting [95], [248] and limited gesture-to-Rx distances [139]. Ongoing efforts aim to enable real-world gesture recognition using ML techniques (e.g., KNN [246], SVM [141], [155]) and advanced signal processing (e.g., S-streams [141]). Fluctuations in illuminance or ambient lightingsuch as turning lights on or off or interference from natural light (e.g., through windows)can impact signal patterns and reduce ML classification accuracy, as seen in SemiGest [139], where accuracy dropped from 95% to 85% with changes in illuminance. Additionally, VLS systems typically operate at short distances (cm scale), which poses challenges for detecting distant (e.g., meter-scale) gestures. In [139], accuracy decreased from 86% to 84.75% as the distance increased from 20 cm to 35 cm. Further research is also needed to ensure ML models generalize across users, as shown in SemiGest, where accuracy for one person was 97.5%, but dropped to 83.33% for another user [139].

In shadow-based sensing, the Tx (e.g., LED or ambient light) and the Rx (e.g., PDs or solar cells) are positioned on opposite sides of the gesture (i.e., requiring LoS), with the gesture in between [248]. In reflection-based sensing, the Tx and Rx are co-located (e.g., monostatic), simplifying the setup while maintaining integration [248]. Compared to occupancy detection and localization, the Tx and Rx components in VLS-based gesture recognition are closely spaced, facilitating easier integration for powering the components, as well as collecting and processing the data. Optimizing the number and placement of PDs is crucial for VLS-based gesture recognition systems using PDs arrays [258]. For instance, SolarGest [105] uses a single sensor to capture six basic gestures, whereas LightDigit [258] and [262] require nine and sixteen sensors, respectively, for more complex gestures [258]. The distance between PDs is also critical: if the sensors are too close, gestures may become indistinguishable due to minimal signal time differences; if they are too far apart, gestures may not be fully captured [258].

Utilizing existing VLS sensing methods may pose several challenges for electronic devices [95], [105], [253], [260], [261], [263], [264]. Firstly, these systems consume significant power (e.g., in the range of milliwatts), which can be problematic for battery-powered systems [95], [260], [261], [264]. Additionally, integrating sensors into compact IoT devices requires more space, such as an array of light sensors, complicating the process of device miniaturization [261]. Gesture recognition systems like LiSense [47], StarLight [111], and GestureLite [246] utilize traditional light sensing mechanisms with components (e.g., TIAs, analog-to-digital converters (ADCs), and computational blocks comprising microcontrollers (MCUs) or FPGAs), which hinder widespread adoption [95], [264]. For instance, TIAs are susceptible to saturation under bright light conditions, limiting continuous operation in natural and ambient lighting [95], [260], [264]. Moreover, incorporating these components significantly increases sensor costs, posing challenges for large-scale deployment due to the associated expenses [95], [260], [264]. In response, future IoT devices may adopt solar panels for energy harvesting [95], [253], [260], [261], [263], [264]. These solar cells leverage the photovoltaic effect [265] to convert incident light into electrical current, known as photocurrent. However, most current VLS systems for gesture recognition employ PD receivers due to their higher sensitivity, faster reaction times, and better SNR compared to solar cells.

F. Comparison With Other Technologies

Gesture recognition techniques, particularly for hand movements, are divided into two main groups: DB and DF (e.g., non-contact) sensing methods [135]. Among the latter, popular approaches include RF-based systems such as WiFi (e.g., WiADG [266] employing CSI measurements), RFID (e.g., GRfid using phase information [267]), mmWave (e.g., DFHGR [268]), and UWB (e.g., IR-UWB [269]). These RF systems mainly analyze changes in RSS [270] and CSI [266] values due to gestures, with some also employing software defined radios for measuring finer characteristics like angle of arrival (AoA) (e.g., ArrayTrack [271]) and Doppler shifts (e.g., WiSee [272]). While RF technology shows promise, it is sensitive to channel noise and environmental changes [141]. Its main advantage lies in being non-intrusive, as it does not require video capture or wearable sensors [141].

In addition, camera-based solutions rely on images, as demonstrated in [273], [274], or video-based approaches [275] often employ computer vision algorithms for signal processing, which require substantial amounts of data for training to achieve satisfactory accuracy [141]. Besides, capturing and storing raw camera data raises significant privacy concerns [141]. Sound-based systems, such as LLAP [276], leverage speakers and microphones on mobile devices to figure out hand/finger movements via acoustic phase measurement. Additionally, ultrasonic-based gesture recognition systems (e.g., Dolphin [277]), have demonstrated good accuracy and benefit from immunity to environmental noise. Nevertheless, the frequencies utilized pose potential risks to the well-being of children and pets [135], [278]. Furthermore, Terahertz technology also has possibilities in this field [279].

Lastly, the traditional approach for gesture recognition relies on vision-based techniques (e.g., using images or videos) with FPGA processing [280]. FPGAs are well-suited for this task due to their low power requirements, reconfigurability, and reasonable cost [281]. However, vision-based techniques remain computationally intensive. VLS is being researched as an alternative that is cheaper, less complex, and more energy-efficient. FPGAs could also be applied in this context, as shown in [97], [139].

Last but not least, most existing gesture recognition systems are based on a single technology and can only handle a small number of hand gestures (e.g., around nine) and users (e.g., often less than fifteen) [282]. To address these constraints, cross-technology frameworks may offer a solution by allowing many technologies to be integrated to increase gesture detection capabilities [283].

VI. Exploratory Applications of DF-VLS

This section explores other applications of DF-VLS that warrant further investigation, including both DF-VLS for healthcare applications (e.g., vital signs monitoring, fall detection, etc.) and DF-VLS for vehicular automation.

A. VLS for Healthcare

There exists a notable gap in research regarding DF-VLS in healthcare. This section overviews the few studies focusing on vital sign monitoring and fall detection utilizing DF-VLS systems.

1) Vital Sign Monitoring: Regular monitoring of vital signs (e.g., heart rate, respiration rate) is critical for ensuring timely and accurate assessments of patients' physiological conditions [284], [285]. Within this framework, Abuella and Ekin [284] developed an unmodulated-passive bistatic VLS system tailored specifically for monitoring vital signs and heart rates through reflection-based sensing [284]. Participants were directed to sit facing the VLS setup and breathe naturally while VL was projected onto their chest [284]. As participants inhaled, the intensity of the received light increased, decreasing as they exhaled, thereby generating data showcasing periodic respiration patterns intertwined with heartbeats [284]. The system analyzed these reflected signals (e.g., RSS) using bandpass filters, subsequently transferring them to the frequency domain to pinpoint frequency peaks, thereby discerning respiration and heart rates [284]. The study demonstrated an accuracy rate exceeding 94% across various scenarios, including both breathing and heartbeat rates, surpassing the performance of conventional contact-based vital sign monitoring devices [284]. Additionally, the study found that the standing posture under light conditions exhibited the highest absolute percentage error, approximately 8%, compared to sitting in darkness, sitting in light, and sleeping in light [284].

At the moment, DF-VLS for vital signs monitoring is a freshly developed technique and is still confined to highly controlled scenarios, demanding further investigation to properly understand its limitations [284], [286]. DF-VLS is sensitive to variations in ambient illumination during data collection, which must be minimizedfor reliable data extraction [286]. In addition, this approach is not feasible at night without active light sources and may be affected by interference from other light sources [286], [287], [288], [289]. Also, its success depends on recognizingthe optoelectronicrelations, including the quantitative elements of light intensity, receiver sensitivity, and the features of the individual under test (e.g., clothes, skin color, blankets, and bedding) [284], [286].

2) Fall Detection: Majeed and Hranilovic [119] proposed a passive fall detection system based on DF-VLS within a realistically simulated indoor environment. This system employs neural networks to predict the output state of a target individual. Operating as an unmodulated-passive VLS monostatic system, it features luminaires and receivers positioned together on the ceiling [117], [118]. The methodology involves simulating a set of CIRs between various source-receiver pairs within the stduy area, corresponding to either upright or prone states of the target [119]. Then, through the neural network architecture, the study establishes the correlation between the simulated CIRs and the target's states [119]. By scrutinizing the nuances within the CIR waveforms, the proposed method effectively discerns between prone and non-prone states [119]. The study also evaluates the method's robustness, particularly when excluding one of the non-prone states (e.g., tilted) from the network training [119]. Results indicate an accuracy surpassing 97% when utilizing a large number of training samples, with luminaires set to full brightness. It is important to note that this approach assumes the presence of a person within the room, differing from occupancy sensing methods that primarily focus on detecting human presence within the room [119].

In [290], LiFall was developed as a wall-mounted unmodulated-passive VLS system using ceiling-mounted

LEDs and open VLC devices placed on a table to simulate the transmission of VLC signals for fall detection [290]. This system is based on RSS signals obtained from both LoS (e.g., unobstructed light) and NLoS (e.g., reflected light) conditions, which are affected by human body movements (e.g., walking, sitting, and picking up objects) [290]. LiFall was tested in real-world settings in two environments: a laboratory (with greater complexity than a classroom) and a classroom with four people (three males and one female) [290]. After processing the raw RSS signals (with a combination of BW and Savitzky-Golay (SG) filters) and feature extraction, random forest and SVM classifiers were tested. Real-world experiments showed that random forest performed better than SVM and was also less sensitive to environmental changes, with fall detection accuracy of over 90% [290]. Under environmental changes, the proposed system maintained a sensitivity of over 95% [290]. However, this system was evaluated under fixed illuminance conditions and needs further investigation to assess its performance under variable illuminance. Additionally, the subtle characteristics of human activity signals differ under changing NLoS conditions, which could lead to performance degradation [290].

B. VLS for Vehicular Automation

According to [291], there is a need to implement Industrial Internet of Things (IIoT) applications to support industrial goals centered around sustainability and energy efficiency. This is essential for addressing the anticipated rise in energy consumption and the growing volume of electronic waste generated by batteries, sensors, and accumulators widely used in sensing and communication applications [291], [292]. DF configurations, including those associated with the concept of "green IoT," have the potential to mitigate environmental consequences, with VL technologies emerging as a viable option in this context [291], [292], [293]. While the integration of DF-VLS systems in the vehicular automation sector is still in its infancy, there is existing literature on this topic.

1) VLS for Vehicle Speed Estimation: Several investigations as reported in [287], [288], [289], have looked into the potential for estimating vehicle speed in the DF-VLS framework [287], [288], [289]. These studies simulated different situations and assessed the accuracy of speed estimation, taking into account aspects such as continuous vehicle velocity and alignment of the vehicle headlight and roadside light sensor at the same heights [287], [288], [289]. The results obtained demonstrate that DF-VLS, especially with vehicle headlamps, is a potential candidate alternative to standard RADAR/LiDAR-based speed estimation techniques [287], [288], [289]. Specifically, the study [287] proposed Visible Light Detection and Ranging (ViLDAR), a new system for estimating speed that capitalizes on fluctuations in VL emitted by a vehicle's headlamp acting as a transmitter [287], [288], [289]. They initially built a model for how light propagates in the environment for vehicle sensing and communication, based on the mentionedassumptions [287], [288], [289]. Their study concluded that the irradiance angle (e.g., ϕ) and incident angle (e.g., θ) became comparable under particular circumstances [287], [288], [289]. When the vehicle's headlights and light sensor are at the same height, the distance between two headlights is small, and the angles become negligible when the detector is close tothe road and the vehicle itself is far away [287], [288], [289]. They claim that with knowledge of the path loss model and received power values at different points in time, the received power can be utilizedfor determining distance values [287], [288], [289]. Employingthe difference in distance and time between two measurements allows for instantaneous speed estimate, which is the core technique of speed estimation utilizingVLS [287], [288], [289]. The performance of the ViLDAR system was assessed in a variety of road conditions, including both straight and curved pathways [287], [288], [289]. Results from the simulation demonstrate that using received light intensity from a vehicle's headlight allows for valid speed estimation, achieving over 90% accuracy across a broader range of incidence angles (up to 70-80% of the simulation's duration) [287], [288], [289]. A comparison of ViLDAR and RADAR systems revealed that the latter performed poorly in settings with rapidly changing incidence angles, but ViLDAR showed promise. Despite encouraging results, this work is still restricted to simulations and requires further investigation in actual situations, particularly in open-sky and urban environments [287], [288], [289].

2) VLS for Vehicle Detection and Traffic Monitoring: Xue et al. [294] proposed a bistatic unmodulated-passive VLS system for vehicle detectionand traffic flow monitoring employing sunlight. By implementing a simple amplification circuit connected to the power supply of streetlights, the LED array within these lamps functions as a light sensor, detecting variations in ambient light intensity triggered by passing vehicles. Following capturing and smoothing the reflected signals, they are used as input for the SVM classification method. To evaluate the system's accuracy, the researchers constructed an indoor testing setting and employed the SVM algorithm. However, future efforts should focus on implementing the system in outdoor settings and expanding its utility to include additional intelligent systems that rely on traffic flow monitoring [294].

VII. Open Challenges and Future Roadmap

A. Open Challenges

1) Issues in Shadow-Based DF-VLS: The main challenges in shadow-based DF-VLS systems include shadow interference in multi-target DFL systems, which occurs when targets are in close proximity and makes it difficult to distinguish between the signals from multiple targets. Additionally, LoS blockage caused by unexpected obstacles, such as moving objects in industrial environments (e.g., IIoT), can suddenly obstruct the LoS between Tx and Rx, disrupting the sensing of the target object.

2) Challenges in Reflection-Based DF-VLS:

a) Limited sensing range: Reflection-based VLS systems face limitations due to the rapid attenuation of reflected VL signals. This attenuation limits the effective sensing range—i.e., the maximum distance from the target to

TABLE VII
OVERVIEW OF EXPLORATORY IoT APPLICATIONS ENABLED BY DF-VLS SYSTEMS

	Scheme	VLS Type & Configuration	VLS Hardwares (Tx vs. Rx)	Design Goal(s)	VLS Sensing Technique & Feature	Key Contributions	Limitations
Healthcare	**Abuella et al. [284]**	Bistatic VLS Unmodulated-passive VLS	Tx: One fixed power LED Rx: one PD in front of human subject	Vital signs (respiration and heartbeat) monitoring	Reflection-based RSS (Light intensity)	Accuracy exceeding 94%	Real-World validation needed (e.g., dynamic environments)
Healthcare	**Majeed et al. [119]**	Monostatic VLS Unmodulated-passive VLS	Tx-Rx: Several co-located LED & PD on the ceiling	Human fall detection	Reflection-based CIR (Light intensity)	Accuracy exceeding 97% in detecting human falls	Real-World validation needed
Healthcare	**LiFall et al. [290]**	Multistatic VLS Unmodulated-passive VLS	Tx-Rx: LEDs on the ceiling & OpenVLC on a table & PDs on the wall	Human fall detection	Shadow- and Reflection-based RSS (Light intensity)	Accuracy exceeding 90% in detecting human falls	Performance degraded in environmental changes
Vehicular Automation	**ViLDAR [287]**	Bistatic VLS Unmodulated-passive VLS	Tx:Vehicle's headlamp & Rx: One PD	Vehicle speed estimation	Reflection-based RSS (Light intensity)	Estimation accuracy decreased from 100% to 10% as the incidence angle rose from 0° to 75° and from 100% to 85% as SNR dropped from 45 dB to 30 dB. At a 50° incidence angle, a 90% accuracy in 0.3 seconds, outperforming RADAR/LiDAR (62%)	Real-World validation needed
Vehicular Automation	**Xue et al. [294]**	Bistatic VLS Unmodulated-passive VLS	Tx: Ambient light & Rx: One LED	Vehicle detecion & Traffic flow monitoring	Reflection-based RSS (Light intensity)	Within the $[0, 1]$ voltage threshold interval, SVM achieved over 95% accuracy in detecting and monitoring vehicle movement under LED streetlights	Real-World validation needed

the receiver at which detection remains feasible—to distances typically ranging from a few centimeters to several meters [37], [45], [125], [295], [296].

b) Object properties recognizing: Unlike DB-VLP configurations, DF-VLS relies on sensing through the external surfaces of objects [9], [10], [37], [45]. The efficacy and design of this approach are heavily influenced by the inherent properties of the object, including its shape, size, color, reflection coefficient, and even its movement direction [9], [10], [37], [45]. The shape of the object determines the trajectory of reflected light, while its size affects the extent of light obstruction. Additionally, variations in object color and reflection coefficient produce unique RSS patterns, impacting object recognition [9], [10], [37], [45], [82]. These diverse considerations highlight the absence of a standardized object model for sensing applications [9], [10], [37], [45]. The primary challenge lies in understanding the specific characteristics of the object under observation and designing VLS systems capable of accurately sensing and identifying a broad array of objects with varied shapes, sizes, colors, surface textures, chemical makeup, and reflective properties [9], [10], [37], [45], [297], [298], [299], [300].

3) Impact of Ambient Light and VL Interference on DF-VLS Performance: VL interference can be caused by other light sources (outside light, non-VLS light sources, or other dedicated VLS sources in the area) or by the propagation medium itself (e.g., scattering due to dust, smoke, or mist) [45]. Outside light is usually sunlight or daylight, whose intensity can fluctuate significantly throughout the day [45], [86]. VLS and non-VLS sources include artificial lighting, such as fluorescent, LED, and incandescent lights, and their interference can be reinforced by reflections (e.g., from walls, glass, polished floors, metallic surfaces, ceilings, etc.). VL interference is generally less severe than RF interference due to its shorter range and localized nature, i.e., it does not penetrate through walls, but it can also be very pronounced in specific settings, such as rooms with many light sources or areas exposed to fluctuating sunlight. Note that the term ambient light' usually refers to (unmodulated) light naturally present in the area, and is either considered as interference, or as intended for VLS usage (in which case it is not considered as interference). VL interference remains a critical concern in environments requiring precise light-based communication or sensing [301], [302], [303], [304], [305], [306]: it can saturate the photodetector, reduce the SNR, distort the signal (e.g., in scenarios with significant reflection), and eventually impact the performance of RSS-based approaches (e.g., decreased positioning accuracy, faulty occupancy detections, etc.). Ambient light can be particularly challenging as it varies over space and (relatively randomly) over time [307], which can affect DF-VLS performance (e.g., EyeLight requires recalibration multiple times a day [125]). Most systems developed in this context have been tested in environments with minimal or no variation in ambient light (e.g., no windows or at night [81], [86]) or under controlled lighting conditions. When striving for commercial adoption of DF-VLS systems, it is crucial to minimize possible interference or mitigate its impact. Possible approaches are signal processing based (see Section VII-B2) or involve adjusting PD placement (see Section VII-B1).

4) Cost and Performance Trade-Offs in DF-VLS Systems: In DF-VLS systems, where Rx devices are placed at predefined locations (e.g., fixed PDs on walls [81], floors [47], or ceilings [37], [45]), Rx can only provide information when targets (e.g., individuals) move through the PDs's FoV [9], [10], [37], [45]. Achieving full coverage of the study area often requires a dense array of PDs installed at optimal locations, significantly increasing costs. For example, LiSense employs 324 PDs on the floor to achieve full coverage [47]. This challenge becomes even more pronounced in environments such as IIoT settings, where objects (e.g., forklifts) or people frequently move, and in office environments with continuous human activity. Such scenarios can impact DF-VLS performance (e.g., in shadow-based VLS), as its accuracy is influenced by the properties of the object's shadow [9], [10]. These properties fluctuate as the object moves, necessitating the use of multiple light sensors, which further increases the sensing cost.

B. Roadmap for DF-VLS

This section will shed light on some promising research directions in DF-VLS, some of which directly address one or more of the aforementioned challenges.

1) Physical Tx and Rx Deployment Strategies: A first research topic relates to the optimal placement, orientation, and configuration of Tx and Rx. Intelligently placing LEDs and/or PDs at well-chosen locations and tilts can improve the system's spatial discrimination capabilities and overall accuracy of shadow-based DF-VLS (e.g., in multi-target DFL). It can provide redundant detection links in case of unforeseen LoS blockages.

Further, utilizing multiple PDs with different tilting directions and/or FoVs could extend the reflection-based DF-VLS sensing range by capturing light signals from a wider array of angles or limiting exposure to interfering light. However, this approach can be costly and requires further investigation to balance cost and accuracy [9], [10], [37], [45]. To overcome the challenge of costly and dense PD deployment in DF-VLS systems, algorithms for careful planning of PD and LED placement are essential [9], [10], [37], [45]. By optimizing sensor locations, tilts, and FoVs, it could be possible to minimize the number of PDs while still ensuring effective coverage range [9], [10], [37], [45]. In dynamic environments, adaptive placement techniques might help optimize PD positions in response to changing conditions. Furthermore, using higher-intensity light sourcessuch as brighter LEDs, LEDs with greater transmit power, laser diode arrays, or integrated lenses for focused lightcan expand the range of the DF-VLS system, though considerations around power consumption, heat dissipation, and safety remain crucial [308].

Some approaches have investigated LED designs specifically tailored to their applications. For instance, LiSense [47], which leverages shadow-based DF-VLS for 3D human skeleton posture reconstruction, utilizes five customized ceiling LEDs arranged in a cross-like pattern to mitigate shadow interference (e.g., separating light from different LEDs and ambient light) [47]. In [25], Okuli used a customized LED with a narrower (e.g., 30°) vertical FoV mounted on a custom-designed structure to control the light reflected by a finger on a tracking pad, improving the sensing range and mitigating multipath interference [25]. However, this approach requires careful consideration of the associated costs [9].

2) Signal Processing and ML Techniques for DF-VLS: Further enhancements can also be applied to the level of processing in a DF-VLS system, either through traditional signal processing or ML techniques.

a) Signal processing techniques: Advanced signal processing algorithms (e.g., combined with ML-based feature extraction techniques) are essential for extracting relevant information from received signals e.g., in the exploration of multi-target DFL using VLS for mitigating shadow interferences problems.

In reflection-based VLS, techniques such as noise cancellation [296] and filtering algorithms are instrumental in handling low SNR and enhancing detection range and accuracy. Furthermore, integrating DF-VLS with other sensing modalities (e.g., infrared or ultrasonic sensing) offers an opportunity to expand its capabilities and sensing range [309], but requires the design of advanced hybrid signal processing algorithms.

Signal processing approaches could also mitigate VL interference. Changes in light levels due to DF-VLS operation are usually either faster than those due to external changes in sunlight or more continuous in nature than those caused by switching on/off other light sources, particularly for reflection-based systems. Background subtraction methods (e.g., the ΔRSS [37], [45]) can aid in isolating modulated or unmodulated signals from slowly changing ambient light sources, thereby maintaining VLC and VLS performance [125], [127], [139], [150]. In the case of modulated DF-VLS, distinct frequency bands can be separated, and direct current light can be filtered out.

b) ML and artificial intelligence (AI) integration: ML and artificial intelligence (AI) approaches have the potential to address several of aforementioned challenges. E.g., ML may be explored to determine the minimum number and optimal placement of PDs to minimize shadow interference (e.g., in multi-target DFL) and LoS blockage in shadow-based DF-VLS.

A particular challenge where ML approaches could be useful, is identifying object properties in both modulated and unmodulated DF-VLS (e.g., reflection-based) systems [25], [125], [127], [150]. Furthermore, ML algorithms may be employed to facilitate object identification by learning distinct characteristics and patterns associated with various objects in training data [9], [10]. For DFL, ML algorithms might be designed to predict the precise location or movement of different objects within the system's FoV. Anomaly detection models could also be investigated to enhance security by identifying unusual patterns or events [9], [10]. Additionally, ML techniques should be assessed to optimize system parameters, such as adjusting sensitivity levels, filtering mechanisms, and other settings to improve overall performance [9], [10].

Finally, strategies such as incorporating convex lenses with different refractive indices for various wavelengths [310] or utilizing multiple PDs with different wavelength ranges [311] may be tested as inputs for ML techniques to improve system performance. These approaches are worth investigating to mitigate the effects of variable object properties, thereby enhancing the overall performance of reflection-based DF-VLS systems in diverse environments [9], [10].

3) Reconfigurable Intelligent Surfaces (RISs) and Mirrors: Optical reconfigurable intelligent surfaces (RISs) generally use passive elements like metasurfaces, mirror arrays, and liquid crystals (LCs) [312]. These elements dynamically guide and control incident light based on Snell's law, enhancing overall performance in VLC [312], [313], [314], [315]. In VLC, optical RISs have primarily been studied to address receiver orientation and LoS light-blocking issues [312], [313], [314], [315]. However, they can also potentially be used to manage unwanted (sudden) blockages (e.g., from tables, moving objects, etc.) by redirecting the transmitted signal toward the receiver through strategic RIS deployment in the environment [312], thereby enhancing shadow-based VLS performance for sensing the intended target objects.

Optical RISs (e.g., LC-enabled RIS) use low-loss materials at reflection points, enabling efficient signal transitions (e.g., incident light steering and intensity amplification [316]) and achieving higher SNR at the PD compared to standard wall reflections [313], [314], [315]. This capability makes RISs promising for extending both coverage and sensing range in reflection-based VLS. Finally, micro-electro-mechanical systems mirror-based RISs [312], which reflect all incident light with the same intensity (i.e., no absorption), along with other benefits detailed in [317], can be used in the environment with optimized orientation angles (e.g., yaw and roll [312]) to potentially enhance the sensing range.

4) Integrated Sensing and Communication (ISAC) in DF-VLS: We are entering an era where passive object sensing could be seamlessly integrated with active positioning and communications, fostering reciprocal mutual benefits. Recent advancements in both cellular (fifth-generation wireless networks (5G) and 6G) and non-cellular systems (e.g., 802.11bf) showcase a growing focus on integrated sensing and communication (ISAC) functionality, as it can reduce costs in the long term.

While DF-VLS technology remains in its nascent stages, the pioneering work of Zhou et al. [115] introduced the concept of ISAC systems through their iVLC proposal. This innovative approach extends VLC for sensing applications, marking a significant advancement in smart space technology. By repurposing light for both communication and sensing tasks, iVLC could integrate seamlessly into smart environments, enabling transformative interactions for users. One of the key features of iVLC is its ability to provide reliable VLC networking for mobile users across a room. Concurrently, the system utilizes light sensors embedded in the floor to measure the illumination levels from each light source, facilitated by embedded beacons. This data is then leveraged to generate shadow maps, enabling efficient tracking of user mobility within the environment [115]. The integration of DF-VLS and VLC presents a novel research area with the potential to unlock innovative applications and advancements in both sensing and communication, demanding further exploration to optimize performance and uncover new use cases. More recently, lighting, sensing, and communication (LiSAC), derived from ISAC and proposed in Liang et al. [153], aims to integrate lighting, sensing, and communication into a unified system. This concept represents a promising advancement in the evolving landscape of wireless communication.

Amjad et al. [318] evaluated the visible light communication and sensing (VLCS) system for IIoT applications, serving communication and vibration sensing purposes in structural health monitoring [318]. Dark Light Communication (DarkVLC) was incorporated to boost communication throughput, and its impact on the frequency sensing capacity of the VLCS system was explored [318]. This modulated-passive VLS system employs LED arrays using differential binary phase shift keying for baseband modulation and demodulation of the input bitstream. Meanwhile, PDs, arranged in a bistatic configuration, serve for sensing (strobing) signal pulses to determine the vibration frequency of observed machinery. The maximum achievable data rate with the current setup could reach 640 kbit/s with 100% dark light communication intensity. In a similar context of machinery vibration sensing and communication, Gokarn and Misra [319] developed VibranSee, a modulated-passive VLS system. This system utilizes OOK modulation for transmitting light signals, serving both sensing and communication purposes within a bistatic configuration. Through experimental evaluation, they demonstrated that VibranSee achieves a VLC data throughput that is ideally only 18.6% lower (and 23.9% lower for a functional prototype) than the maximum communication rate. Additionally, it may accurately infer over 96.6% (100% for the prototype) of possible vibration frequencies.

5) Current Status and Commercial Viability of DF-VLS Technology: Current commercial DF-VLS systems are relatively simple in their functionality. A notable example is the ALS, which is already present in many smartphones, for detecting ambient brightness and automatically adjusting the screen brightness accordingly [320]. In smart homes, Philips Hue lamps offer another example, providing adjustable lighting that responds to environmental changes and user presence [321]. These systems primarily focus on basic tasks, such as adjusting brightness or color, enhancing energy efficiency, and improving user comfort [321].

The commercial viability of DF-VLS technology for more complex applications discussed in Section II-D depends for a large part on addressing the challenges discussed in Section VII-A to make DF-VLS systems more robust and mature. Compared to RF-based systems, DF-VLS offers a more cost-effective solution, making it particularly appealing for budget-conscious applications. For instance, a study detailed in [149] benchmarked RF-based approaches using WiFi and UWB for occupancy estimation. It showed that DF-VLS is a competitive option, providing accuracy comparable to that of RF-based systems but at a fraction of the cost [149].

VIII. Conclusion

This survey explored recent advances in device-free (DF) visible light sensing (VLS) systems, highlighting their potential to facilitate various Internet of Things (IoT) applications within the framework of sixth-generation wireless networks (6G). We provided an in-depth overview of the DF-VLS system taxonomy and proposed a redefinition of VLS systems based on the DF and device-based concepts prevalent in the literature. The components of VLS systems were examined, focusing on sensing techniques rooted in visible light—such as shadow- and reflection-based methods—and key configuration setups like monostatic and bi-/multistatic systems.

Our investigation into DF-VLS applications for IoT systems concentrated on three extensively researched areas: occupancy detection, gesture recognition, and passive target localization and tracking, commonly referred to as device-free localization (DFL). In occupancy detection, we found that DF-VLS systems primarily rely on ceiling-mounted reflection-based sensing, wall-mounted reflection and shadowing, and floor-mounted shadow signals. Most studies on passive target localization focus on single targets, with less attention given to multi-target positioning due to complexities such as shadow interference when targets are in close proximity. For gesture recognition, both shadow- and reflection-based approaches using photodiodes and solar cells were explored. Additionally, we identified three emerging DF-VLS applications—fall detection, vital sign monitoring, and vehicular applications (e.g., vehicle speed estimation)—which are mainly investigated through simulations, indicating a need for further real-world exploration.

Finally, we identified several open challenges in DF-VLS, including shadow interference and line-of-sight (LoS) blockages in shadow-based DF-VLS, the limited sensing range and object recognition difficulties in reflection-based DF-VLS, the impact of ambient light and visible light interference on sensing performance, and balancing cost and performance trade-offs. Potential research pathways relate to optimizing physical transmitter and receiver deployment strategies, advancing signal processing and machine learning techniques, integrating sensing and communication (ISAC) capabilities, and leveraging reflecting intelligent surface (RIS)-assisted platforms for DF-VLS IoT applications.

List of Acronyms

2D two-dimensional
3D three-dimensional
5G fifth-generation wireless networks
6G sixth-generation wireless networks
ADC analog-to-digital converter
AI artificial intelligence
ALS ambient light sensor
AMTP adaptive multi-target positioning
BLE bluetooth low energy
BW Butterworth
CDF cumulative distribution function
CF characteristic frequency
CIR channel impulse response
cm centimeters
CNN convolutional neural networks
CSI channel state information
DAQ data acquisition
DB device-based
DFL device-free localization
DFWS device-free wireless sensing
DF device-free
DLS dynamic lighting system
DT decision tree
DWT discrete wavelet transform
FDM frequency division multiplexing
FFT Fast Fourier transform
FMCW frequency modulated continuous wave
FoV field of view
FPGA field-programmable gate array
GL geometrical localization
HCI human-computer interaction
HVAC heating, ventilation, and air conditioning
IIoT Industrial Internet of Things
IoT Internet of Things
IR impulse response
ISAC integrated sensing and communication
KL Kullback-leibler
KNN K-nearest neighbor
LC liquid crystal
LED light emitting diode
LiDAR light detection and ranging
LiSAC lighting, sensing, and communication
LoS line of sight
LSI light spectral information
MHz megahertz
MLE maximum likelihood estimation
ML machine learning
mmWave millimeter wave
MSE mean squared error
NIR near-infrared
NLoS none line of sight
OOK on–off keying
OWC optical wireless channel
PDF probability density function
PD photodiode
PIR passive infrared sensor
RADAR radio detection and ranging
RBS reflection-based sensing
RFID radio-frequency identification
RF radio frequency
RGB red, green and blue
RIS reconfigurable intelligent surface
RNN recurrent neural network
RSS received signal strength
Rx receiver
SBS shadow-based sensing
SNR signal-to-noise ratio
SSL semi-supervised learning
SVM support vector machine
SVR support vector regression
SWT stationary wavelet transform
TDM time-division multiplexing
TIA transimpedance amplifier
ToA time-of-arrival
Tx transmitter
uVLP unmodulated visible light positioning
UV ultraviolet
UWB ultraWide band
VLBC visible light backscatter communication
VLBP visible light backscatter positioning
VLB visible light backscattering
VLCS visible light communication and sensing
VLC visible light communication
VLP visible light positioning
VLS-RCNN VLS-Region Convolutional Neural Network
VLS visible light sensing
VL visible light
WiFi wireless fidelity
WoW watchers on the wall
WSN wireless sensor network

Acknowledgment

The authors would like to thank *Jeroen Van der Straeten* for his valuable assistance during the preparation of this manuscript.

References

[1] C. De Lima et al., "Convergent communication, sensing and localization in 6G systems: An overview of technologies, opportunities and challenges," *IEEE Access*, vol. 9, pp. 26902–26925, 2021. [Online]. Available: http://dx.doi.org/10.1109/ACCESS.2021.3053486

[2] M. Youssef, M. Mah, and A. Agrawala, "Challenges: Device-free passive localization for wireless environments," in *Proc. ACM 13th Annu. Int. Conf. Mobile Comput. Netw. (MobiCom/MobiHoc)*, Sep. 2007, pp. 222–229. [Online]. Available: http://dx.doi.org/10.1145/1287853.1287880

[3] S. Denis, R. Berkvens, and M. Weyn, "A survey on detection, tracking and identification in radio frequency-based device-free localization," *Sensors*, vol. 19, no. 23, p. 5329, Dec. 2019. [Online]. Available: http://dx.doi.org/10.3390/s19235329

[4] R. C. Shit et al., "Ubiquitous localization (UbiLoc): A survey and taxonomy on device free localization for smart world," *IEEE Commun. Surveys Tuts.*, vol. 21, no. 4, pp. 3532–3564, 4th Quart., 2019. [Online]. Available: http://dx.doi.org/10.1109/COMST.2019.2915923

[5] S. Palipana, B. Pietropaoli, and D. Pesch, "Recent advances in RF-based passive device-free localization for indoor applications," *Ad Hoc Netw.*, vol. 64, pp. 80–98, Sep. 2017. [Online]. Available: http://dx.doi.org/10.1016/j.adhoc.2017.06.007

[6] J. Wang, Q. Gao, M. Pan, and Y. Fang, "Device-free wireless sensing: Challenges, opportunities, and applications," *IEEE Netw.*, vol. 32, no. 2, pp. 132–137, Mar./Apr. 2018. [Online]. Available: http://dx.doi.org/10.1109/MNET.2017.1700133

[7] F. Alam, N. Faulkner, and B. Parr, "Device-free localization: A review of non-RF techniques for unobtrusive indoor positioning," *IEEE Internet Things J.*, vol. 8, no. 6, pp. 4228–4249, Mar. 2021.

[8] J. Xiao, Z. Zhou, Y. Yi, and L. M. Ni, "A survey on wireless indoor localization from the device perspective," *ACM Comput. Surveys*, vol. 49, no. 2, pp. 1–31, Jun. 2016. [Online]. Available: http://dx.doi.org/10.1145/2933232

[9] Q. Wang and M. Zuniga, "Passive visible light networks: Taxonomy and opportunities," in *Proc. Workshop Light Up IoT (MobiCom)*, vol. 201, Sep. 2020, pp. 42–47. [Online]. Available: http://dx.doi.org/10.1145/3412449.3412551

[10] J. Singh and U. Raza, "Passive visible light positioning systems: An overview," in *Proc. ACM Workshop Light Up IoT (MobiCom)*, Sep. 2020, pp. 48–53. [Online]. Available: http://dx.doi.org/10.1145/3412449.3412553

[11] H. F. T. Ahmed, H. Ahmad, and C. V. Aravind, "Device free human gesture recognition using Wi-Fi CSI: A survey," *Eng. Appl. Artif. Intell.*, vol. 87, Jan. 2020, Art. no. 103281. [Online]. Available: http://dx.doi.org/10.1016/j.engappai.2019.103281

[12] A. Shastri et al., "A review of millimeter wave device-based localization and device-free sensing technologies and applications," *IEEE Commun. Surveys Tuts.*, vol. 24, no. 3, pp. 1708–1749, 3rd Quart., 2022. [Online]. Available: http://dx.doi.org/10.1109/COMST.2022.3177305

[13] C. Mariotti, G. Orecchini, M. Virili, F. Alimenti, and L. Roselli, "Wireless localization in buildings by smart tiles," in *Proc. IEEE Workshop Environ. Energy Struct. Monit. Syst. (EESMS)*, Sep. 2012, pp. 1–9. [Online]. Available: http://dx.doi.org/10.1109/EESMS.2012.6348398

[14] Z. D. Tekler, R. Low, C. Yuen, and L. Blessing, "Plug-mate: An IoT-based occupancy-driven plug load management system in smart buildings," *Building Environ.*, vol. 223, Sep. 2022, Art. no. 109472. [Online]. Available: http://dx.doi.org/10.1016/j.buildenv.2022.109472

[15] T. Fryza, T. Bravenec, and Z. Kohl, "Security and reliability of room occupancy detection using probe requests in smart buildings," in *Proc. IEEE 33rd Int. Conf. Radioelektronika (RADIOELEKTRONIKA)*, Apr. 2023, pp. 1–6. [Online]. Available: http://dx.doi.org/10.1109/RADIOELEKTRONIKA57919.2023.10109085

[16] U. M. Khan, Z. Kabir, and S. A. Hassan, "Wireless health monitoring using passive WiFi sensing," in *Proc. IEEE 13th Int. Wireless Commun. Mobile Comput. Conf. (IWCMC)*, Jun. 2017, pp. 1771–1776. [Online]. Available: http://dx.doi.org/10.1109/IWCMC.2017.7986552

[17] W. Cao, X. Liu, and F. Li, "Robust device-free fall detection using fine-grained Wi-Fi signatures," in *Proc. IEEE 2nd Adv. Inf. Technol. Electron. Autom. Control Conf. (IAEAC)*, Mar. 2017, pp. 1–9. [Online]. Available: http://dx.doi.org/10.1109/IAEAC.2017.8054245

[18] A. Shojaei-Hashemi, P. Nasiopoulos, J. J. Little, and M. T. Pourazad, "Video-based human fall detection in smart homes using deep learning," in *Proc. IEEE Int. Symp. Circuits Syst. (ISCAS)*, May 2018, pp. 1–5. [Online]. Available: http://dx.doi.org/10.1109/ISCAS.2018.8351648

[19] Y. Bai, Z. Wang, K. Zheng, X. Wang, and J. Wang, "WiDrive: Adaptive WiFi-based recognition of driver activity for real-time and safe takeover," in *Proc. IEEE 39th Int. Conf. Distrib. Comput. Syst. (ICDCS)*, Jul. 2019, pp. 901–911. [Online]. Available: http://dx.doi.org/10.1109/ICDCS.2019.00094

[20] Q. Xu, B. Wang, F. Zhang, D. S. Regani, F. Wang, and K. J. R. Liu, "Wireless AI in smart car: How smart a car can be?" *IEEE Access*, vol. 8, pp. 55091–55112, 2020. [Online]. Available: http://dx.doi.org/10.1109/ACCESS.2020.2978531

[21] H. Song, B. Wei, Q. Yu, X. Xiao, and T. Kikkawa, "WiEps: Measurement of dielectric property with commodity WiFi device—An application to ethanol/water mixture," *IEEE Internet Things J.*, vol. 7, no. 12, pp. 11667–11677, Dec. 2020. [Online]. Available: http://dx.doi.org/10.1109/JIOT.2020.2999210

[22] Y. Gu, Y. Zhu, J. Li, and Y. Ji, "WiMate: Location-independent material identification based on commercial WiFi devices," in *Proc. IEEE Global Commun. Conf. (GLOBECOM)*, Dec. 2021, pp. 1–6. [Online]. Available: http://dx.doi.org/10.1109/GLOBECOM46510.2021.9685094

[23] P. H. Pathak, X. Feng, P. Hu, and P. Mohapatra, "Visible light communication, networking, and sensing: A survey, potential and challenges," *IEEE Commun. Surveys Tuts.*, vol. 17, no. 4, pp. 2047–2077, 4th Quart., 2015. [Online]. Available: http://dx.doi.org/10.1109/COMST.2015.2476474

[24] M. H. Ullah, G. Gelli, and F. Verde, "Visible light backscattering with applications to the Internet of Things: State-of-the-art, challenges, and opportunities," *Internet Things*, vol. 22, Jul. 2023, Art. no. 100768. [Online]. Available: http://dx.doi.org/10.1016/j.iot.2023.100768

[25] C. Zhang, J. Tabor, J. Zhang, and X. Zhang, "Extending mobile interaction through near-field visible light sensing," in *Proc. 21st Annu. Int. Conf. Mobile Comput. Netw. (MobiCom)*, Sep. 2015, pp. 345–357. [Online]. Available: http://dx.doi.org/10.1145/2789168.2790115

[26] A. Behravan et al., "Positioning and sensing in 6G: Gaps, challenges, and opportunities," *IEEE Veh. Technol. Mag.*, vol. 18, no. 1, pp. 40–48, Mar. 2023. [Online]. Available: http://dx.doi.org/10.1109/MVT.2022.3219999

[27] IEEE EMBS Committee on Man and Radiation, "Radiofrequency interference with medical devices. A technical information statement," *IEEE Eng. Med. Biol. Mag. Quart. Mag. Eng. Med. Biol. Soc.*, vol. 17, no. 3, pp. 111–114, 1998. [Online]. Available: https://pubmed.ncbi.nlm.nih.gov/9604711/

[28] J. Cho, J. H. Park, J. K. Kim, and E. F. Schubert, "White light-emitting diodes: History, progress, and future," *Laser Photon. Rev.*, vol. 11, no. 2, Mar. 2017, Art. no. 1600147. [Online]. Available: http://dx.doi.org/10.1002/lpor.201600147

[29] S. Bastiaens, M. Alijani, W. Joseph, and D. Plets, "Visible light positioning as a next-generation indoor positioning technology: A tutorial," *IEEE Commun. Surveys Tuts.*, vol. 26, no. 4, pp. 2867–2913, 4th Quart., 2024. [Online]. Available: http://dx.doi.org/10.1109/COMST.2024.3372153

[30] Y. Zhuang et al., "A survey of positioning systems using visible LED lights," *IEEE Commun. Surveys Tuts.*, vol. 20, no. 3, pp. 1963–1988, 3rd Quart., 2018. [Online]. Available: http://dx.doi.org/10.1109/COMST.2018.2806558

[31] S. Bastiaens, M. Alijani, W. Joseph, and D. Plets, "An experimental analysis of visible light positioning in NLoS environments," in *Proc. 13th Int. Conf. Indoor Position. Indoor Navig. Papers (IPIN-WiP)*, 2023, pp. 1–9. [Online]. Available: https://ceur-ws.org/Vol-3581/184_WiP.pdf

[32] G. M. Insights. "Visible light communication market size, industry outlook report, regional analysis, application development, price trends, competitive market share & forecast, 2024–2032." Accessed: Nov. 23, 2023. [Online]. Available: https://www.gminsights.com/industry-analysis/visible-light-communication-market

[33] S. Rehman, S. Ullah, P. Chong, S. Yongchareon, and D. Komosny, "Visible light communication: A system perspective—Overview and challenges," *Sensors*, vol. 19, no. 5, p. 1153, Mar. 2019. [Online]. Available: http://dx.doi.org/10.3390/s19051153

[34] E. C. Strinati et al., "6G: The next frontier: From holographic Messaging to artificial intelligence using subterahertz and visible light communication," *IEEE Veh. Technol. Mag.*, vol. 14, no. 3, pp. 42–50, Sep. 2019. [Online]. Available: http://dx.doi.org/10.1109/MVT.2019.2921162

[35] T. Koonen, "Indoor optical wireless systems: Technology, trends, and applications," *J. Lightw. Technol.*, vol. 36, no. 8, pp. 1459–1467, Apr. 15, 2018. [Online]. Available: http://dx.doi.org/10.1109/JLT.2017.2787614

[36] P. J. Winzer and D. T. Neilson, "From scaling disparities to integrated parallelism: A decathlon for a decade," *J. Lightw. Technol.*, vol. 35, no. 5, pp. 1099–1115, Mar. 1, 2017. [Online]. Available: http://dx.doi.org/10.1109/JLT.2017.2662082

[37] K. Deprez, S. Bastiaens, L. Martens, W. Joseph, and D. Plets, "Passive visible light detection of humans," *Sensors*, vol. 20, no. 7, p. 1902, Mar. 2020. [Online]. Available: http://dx.doi.org/10.3390/s20071902

[38] K. Majeed and S. Hranilovic, "Passive positioning using visible light systems," in *Proc. Opt. Fiber Commun. Conf. Exhibit. (OFC)*, 2021, pp. 1–3, [Online]. Available: https://api.semanticscholar.org/CorpusID:236481319

[39] E. Di Lascio, A. Varshney, T. Voigt, and C. Perez-Penichet, "Poster abstract: LocaLight—A battery-free passive localization system using visible light," in *Proc. 15th ACM/IEEE Int. Conf. Inf. Process. Sensor Netw. (IPSN)*, Apr. 2016, pp. 1–2. [Online]. Available: http://dx.doi.org/10.1109/IPSN.2016.7460707

[40] G. Lee, J. K. Park, and J. T. Kim, "Multitarget passive indoor visible light positioning method based on specular reflection," *IEEE Sensors J.*, vol. 23, no. 24, pp. 31196–31208, Dec. 2023. [Online]. Available: http://dx.doi.org/10.1109/JSEN.2023.3328646

[41] W. Wang, J. Zhang, Q. Wang, and M. Zuniga, "Leveraging smart lights for passive localization," in *Proc. IEEE 15th Int. Conf. Mobile Ad Hoc Sensor Syst. (MASS)*, Oct. 2018, pp. 272–280. [Online]. Available: http://dx.doi.org/10.1109/MASS.2018.00049

[42] C. Carver, S. Wu, A. Rogers, M. Stafford, N. S. Artan, and Z. Dong, "Indoor localization through visible light characterization using front-facing smartphone camera," in *Proc. IEEE 14th Int. Conf. Mobile Ad Hoc Sensor Syst. (MASS)*, Oct. 2017, pp. 575–579. [Online]. Available: http://dx.doi.org/10.1109/MASS.2017.102

[43] H. Abuella et al., "Hybrid RF/VLC systems: A comprehensive survey on network topologies, performance analyses, applications, and future directions," *IEEE Access*, vol. 9, pp. 160402–160436, 2021. [Online]. Available: http://dx.doi.org/10.1109/ACCESS.2021.3129154

[44] S. Zhang, K. Liu, Y. Ma, X. Huang, X. Gong, and Y. Zhang, "An accurate geometrical multi-target device-free localization method using light sensors," *IEEE Sensors J.*, vol. 18, no. 18, pp. 7619–7632, Sep. 2018. [Online]. Available: http://dx.doi.org/10.1109/JSEN.2018.2862412

[45] M. Alijani, W. Joseph, E. De Poorter, M. Deruyck, and D. Plets, "ChickSense: Toward poultry welfare with machine learning-assisted visible light sensing," *IEEE Sensors J.*, vol. 24, no. 21, pp. 36178–36193, Nov. 2024. [Online]. Available: http://dx.doi.org/10.1109/JSEN.2024.3463209

[46] G. Deak, K. Curran, and J. Condell, "A survey of active and passive indoor localisation systems," *Comput. Commun.*, vol. 35, no. 16, pp. 1939–1954, Sep. 2012. [Online]. Available: http://dx.doi.org/10.1016/j.comcom.2012.06.004

[47] T. Li, C. An, Z. Tian, A. T. Campbell, and X. Zhou, "Human sensing using visible light communication," in *Proc. 21st Annu. Int. Conf. Mobile Comput. Netw. (MobiCom)*, Sep. 2015, pp. 331–344. [Online]. Available: http://dx.doi.org/10.1145/2789168.2790110

[48] J. Luo, L. Fan, and H. Li, "Indoor positioning systems based on visible light communication: State of the art," *IEEE Commun. Surveys Tuts.*, vol. 19, no. 4, pp. 2871–2893, 4th Quart., 2017. [Online]. Available: http://dx.doi.org/10.1109/COMST.2017.2743228

[49] T.-H. Do and M. Yoo, "An in-depth survey of visible light communication based positioning systems," *Sensors*, vol. 16, no. 5, p. 678, May 2016. [Online]. Available: http://dx.doi.org/10.3390/s16050678

[50] R. Wang, G. Niu, Q. Cao, C. S. Chen, and S.-W. Ho, "A survey of visible-light-communication-based indoor positioning systems," *Sensors*, vol. 24, no. 16, p. 5197, Aug. 2024. [Online]. Available: http://dx.doi.org/10.3390/s24165197

[51] Z. Zhu, Y. Yang, M. Chen, C. Guo, J. Cheng, and S. Cui, "A survey on indoor visible light positioning systems: Fundamentals, applications, and challenges," *IEEE Commun. Surveys Tuts.*, early access, Oct. 1, 2024, [Online]. Available: http://dx.doi.org/10.1109/COMST.2024.3471950

[52] S. Bastiaens, K. Deprez, L. Martens, W. Joseph, and D. Plets, "A comprehensive study on light signals of opportunity for subdecimetre unmodulated visible light positioning," *Sensors*, vol. 20, no. 19, p. 5596, Sep. 2020. [Online]. Available: http://dx.doi.org/10.3390/s20195596

[53] T. Desquins, F. Bousefsaf, A. Pruski, and C. Maaoui, "A survey of photoplethysmography and imaging photoplethysmography quality assessment methods," *Appl. Sci.*, vol. 12, no. 19, p. 9582, Sep. 2022. [Online]. Available: http://dx.doi.org/10.3390/app12199582

[54] F. Scardulla et al., "Photoplethysmograhic sensors, potential and limitations: Is it time for regulation? a comprehensive review," *Measurement*, vol. 218, Aug. 2023, Art. no. 113150. [Online]. Available: http://dx.doi.org/10.1016/j.measurement.2023.113150

[55] C. Mai et al., "Laser sensing and vision sensing smart blind cane: A review," *Sensors*, vol. 23, no. 2, p. 869, Jan. 2023. [Online]. Available: http://dx.doi.org/10.3390/s23020869

[56] F. Zafar, M. Bakaul, and R. Parthiban, "Laser-diode-based visible light communication: Toward gigabit class communication," *IEEE Commun. Mag.*, vol. 55, no. 2, pp. 144–151, Feb. 2017. [Online]. Available: http://dx.doi.org/10.1109/MCOM.2017.1500672CM

[57] W. A. Cahyadi, Y. H. Chung, Z. Ghassemlooy, and N. B. Hassan, "Optical camera communications: Principles, modulations, potential and challenges," *Electronics*, vol. 9, no. 9, p. 1339, Aug. 2020. [Online]. Available: http://dx.doi.org/10.3390/electronics9091339

[58] M. K. Hasan, M. O. Ali, M. H. Rahman, M. Z. Chowdhury, and Y. M. Jang, "Optical camera communication in vehicular applications: A review," *IEEE Trans. Intell. Transp. Syst.*, vol. 23, no. 7, pp. 6260–6281, Jul. 2022. [Online]. Available: http://dx.doi.org/10.1109/TITS.2021.3086409

[59] S. Aleksic, "A survey on optical technologies for IoT, smart industry, and smart infrastructures," *J. Sensor Actuator Netw.*, vol. 8, no. 3, p. 47, Sep. 2019. [Online]. Available: http://dx.doi.org/10.3390/jsan8030047

[60] O. Svelto et al., *Lasers and Coherent Light Sources*. New York, NY, USA: Springer, 2007, pp. 583–936. [Online]. Available: http://dx.doi.org/10.1007/978-0-387-30420-5_11

[61] W. T. Silfvast, *Laser Fundamentals*. Cambridge, U.K.: Cambridge Univ. Press, Jan. 2004. [Online]. Available: http://dx.doi.org/10.1017/CBO9780511616426

[62] A. Saha and B. C. Dhara, "3-D LiDAR-based obstacle detection and tracking for autonomous navigation in dynamic environments," *Int. J. Intell. Robot. Appl.*, vol. 8, no. 1, pp. 39–60, Nov. 2023. [Online]. Available: http://dx.doi.org/10.1007/s41315-023-00302-1

[63] L.-Q. Tao, Y. Liu, S. Zou, Z. Zhang, and X. Zhao, "Enhancing gesture recognition in low-light conditions using laser-induced graphene flexible strain sensors," *IEEE Sensors J.*, vol. 24, no. 4, pp. 5256–5265, Feb. 2024. [Online]. Available: http://dx.doi.org/10.1109/JSEN.2023.3345344

[64] J. A. S. D. Fonseca, A. Baptista, M. J. Martins, and J. P. N. Torres, "Distance measurement systems using lasers and their applications," *Appl. Phys. Res.*, vol. 9, no. 4, p. 33, Jul. 2017. [Online]. Available: http://dx.doi.org/10.5539/apr.v9n4p33

[65] M. D. Soltani et al., "Safety analysis for laser-based optical wireless communications: A tutorial," *Proc. IEEE*, vol. 110, no. 8, pp. 1045–1072, Aug. 2022. [Online]. Available: http://dx.doi.org/10.1109/JPROC.2022.3181968

[66] J. Kahn and J. Barry, "Wireless infrared communications," *Proc. IEEE*, vol. 85, no. 2, pp. 265–298, Feb. 1997. [Online]. Available: http://dx.doi.org/10.1109/5.554222

[67] Q. Wang, X. Zhang, and K. L. Boyer, "Occupancy distribution estimation for smart light delivery with perturbation-modulated light sensing," *J. Solid-State Light.*, vol. 1, no. 1, p. 17, Oct. 2014. [Online]. Available: http://dx.doi.org/10.1186/s40539-014-0017-2

[68] J. Zhao, P. Ishwar, and J. Konrad, "Privacy-preserving indoor localization via light transport analysis," in *Proc. IEEE Int. Conf. Acoust. Speech Signal Process. (ICASSP)*, Mar. 2017, pp. 3331–3335. [Online]. Available: http://dx.doi.org/10.1109/ICASSP.2017.7952773

[69] M. A. Mestiraihi, H. Abuella, and S. Ekin, "Indoor occupancy estimation using visible light sensing (VLS) system," in *Proc. IEEE 88th Veh. Technol. Conf. (VTC-Fall)*, Aug. 2018, pp. 1–5. [Online]. Available: http://dx.doi.org/10.1109/VTCFall.2018.8690704

[70] E. A. Jarchlo et al., "Li-Tect: 3-D monitoring and shape detection using visible light sensors," *IEEE Sensors J.*, vol. 19, no. 3, pp. 940–949, Feb. 2019. [Online]. Available: http://dx.doi.org/10.1109/JSEN.2018.2879398

[71] X. Liu, X. Wei, and L. Guo, "Indoor passive visible light localization: A case of the novel rake RGB-LED series detector," *IEEE Trans. Instrum. Meas.*, vol. 72, pp. 1–13, 2023. [Online]. Available: http://dx.doi.org/10.1109/TIM.2023.3249254

[72] J. Hu et al., "IRIS: Passive visible light positioning using light spectral information," *Proc. ACM Interact. Mobile Wearable Ubiquitous Technol.*, vol. 7, no. 3, pp. 1–27, Sep. 2023. [Online]. Available: http://dx.doi.org/10.1145/3610913

[73] M. F. Keskin, A. D. Sezer, and S. Gezici, "Localization via visible light systems," *Proc. IEEE*, vol. 106, no. 6, pp. 1063–1088, Jun. 2018. [Online]. Available: http://dx.doi.org/10.1109/JPROC.2018.2823500

[74] S. Bastiaens et al., "Experimental benchmarking of next-gen indoor positioning technologies (unmodulated) visible light positioning and ultra-wideband," *IEEE Internet Things J.*, vol. 9, no. 18, pp. 17858–17870, Sep. 2022. [Online]. Available: http://dx.doi.org/10.1109/jiot.2022.3161791

[75] J. Singh, T. Farnham, and Q. Wang, "When BLE meets light: Multimodal fusion for enhanced indoor localization," in *Proc. 29th Annu. Int. Conf. Mobile Comput. Netw. (ACM MobiCom)*, Oct. 2023, pp. 1–3. [Online]. Available: http://dx.doi.org/10.1145/3570361.3615746

[76] R. Amsters, E. Demeester, N. Stevens, and P. Slaets, "In-depth analysis of unmodulated visible light positioning using the iterated extended Kalman filter," *Sensors*, vol. 19, no. 23, p. 5198, Nov. 2019. [Online]. Available: http://dx.doi.org/10.3390/s19235198

[77] P. Xie, L. Li, J. Wang, and Y. Liu, "Passive visible light tag system for localization and posture estimation," *IEEE Trans. Mobile Comput.*, vol. 23, no. 8, pp. 8541–8556, Aug. 2024. [Online]. Available: http://dx.doi.org/10.1109/TMC.2023.3348802

[78] W. Wang, Q. Wang, J. Zhang, and M. Zuniga, "PassiveVLP: Leveraging smart lights for passive positioning," *ACM Trans. Internet Things*, vol. 1, no. 1, pp. 1–24, Feb. 2020. [Online]. Available: http://dx.doi.org/10.1145/3362123

[79] C. Fragner, C. Krutzler, A. P. Weiss, and E. Leitgeb, "LEDPOS: Indoor visible light positioning based on LED as sensor and machine learning," *IEEE Access*, vol. 12, pp. 46444–46461, 2024. [Online]. Available: http://dx.doi.org/10.1109/ACCESS.2024.3382757

[80] D. Konings, N. Faulkner, F. Alam, E. M.-K. Lai, and S. Demidenko, "FieldLight: Device-free indoor human localization using passive visible light positioning and artificial potential fields," *IEEE Sensors J.*, vol. 20, no. 2, pp. 1054–1066, Jan. 2020. [Online]. Available: http://dx.doi.org/10.1109/JSEN.2019.2944178

[81] N. Faulkner, F. Alam, M. Legg, and S. Demidenko, "Smart wall: Passive visible light positioning with ambient light only," in *Proc. IEEE Int. Instrum. Meas. Technol. Conf. (I2MTC)*, May 2019, pp. 1–6. [Online]. Available: http://dx.doi.org/10.1109/I2MTC.2019.8826875

[82] Y. Wang et al., "Spectral-Loc: Indoor localization using light spectral information," *Proc. ACM Interact. Mobile Wearable Ubiquitous Technol.*, vol. 7, no. 1, pp. 1–26, Mar. 2023. [Online]. Available: http://dx.doi.org/10.1145/3580878

[83] J. Suder, K. Podbucki, T. Marciniak, and A. Dabrowski, "Spectrum sensors for detecting type of airport lamps in a light photometry system," *Opto-Electron. Rev.*, vol. 29, pp. 133–140, May 2021. [Online]. Available: http://dx.doi.org/10.24425/opelre.2021.139383

[84] Z. Yang, Z. Wang, J. Zhang, C. Huang, and Q. Zhang, "Wearables can afford: Light-weight indoor positioning with visible light," in *Proc. 13th Annu. Int. Conf. Mobile Syst. Appl. Services (MobiSys)*, May 2015, pp. 317–330. [Online]. Available: http://dx.doi.org/10.1145/2742647.2742648

[85] D. Konings, F. Alam, F. Noble, and E. M.-K. Lai, "Improved distance metrics for histogram-based device-free localization," *IEEE Sensors J.*, vol. 19, no. 19, pp. 8940–8950, Oct. 2019. [Online]. Available: http://dx.doi.org/10.1109/JSEN.2019.2922772

[86] N. Faulkner, F. Alam, M. Legg, and S. Demidenko, "Watchers on the wall: Passive visible light-based positioning and tracking with embedded light-sensors on the wall," *IEEE Trans. Instrum. Meas.*, vol. 69, no. 5, pp. 2522–2532, May 2020. [Online]. Available: http://dx.doi.org/10.1109/TIM.2019.2953373

[87] H. Rizk, D. Ma, M. Hassan, and M. Youssef, "Indoor localization using solar cells," in *Proc. IEEE Int. Conf. Pervasive Comput. Commun. Workshops (PerCom Workshops)*, Mar. 2022, pp. 38–41. [Online]. Available: http://dx.doi.org/10.1109/PerComWorkshops53856.2022.9767256

[88] N. U. Hassan, A. Naeem, M. A. Pasha, T. Jadoon, and C. Yuen, "Indoor positioning using visible LED lights: A survey," *ACM Comput. Surveys*, vol. 48, no. 2, pp. 1–32, Nov. 2015. [Online]. Available: http://dx.doi.org/10.1145/2835376

[89] M. Kavehrad and R. Aminikashani, *Visible Light Communication Based Indoor Localization*. Hoboken, NJ, USA: CRC Press, Nov. 2019. [Online]. Available: http://dx.doi.org/10.1201/9780429355806

[90] A. A. Al-Hameed. "Detection and localisation using light." 2019. [Online]. Available: https://etheses.whiterose.ac.uk/24327/

[91] *Visible Light Communications: Theory and Applications*. Hoboken, NJ, USA: CRC Press, Jun. 2017. [Online]. Available: http://dx.doi.org/10.1201/9781315367330

[92] E. F. Schubert and J. K. Kim, "Solid-state light sources getting smart," *Science*, vol. 308, no. 5726, pp. 1274–1278, May 2005. [Online]. Available: http://dx.doi.org/10.1126/science.1108712

[93] Q. Wang, M. Zuniga, and D. Giustiniano, "Passive communication with ambient light," in *Proc. 12th Int. Conf. Emerg. Netw. Exp. Technol. (CoNEXT)*, Dec. 2016, pp. 97–104. [Online]. Available: http://dx.doi.org/10.1145/2999572.2999584

[94] S. Bastiaens, "Towards centimetre-order indoor localisation with RSS-based visible light positioning," Ph.D. dissertation, Dept. Inf. Eng., Ghent Univ., Ghent, Belgium, 2022.

[95] A. Varshney, A. Soleiman, L. Mottola, and T. Voigt, "Battery-free visible light sensing," in *Proc. 4th ACM Workshop Vis. Light Commun. Syst. (MobiCom)*, Oct. 2017, pp. 582–584. [Online]. Available: http://dx.doi.org/10.1145/3129881.3129890

[96] R. H. Venkatnarayan and M. Shahzad, "Recognizing gestures with ambient light," in *Proc. 10th Wireless Students Workshop (MobiCom)*, Oct. 2018, pp. 19–21. [Online]. Available: http://dx.doi.org/10.1145/3264877.3264883

[97] H. Duan, M. Huang, Y. Yang, J. Hao, and L. Chen, "Ambient light based hand gesture recognition enabled by recurrent neural network," *IEEE Access*, vol. 8, pp. 7303–7312, 2020. [Online]. Available: http://dx.doi.org/10.1109/ACCESS.2019.2963440

[98] A. P. Weiss, S. Z. Rad, and F. P. Wenzl, "Pose detection with backscattered visible light sensing utilizing a single RGB photodiode: A model based feasibility study," in *Proc. Int. Wireless Commun. Mobile Comput. (IWCMC)*, Jun. 2020, pp. 137–142. [Online]. Available: http://dx.doi.org/10.1109/IWCMC48107.2020.9148177

[99] J. Hu et al., "Passive light spectral indoor localization," in *Proc. 28th Annu. Int. Conf. Mobile Comput. And Netw. (MobiCom)*, Oct. 2022, pp. 832–834. [Online]. Available: http://dx.doi.org/10.1145/3495243.3558253

[100] A. A. Al-Hameed, S. H. Younus, A. T. Hussein, M. T. Alresheed, and J. M. H. Elmirghani, "LiDAL: Light detection and localization," *IEEE Access*, vol. 7, pp. 85645–85687, 2019. [Online]. Available: http://dx.doi.org/10.1109/ACCESS.2019.2925076

[101] R. Hui, *Photodetectors*. Amsterdam, The Netherlands: Elsevier, 2020, pp. 125–154. [Online]. Available: http://dx.doi.org/10.1016/B978-0-12-805345-4.00004-4

[102] T. Xu. "IntI: Indoor tracking with solar cells." 2022. Accessed: Apr. 18, 2024. [Online]. Available: https://repository.tudelft.nl/islandora/object/uuid:e614ca94-0e84-414b-b78c-9491f1a19f22

[103] K. W. Boer. "Solar cells." 2024. Accessed: Apr. 17, 2024. [Online]. Available: https://www.chemistryexplained.com/Ru-Sp/Solar-Cells.html

[104] R. Paschotta, *Photodiodes—An Encyclopedia Article*, RP Photonics AG, Frauenfeld, Switzerland, 2006. [Online]. Available: http://dx.doi.org/10.61835/8jq

[105] D. Ma et al., "SolarGest: Ubiquitous and battery-free gesture recognition using solar cells," in *Proc. ACM 25th Annu. Int. Conf. Mobile Comput. Netw. (MobiCom)*, Aug. 2019, pp. 1–15. [Online]. Available: http://dx.doi.org/10.1145/3300061.3300129

[106] SPECIM. "How does spectral sensing work? Understanding the basics of spectroscopy and spectral sensors." 2024. Accessed: Apr. 23, 2024. [Online]. Available: https://www.specim.com/technology/how-does-spectral-sensing-work/

[107] SparkFun. "AS726X NIRV-IS tutorial." Accessed: Nov. 21, 2024. [Online]. Available: https://learn.sparkfun.com/tutorials/as726x-nirvi/all

[108] SparkFun. "SparkFun triad spectroscopy sensor—AS7265x (Qwiic)." Accessed: Apr. 17, 2024. [Online]. Available: https://www.sparkfun.com/products/15050

[109] National Instruments. "USB-6212 specifications." Accessed: Nov. 21, 2024. [Online]. Available: https://www.ni.com/docs/en-U.S./bundle/usb-6212-specs/page/specs.html

[110] Thorlabs. "PDA100A2 photodiode amplifier." Accessed: Nov. 21, 2024. [Online]. Available: https://www.thorlabs.com/thorproduct.cfm?partnumber=PDA100A2

[111] T. Li, Q. Liu, and X. Zhou, "Practical human sensing in the light," in *Proc. 14th Annu. Int. Conf. Mobile Syst. Appl. Services (MobiSys)*, Jun. 2016, pp. 71–84. [Online]. Available: http://dx.doi.org/10.1145/2906388.2906401

[112] M. Jawahar. "Device-free positioning using a ceiling-based visible light sensing system." 2018. [Online]. Available: https://rucore.libraries.rutgers.edu/rutgers-lib/56021/

[113] Y. Zhang, O. Cai, and Y. Yang, "Shadow effect of human obstacles on indoor visible light communication system with multiple light sources," *Appl. Sci.*, vol. 13, no. 11, p. 6356, May 2023. [Online]. Available: http://dx.doi.org/10.3390/app13116356

[114] T. Tang, T. Shang, and Q. Li, "Impact of multiple shadows on visible light communication channel," *IEEE Commun. Lett.*, vol. 25, no. 2, pp. 513–517, Feb. 2021. [Online]. Available: http://dx.doi.org/10.1109/LCOMM.2020.3031645

[115] X. Zhou and A. T. Campbell, "Visible light networking and sensing," in *Proc. 1st ACM Workshop Hot Topics Wireless (MobiCom)*, Sep. 2014, pp. 55–60. [Online]. Available: http://dx.doi.org/10.1145/2643614.2643621

[116] V. Amacker, H. Lohse-Bossenz, M. Wilhelm, and D. Brovelli, "Concept test on reflection and transmission in the range of visible and infrared optics," *Int. J. Sci. Educ.*, vol. 46, no. 9, pp. 913–933, Oct. 2023. [Online]. Available: http://dx.doi.org/10.1080/09500693.2023.2263917

[117] K. Majeed and S. Hranilovic, "Passive indoor visible light positioning system using deep learning," *IEEE Internet Things J.*, vol. 8, no. 19, pp. 14810–14821, Oct. 2021. [Online]. Available: http://dx.doi.org/10.1109/JIOT.2021.3072201

[118] K. Majeed and S. Hranilovic, "Passive indoor localization for visible light communication systems," in *Proc. IEEE Global Commun. Conf. (GLOBECOM)*, 2018, pp. 1–6.

[119] K. Majeed and S. Hranilovic, "Passive indoor visible light-based fall detection using neural networks," *Opt. Exp.*, vol. 29, no. 26, pp. 43389–43402, Dec. 2021. [Online]. Available: https://opg.optica.org/oe/abstract.cfm?URI=oe-29-26-43389

[120] W. Zhang, M. I. S. Chowdhury, and M. Kavehrad, "Asynchronous indoor positioning system based on visible light communications," *Opt. Eng.*, vol. 53, no. 4, Apr. 2014, Art. no. 45105. [Online]. Available: http://dx.doi.org/10.1117/1.OE.53.4.045105

[121] S.-H. Yang, H.-S. Kim, Y.-H. Son, and S.-K. Han, "Three-dimensional visible light indoor localization using AOA and RSS with multiple optical receivers," *J. Lightw. Technol.*, vol. 32, no. 14, pp. 2480–2485, Jul. 1, 2014. [Online]. Available: http://dx.doi.org/10.1109/JLT.2014.2327623

[122] R. Zhang, W.-D. Zhong, K.-M. Qian, and D.-h. Wu, "Image sensor based visible light positioning system with improved positioning algorithm," *IEEE Access*, vol. 5, pp. 6087–6094, 2017. [Online]. Available: http://dx.doi.org/10.1109/ACCESS.2017.2693299

[123] E. W. Lam and T. D. C. Little, "Refining light-based positioning for indoor smart spaces," in *Proc. 4th ACM MobiHoc Workshop Exp. Design Implement. Smart Objects (Mobihoc)*, Jun. 2018, pp. 1–8. [Online]. Available: http://dx.doi.org/10.1145/3213299.3213308

[124] S. Bastiaens, W. Raes, N. Stevens, L. Martens, W. Joseph, and D. Plets, "Impact of a photodiode's angular characteristics on RSS-based VLP accuracy," *IEEE Access*, vol. 8, pp. 83116–83130, 2020. [Online]. Available: http://dx.doi.org/10.1109/ACCESS.2020.2991298

[125] V. Nguyen, M. Ibrahim, S. Rupavatharam, M. Jawahar, M. Gruteser, and R. Howard, "Eyelight: Light-and-shadow-based occupancy estimation and room activity recognition," in *Proc. IEEE Conf. Comput. Commun. (IEEE INFOCOM)*, Apr. 2018, pp. 351–359. [Online]. Available: http://dx.doi.org/10.1109/INFOCOM.2018.8485867

[126] T.-K. Woodstock, R. J. Radke, and A. C. Sanderson, "Sensor fusion for occupancy detection and activity recognition using time-of-flight sensors," in *Proc. 19th Int. Conf. Inf. Fusion (FUSION)*, 2016, pp. 1695–1701, [Online]. Available: https://ieeexplore.ieee.org/stamp/stamp.jsp?tp=&arnumber=7528087

[127] Y. Yang, J. Hao, J. Luo, and S. J. Pan, "CeilingSee: Device-free occupancy inference through lighting infrastructure based LED sensing," in *Proc. IEEE Int. Conf. Pervasive Comput. Commun. (PerCom)*, Mar. 2017, pp. 247–256. [Online]. Available: http://dx.doi.org/10.1109/PERCOM.2017.7917871

[128] S. Yahia, Y. Meraihi, A. Ramdane-Cherif, A. B. Gabis, D. Acheli, and H. Guan, "A survey of channel modeling techniques for visible light communications," *J. Netw. Comput. Appl.*, vol. 194, Nov. 2021, Art. no. 103206. [Online]. Available: http://dx.doi.org/10.1016/j.jnca.2021.103206

[129] M. I. S. Chowdhury, W. Zhang, and M. Kavehrad, "Combined deterministic and modified Monte Carlo method for calculating impulse responses of indoor optical wireless channels," *J. Lightw. Technol.*, vol. 32, no. 18, pp. 3132–3148, Sep. 15, 2014. [Online]. Available: http://dx.doi.org/10.1109/JLT.2014.2339131

[130] J. Barry, J. Kahn, W. Krause, E. Lee, and D. Messerschmitt, "Simulation of multipath impulse response for indoor wireless optical channels," *IEEE J. Sel. Areas Commun.*, vol. 11, no. 3, pp. 367–379, Apr. 1993. [Online]. Available: http://dx.doi.org/10.1109/49.219552

[131] W. Gu, M. Aminikashani, P. Deng, and M. Kavehrad, "Impact of multipath reflections on the performance of indoor visible light positioning systems," *J. Lightw. Technol.*, vol. 34, no. 10, pp. 2578–2587, May 15, 2016. [Online]. Available: http://dx.doi.org/10.1109/JLT.2016.2541659

[132] F. Miramirkhani and M. Uysal, "Channel modeling and Characterization for visible light communications," *IEEE Photon. J.*, vol. 7, no. 6, pp. 1–16, Dec. 2015. [Online]. Available: http://dx.doi.org/10.1109/JPHOT.2015.2504238

[133] M. Uysal, F. Miramirkhani, O. Narmanlioglu, T. Baykas, and E. Panayirci, "IEEE 802.15.7r1 reference channel models for visible light communications," *IEEE Commun. Mag.*, vol. 55, no. 1, pp. 212–217, Jan. 2017. [Online]. Available: http://dx.doi.org/10.1109/MCOM.2017.1600872CM

[134] S. V. Tiwari, A. Sewaiwar, and Y.-H. Chung, "Smart home technologies using visible light communication," in *Proc. IEEE Int. Conf. Consum. Electron. (ICCE)*, Jan. 2015, pp. 379–380. [Online]. Available: http://dx.doi.org/10.1109/ICCE.2015.7066453

[135] L. Yu, H. Abuella, M. Z. Islam, J. F. O'Hara, C. Crick, and S. Ekin, "Gesture recognition using reflected visible and infrared lightwave signals," *IEEE Trans. Human–Mach. Syst.*, vol. 51, no. 1, pp. 44–55, Feb. 2021. [Online]. Available: http://dx.doi.org/10.1109/THMS.2020.3043302

[136] Y. Almadani et al., "Visible light communications for industrial applications—challenges and potentials," *Electronics*, vol. 9, no. 12, p. 2157, Dec. 2020. [Online]. Available: http://dx.doi.org/10.3390/electronics9122157

[137] J. Straub, "Characterization of internal geometry—Covered surface defects with a visible light sensing system," in *Proc. Image Sens. Technol. Mater. Devices Syst. Appl. III*, May 2016, Art. no. 98540W. [Online]. Available: http://dx.doi.org/10.1117/12.2227802

[138] M. Ibrahim, V. Nguyen, S. Rupavatharam, M. Jawahar, M. Gruteser, and R. Howard, "Visible light based activity sensing using ceiling photosensors," in *Proc. 3rd Workshop Vis. Light Commun. Syst. (MobiCom)*, Oct. 2016, pp. 837–842. [Online]. Available: http://dx.doi.org/10.1145/2981548.2981554

[139] J. Zhu, Z. Liu, Y. Sun, and Y. Yang, "SemiGest: Recognizing hand gestures via visible light sensing with fewer labels," in *Proc. 19th Int. Conf. Mobility Sens. Netw. (MSN)*, vol. 32, Dec. 2023, pp. 837–842. [Online]. Available: http://dx.doi.org/10.1109/MSN60784.2023.00123

[140] Z. Chen, Y. Yang, C. Jiang, J. Hao, and L. Zhang, "Light sensor based occupancy estimation via Bayes filter with neural networks," *IEEE Trans. Ind. Electron.*, vol. 67, no. 7, pp. 5787–5797, Jul. 2020. [Online]. Available: http://dx.doi.org/10.1109/TIE.2019.2934028

[141] R. H. Venkatnarayan and M. Shahzad, "Gesture recognition using ambient light," *Proc. ACM Interact. Mobile Wearable Ubiquitous Technol.*, vol. 2, no. 1, pp. 1–28, Mar. 2018. [Online]. Available: http://dx.doi.org/10.1145/3191772

[142] M. Roscia, V. Dancu, and G. C. Lazaroiu, "Smart home survey analysis," in *Proc. IEEE Int. Smart Cities Conf. (ISC2)*, Sep. 2023, pp. 1–5. [Online]. Available: http://dx.doi.org/10.1109/ISC257844.2023.10293364

[143] M. Figueiredo, L. N. Alves, and C. Ribeiro, "Lighting the wireless world: The promise and challenges of visible light communication," *IEEE Consum. Electron. Mag.*, vol. 6, no. 4, pp. 28–37, Oct. 2017. [Online]. Available: http://dx.doi.org/10.1109/MCE.2017.2714721

[144] K. P. Pujapanda, "LiFi integrated to power-lines for smart illumination cum communication," in *Proc. Int. Conf. Commun. Syst. Netw. Technol.*, Apr. 2013, pp. 1–9. [Online]. Available: http://dx.doi.org/10.1109/CSNT.2013.189

[145] L. Rodrigues, M. Figueiredo, and L. N. Alves, "Analog m-CAP demodulation for VLC-based IoT systems," in *Proc. 12th Int. Symp. Commun. Syst. Netw. Digit. Signal Process. (CSNDSP)*, Jul. 2020, pp. 1–6. [Online]. Available: http://dx.doi.org/10.1109/CSNDSP49049.2020.9249493

[146] M. A. Mestiraihi. "Occupancy estimation through visible light sensing (VLS)." 2019. [Online]. Available: https://shareok.org/handle/11244/321536?show=full

[147] L. AG. "Autonomous lighting system." Accessed: Nov. 23, 2023. [Online]. Available: https://solarimpulse.com/solutions-explorer/autonomous-lighting-system

[148] K. Sun, Q. Zhao, and J. Zou, "A review of building occupancy measurement systems," *Energy Buildings*, vol. 216, Jun. 2020, Art. no. 109965. [Online]. Available: http://dx.doi.org/10.1016/j.enbuild.2020.109965

[149] H. Mohammadmoradi, S. Yin, and O. Gnawali, "Room occupancy estimation through WiFi, UWB, and light sensors mounted on doorways," in *Proc. Int. Conf. Smart Digit. Environ. (ICSDE)*, Jul. 2017, pp. 27–34. [Online]. Available: http://dx.doi.org/10.1145/3128128.3128133

[150] Y. Yang, J. Luo, J. Hao, and S. J. Pan, "Counting via LED sensing: Inferring occupancy using lighting infrastructure," *Pervasive Mobile Comput.*, vol. 45, pp. 35–54, Apr. 2018. [Online]. Available: http://dx.doi.org/10.1016/j.pmcj.2018.01.003

[151] O. E. Ouahabi, C. Fragner, A. P. Weiss, and E. Leitgeb, "Occupancy determination by backscattered visible light sensing," in *Proc. 46th MIPRO ICT Electron. Conv. (MIPRO)*, May 2023, pp. 280–285. [Online]. Available: http://dx.doi.org/10.23919/MIPRO57284.2023.10159964

[152] J. Hao, X. Yuan, Y. Yang, R. Wang, Y. Zhuang, and J. Luo, "Visible light based occupancy inference using ensemble learning," *IEEE Access*, vol. 6, pp. 16377–16385, 2018. [Online]. Available: http://dx.doi.org/10.1109/ACCESS.2018.2809612

[153] C. Liang et al., "Integrated sensing, lighting and communication based on visible light communication: A review," *Digit. Signal Process.*, vol. 145, Feb. 2024, Art. no. 104340. [Online]. Available: http://dx.doi.org/10.1016/j.dsp.2023.104340

[154] J. Li et al., "DEMO: SolarSense: A self-powered ubiquitous gesture recognition system for industrial human–computer interaction," in *Proc. 22nd Annu. Int. Conf. Mobile Syst. Appl. Services (MOBISYS)*, Jun. 2024, pp. 600–601. [Online]. Available: http://dx.doi.org/10.1145/3643832.3661838

[155] X. Liang et al., "Gesture recognition and control based on visible light communication," in *Proc. 43rd Chin. Control Conf. (CCC)*, vol. 16, Jul. 2024, pp. 6164–6169. [Online]. Available: http://dx.doi.org/10.23919/CCC63176.2024.10661455

[156] J. Ahmad, H. Larijani, R. Emmanuel, M. Mannion, and A. Javed, "Occupancy detection in non-residential buildings—A survey and novel privacy preserved occupancy monitoring solution," *Appl. Comput. Inf.*, vol. 17, no. 2, pp. 279–295, Sep. 2020. [Online]. Available: http://dx.doi.org/10.1016/J.ACI.2018.12.001

[157] S. Hu, P. Wang, C. Hoare, and J. O'Donnell, "Building occupancy detection and localization using CCTV camera and deep learning," *IEEE Internet Things J.*, vol. 10, no. 1, pp. 597–608, Jan. 2023. [Online]. Available: http://dx.doi.org/10.1109/JIOT.2022.3201877

[158] T.-K. Woodstock and R. F. Karlicek, "RGB color sensors for occupant detection: An alternative to PIR sensors," *IEEE Sensors J.*, vol. 20, no. 20, pp. 12364–12373, Oct. 2020. [Online]. Available: http://dx.doi.org/10.1109/JSEN.2020.3000170

[159] K. E. Caine, A. D. Fisk, and W. A. Rogers, "Benefits and privacy concerns of a home equipped with a visual sensing system: A perspective from older adults," in *Proc. Human Factors Ergonom. Soc. Annu. Meeting*, vol. 50, Oct. 2006, pp. 180–184, [Online]. Available: http://dx.doi.org/10.1177/154193120605000203

[160] Y. P. Raykov, E. Ozer, G. Dasika, A. Boukouvalas, and M. A. Little, "Predicting room occupancy with a single passive infrared (PIR) sensor through behavior extraction," in *Proc. ACM Int. Joint Conf. Pervasive Ubiquitous Comput. (UbiComp)*, Sep. 2016, pp. 1016–1027. [Online]. Available: http://dx.doi.org/10.1145/2971648.2971746

[161] A. Hammoud, M. Deriaz, and D. Konstantas, "UltraSense: A self-calibrating ultrasound-based room occupancy sensing system," *Procedia Comput. Sci.*, vol. 109, pp. 75–83, Jun. 2017. [Online]. Available: http://dx.doi.org/10.1016/j.procs.2017.05.297

[162] L. Ada. "IR breakbeam sensors." 2014. Accessed: Nov. 15, 2024. [Online]. Available: https://learn.adafruit.com/ir-breakbeam-sensors/overview

[163] N. Lasla, M. Doudou, D. Djenouri, A. Ouadjaout, and C. Zizoua, "Wireless energy efficient occupancy-monitoring system for smart buildings," *Pervasive Mobile Comput.*, vol. 59, Oct. 2019, Art. no. 101037. [Online]. Available: http://dx.doi.org/10.1016/j.pmcj.2019.101037

[164] R. J. Orr and G. D. Abowd, "The smart floor: A mechanism for natural user identification and tracking," in *Proc. Extended Abstracts Human Factors Comput. Syst. (CHI)*, Apr. 2000, pp. 275–276. [Online]. Available: http://dx.doi.org/10.1145/633292.633453

[165] M. Valtonen, J. Maentausta, and J. Vanhala, "TileTrack: Capacitive human tracking using floor tiles," in *Proc. IEEE Int. Conf. Pervasive Comput. Commun.*, Mar. 2009, pp. 1–10. [Online]. Available: http://dx.doi.org/10.1109/PERCOM.2009.4912749

[166] S. Lim, S. Lee, J. Jung, and S.-C. Kim, "Detection and localization of people inside vehicle using impulse radio ultra-wideband radar sensor," *IEEE Sensors J.*, vol. 20, no. 7, pp. 3892–3901, Apr. 2020. [Online]. Available: http://dx.doi.org/10.1109/JSEN.2019.2961107

[167] M. Alizadeh, H. Abedi, and G. Shaker, "Low-cost low-power in-vehicle occupant detection with mm-Wave FMCW radar," in *Proc. IEEE SENSORS*, Oct. 2019, pp. 1–4. [Online]. Available: http://dx.doi.org/10.1109/SENSORS43011.2019.8956880

[168] C. Brennan, G. W. Taylor, and P. Spachos, "Designing learned CO_2-based occupancy estimation in smart buildings," *IET Wireless Sensor Syst.*, vol. 8, no. 6, pp. 249–255, Nov. 2018. [Online]. Available: http://dx.doi.org/10.1049/iet-wss.2018.5027

[169] C. Jiang, M. K. Masood, Y. C. Soh, and H. Li, "Indoor occupancy estimation from carbon dioxide concentration," *Energy Build.*, vol. 131, pp. 132–141, Nov. 2016. [Online]. Available: http://dx.doi.org/10.1016/j.enbuild.2016.09.002

[170] L. Wu and Y. Wang, "Stationary and moving occupancy detection using the SLEEPIR sensor module and machine learning," *IEEE Sensors J.*, vol. 21, no. 13, pp. 14701–14708, Jul. 2021. [Online]. Available: http://dx.doi.org/10.1109/JSEN.2021.3071402

[171] A. Milan, S. Roth, K. Schindler, and M. Kudo, *Privacy Preserving Multi-Target Tracking*. Cham, Switzerland: Springer, 2015, pp. 519–530. [Online]. Available: http://dx.doi.org/10.1007/978-3-319-16634-6_38

[172] M. Crawford, "LEDs for solid-state lighting: Performance challenges and recent advances," *IEEE J. Sel. Topics Quant. Electron.*, vol. 15, no. 4, pp. 1028–1040, Jul./Aug. 2009. [Online]. Available: http://dx.doi.org/10.1109/JSTQE.2009.2013476

[173] J. Grubor, O. Gaete, J. W. Walewski, S. Randel, and K.-D. Langer. "High-speed wireless indoor communication via visible light." 2007. [Online]. Available: https://api.semanticscholar.org/CorpusID:18142257

[174] K. Verniers and N. Stevens, "Impact of LED optical bandwidth limitation on the performance of power switched signaling," in *Proc. 12th Int. Symp. Commun. Syst. Netw. Digit. Signal Process. (CSNDSP)*, Jul. 2020, pp. 1–6. [Online]. Available: http://dx.doi.org/10.1109/CSNDSP49049.2020.9249510

[175] X. Cui, Y. Li, J. Li, B. Jiang, S. Li, and J. Liu, "UWB wireless positioning method based on LightGBM," *Wireless Pers. Commun.*, vol. 137, no. 2, pp. 1141–1160, Jul. 2024. [Online]. Available: http://dx.doi.org/10.1007/s11277-024-11456-x

[176] A. Alarifi et al., "Ultra wideband indoor positioning technologies: Analysis and recent advances," *Sensors*, vol. 16, no. 5, p. 707, May 2016. [Online]. Available: http://dx.doi.org/10.3390/s16050707

[177] J. Zhou, X. Bao, and W. Zhang, "Performance limits of passive visible light positioning using shadowing effects," *IEEE Commun. Lett.*, vol. 27, no. 12, pp. 3225–3229, Dec. 2023. [Online]. Available: http://dx.doi.org/10.1109/LCOMM.2023.3331540

[178] X. Mao, S. Tang, J. Wang, and X. Y. Li, "iLight: Device-free passive tracking using wireless sensor networks," *IEEE Sensors J.*, vol. 13, no. 10, pp. 3785–3792, Oct. 2013. [Online]. Available: http://dx.doi.org/10.1109/JSEN.2013.2267959

[179] X. Du, Y. Zhang, C. Wang, D. Li, and Y. Zhu, "Visible light sensing based on shadow features using multi-scale region convolutional neural network," *Opt. Exp.*, vol. 31, no. 26, Dec. 2023, Art. no. 43323. [Online]. Available: http://dx.doi.org/10.1364/OE.503488

[180] D. Zhang, Y. Liu, and L. M. Ni, "RASS: A real-time, accurate and scalable system for tracking transceiver-free objects," in *Proc. IEEE Int. Conf. Pervasive Comput. Commun. (PerCom)*, Mar. 2011, pp. 197–204. [Online]. Available: http://dx.doi.org/10.1109/PERCOM.2011.5767585

[181] S. Zhang, K. Liu, Y. Zhang, and X. Huang, "Robust multitarget device-free localization and tracking via visible light sensing," *IEEE Internet Things J.*, vol. 9, no. 17, pp. 16446–16462, Sep. 2022. [Online]. Available: http://dx.doi.org/10.1109/JIOT.2022.3153317

[182] IMEC. "Low-cost and low-energy radar chips for smart building sensors." Accessed: Nov. 23, 2023. [Online]. Available: https://www.imec-int.com/en/79GHz-and-140GHz-radar-solutions/8-GHz-radar-for-smart-buildings

[183] M. Deputter. "UWB versus other tracking technologies in 2024." 2024. Accessed: Feb. 23, 2024. [Online]. Available: https://www.pozyx.io/newsroom/uwb-versus-other-technologies

[184] M. Zywek and M. Malanowski, "Real-time selection of FM transmitter in passive bistatic radar based on short-term bandwidth analysis," in *Proc. 21st Int. Radar Symp. (IRS)*, Jun. 2021, pp. 1–9. [Online]. Available: http://dx.doi.org/10.23919/IRS51887.2021.9466225

[185] F. Zhang et al., "Embracing consumer-level UWB-equipped devices for fine-grained wireless sensing," *Proc. ACM Interact. Mobile Wearable Ubiquitous Technol.*, vol. 6, no. 4, pp. 1–27, Dec. 2022. [Online]. Available: http://dx.doi.org/10.1145/3569487

[186] C. Li et al., "Multistatic UWB radar-based passive human tracking using COTS devices," *IEEE Antennas Wireless Propag. Lett.*, vol. 21, no. 4, pp. 695–699, Apr. 2022. [Online]. Available: http://dx.doi.org/10.1109/LAWP.2022.3141869

[187] C. Li et al., "Device-free pedestrian tracking using low-cost ultrawideband devices," *IEEE Trans. Instrum. Meas.*, vol. 71, pp. 1–4, 2022. [Online]. Available: http://dx.doi.org/10.1109/TIM.2022.3157004

[188] NOVELDA. "NOVELDA ultra-wideband proximity sensor." Accessed: Nov. 29, 2024. [Online]. Available: https://novelda.com/ultra-wideband-proximity-sensor/

[189] X. Wang et al., "Millimeter wave communication: A comprehensive survey," *IEEE Commun. Surveys Tuts.*, vol. 20, no. 3, pp. 1616–1653, 3rd Quart., 2018. [Online]. Available: http://dx.doi.org/10.1109/COMST.2018.2844322

[190] C. Xu et al., "WaveEar: Exploring a mmWave-based noise-resistant speech sensing for voice-user interface," in *Proc. 17th Annu. Int. Conf. Mobile Syst. Appl. Services (MobiSys)*, Jun. 2019, pp. 14–26. [Online]. Available: http://dx.doi.org/10.1145/3307334.3326073

[191] W. Chen et al., "Environment-aware multi-person tracking in indoor environments with mmWave radars," *Proc. ACM Interact. Mobile Wearable Ubiquitous Technol.*, vol. 7, no. 3, pp. 1–29, Sep. 2023. [Online]. Available: http://dx.doi.org/10.1145/3610902

[192] C. Wu, F. Zhang, B. Wang, and K. J. R. Liu, "mmTrack: Passive multi-person localization using commodity millimeter wave radio," in *Proc. IEEE Conf. Comput. Commun. (IEEE INFOCOM)*, Jul. 2020, pp. 2400–2409. [Online]. Available: http://dx.doi.org/10.1109/INFOCOM41043.2020.9155293

[193] J. Lee, K. Park, and Y. Kim, "Deep learning-based device-free localization scheme for simultaneous estimation of indoor location and posture using FMCW radars," *Sensors*, vol. 22, no. 12, p. 4447, Jun. 2022. [Online]. Available: http://dx.doi.org/10.3390/s22124447

[194] V. Pillai, H. Heinrich, D. Dieska, P. V. Nikitin, R. Martinez, and K. V. S. Rao, "An ultra-low-power long range battery/passive RFID tag for UHF and microwave bands with a current consumption of 700 nA at 1.5 V," *IEEE Trans. Circuits Syst. I, Reg. Papers*, vol. 54, no. 7, pp. 1500–1512, Jul. 2007. [Online]. Available: http://dx.doi.org/10.1109/TCSI.2007.897768

[195] J. Halstead. "A breakdown of 7 RFID costs, from hardware to implementation." Accessed: Nov. 23, 2023. [Online]. Available: https://www.link-labs.com/blog/rfid-cost

[196] Y.-H. Su, J. Ren, Z. Qian, D. Fouhey, and A. Sample, "TomoID: A scalable approach to device free indoor localization via RFID tomography," in *Proc. IEEE Conf. Comput. Commun. (IEEE INFOCOM)*, May 2023, pp. 1–10. [Online]. Available: http://dx.doi.org/10.1109/INFOCOM53939.2023.10228938

[197] X. Liang, Z. Huang, S. Yang, and L. Qiu, "Device-free motion & trajectory detection via RFID," *ACM Trans. Embedded Comput. Syst.*, vol. 17, no. 4, pp. 1–27, Jul. 2018. [Online]. Available: http://dx.doi.org/10.1145/3230644

[198] L. Ma, M. Liu, H. Wang, Y. Yang, N. Wang, and Y. Zhang, "WallSense: Device-free indoor localization using wall-mounted UHF RFID tags," *Sensors*, vol. 19, no. 1, p. 68, Dec. 2018. [Online]. Available: http://dx.doi.org/10.3390/s19010068

[199] M. Woolley. "Bluetooth technology protecting your privacy." 2015. Accessed: Nov. 23, 2023. [Online]. Available: https://www.bluetooth.com/blog/bluetooth-technology-protecting-your-privacy/

[200] T. Instruments. "Cc2674r10." 2023. Accessed: Nov. 23, 2023. [Online]. Available: https://www.ti.com/product/CC2674R10#design-development

[201] Y. Zhuang, C. Zhang, J. Huai, Y. Li, L. Chen, and R. Chen, "Bluetooth localization technology: Principles, applications, and future trends," *IEEE Internet Things J.*, vol. 9, no. 23, pp. 23506–23524, Dec. 2022. [Online]. Available: http://dx.doi.org/10.1109/JIOT.2022.3203414

[202] "Maximizing BLE range." Argenox. 2020. Accessed: Feb. 23, 2024. [Online]. Available: https://www.argenox.com/library/bluetooth-low-energy/maximizing-bluetooth-low-energy-ble-range/

[203] N. Kuxdorf-Alkirata, G. Maus, and D. Bruckmann, "A device-free indoor Localization system based on supervised learning and Bluetooth low energy," in *Proc. IEEE Int. Mediterr. Conf. Commun. Netw. (MeditCom)*, Sep. 2021, pp. 413–418. [Online]. Available: http://dx.doi.org/10.1109/MeditCom49071.2021.9647654

[204] G. Iannizzotto, L. Lo Bello, and A. Nucita, "Improving BLE-based passive human sensing with deep learning," *Sensors*, vol. 23, no. 5, p. 2581, Feb. 2023. [Online]. Available: http://dx.doi.org/10.3390/s23052581

[205] Y. Li et al., "DiverSense: Maximizing Wi-Fi sensing range leveraging signal diversity," *Proc. ACM Interact., Mobile, Wearable Ubiquitous Technol.*, vol. 6, no. 2, pp. 1–28, Jul. 2022. [Online]. Available: http://dx.doi.org/10.1145/3536393

[206] A. Khalili, A. Soliman, M. Asaduzzaman, and A. Griffiths, "Wi-Fi sensing: Applications and challenges," *J. Eng.*, vol. 2020, pp. 87–97, Feb. 2020. [Online]. Available: http://dx.doi.org/10.1049/joe.2019.0790

[207] W. Li, B. Tan, and R. J. Piechocki, "WiFi-based passive sensing system for human presence and activity event classification," *Inst. Eng. Technol. Wireless Sensor Syst.*, vol. 8, no. 6, pp. 276–283, Oct. 2018. [Online]. Available: http://dx.doi.org/10.1049/iet-wss.2018.5113

[208] M. Mohsen, H. Rizk, H. Yamaguchi, and M. Youssef, "LocFree: WiFi RTT-based device-free indoor localization system," in *Proc. 2nd ACM SIGSPATIAL Int. Workshop Spatial Big Data AI Ind. Appl.*, Nov. 2023, pp. 32–40. [Online]. Available: http://dx.doi.org/10.1145/3615888.3627813

[209] A. E. Kosba, A. Saeed, and M. Youssef, "RASID: A robust WLAN device-free passive motion detection system," in *Proc. IEEE Int. Conf. Pervasive Comput. Commun.*, Mar. 2012, pp. 180–189. [Online]. Available: http://dx.doi.org/10.1109/PerCom.2012.6199865

[210] X. Rao and Z. Li, "MSDFL: A robust minimal hardware low-cost device-free WLAN localization system," *Neural Comput. Appl.*, vol. 31, no. 12, pp. 9261–9278, Jan. 2019. [Online]. Available: http://dx.doi.org/10.1007/s00521-018-3945-8

[211] I. Akyildiz, W. Su, Y. Sankarasubramaniam, and E. Cayirci, "Wireless sensor networks: A survey," *Comput. Netw.*, vol. 38, no. 4, pp. 393–422, Mar. 2002. [Online]. Available: http://dx.doi.org/10.1016/S1389-1286(01)00302-4

[212] N. Patwari and J. Wilson, "RF sensor networks for device-free localization: Measurements, models, and algorithms," *Proc. IEEE*, vol. 98, no. 11, pp. 1961–1973, Nov. 2010. [Online]. Available: http://dx.doi.org/10.1109/JPROC.2010.2052010

[213] D. Zhang, J. Ma, Q. Chen, and L. M. Ni, "An RF-based system for tracking transceiver-free objects," in *Proc. 5th Annu. IEEE Int. Conf. Pervasive Comput. Commun. (PerCom)*, 2007. [Online]. Available: http://dx.doi.org/10.1109/PERCOM.2007.8

[214] T. Kivimäki, T. Vuorela, P. Peltola, and J. Vanhala, "A review on device-free passive indoor positioning methods," *Int. J. Smart Home*, vol. 8, no. 1, pp. 71–94, Jan. 2014. [Online]. Available: http://dx.doi.org/10.14257/ijsh.2014.8.1.09

[215] "Outdoor cameras." Mobotix. 2024. Accessed: Feb. 23, 2024. [Online]. Available: https://www.mobotix.com/en/products/outdoor-cameras

[216] Y. Sun, K. Zhao, J. Wang, W. Li, G. Bai, and N. Zhang, "Device-free human localization using panoramic camera and indoor map," in *Proc. IEEE Int. Conf. Consum. Electron.-China (ICCE-China)*, Dec. 2016, pp. 1–5. [Online]. Available: http://dx.doi.org/10.1109/ICCE-China.2016.7849743

[217] C. Xu, M. Gao, B. Firner, Y. Zhang, R. Howard, and J. Li, "Towards robust device-free passive localization through automatic camera-assisted recalibration," in *Proc. 10th ACM Conf. Embed. Netw. Sensor Syst.*, Nov. 2012, pp. 339–340. [Online]. Available: http://dx.doi.org/10.1145/2426656.2426697

[218] "Mb1242 i2cxl-maxsonar-ez4." Maxbotix. 2024. Accessed: Nov. 23, 2023. [Online]. Available: https://maxbotix.com/products/mb1242

[219] Y. Bai, L. Lu, J. Cheng, J. Liu, Y. Chen, and J. Yu, "Acoustic-based sensing and applications: A survey," *Comput. Netw.*, vol. 181, Nov. 2020, Art. no. 107447. [Online]. Available: http://dx.doi.org/10.1016/j.comnet.2020.107447

[220] A. García-Requejo, M. C. Perez-Rubio, A. Hernandez, and W. M. D. Wright, "Ultrasonic device-free localization system using orthogonal chirp-based multistatic sonar," *IEEE Trans. Instrum. Meas.*, vol. 73, pp. 1–10, Sep. 2024. [Online]. Available: http://dx.doi.org/10.1109/TIM.2024.3457937

[221] A. García-Requejo, M. Pérez-Rubio, A. Hernández, W. Wright, and L. Marnane, "Ultrasonic device-free localisation system modelling for performance analysis," in *Proc. 13th Int. Conf. Indoor Posit. Indoor Navig. (IPIN)*, Sep. 2023, pp. 1–7. [Online]. Available: http://dx.doi.org/10.1109/IPIN57070.2023.10332222

[222] Y. Ye, C. Zhang, C. He, X. Wang, J. Huang, and J. Deng, "A review on applications of capacitive displacement sensing for capacitive proximity sensor," *IEEE Access*, vol. 8, pp. 45325–45342, 2020. [Online]. Available: http://dx.doi.org/10.1109/ACCESS.2020.2977716

[223] "Fdc1004." Texas Instruments. 2015. Accessed: Nov. 23, 2023. [Online]. Available: https://www.ti.com/product/FDC1004

[224] J. von Wilmsdorff, F. Kirchbuchner, B. Fu, A. Braun, and A. Kuijper, "An experimental overview on electric field sensing," *J. Ambient Intell. Human. Comput.*, vol. 10, no. 2, pp. 813–824, Feb. 2019. [Online]. Available: http://dx.doi.org/10.1007/s12652-018-0877-1

[225] N. Faulkner, B. Parr, F. Alam, M. Legg, and S. Demidenko, "CapLoc: Capacitive sensing floor for device-free localization and fall detection," *IEEE Access*, vol. 8, pp. 187353–187364, 2020. [Online]. Available: http://dx.doi.org/10.1109/ACCESS.2020.3029971

[226] D. Savio and T. Ludwig, "Smart carpet: A footstep tracking interface," in *Proc. 21st Int. Conf. Adv. Inf. Netw. Appl. Workshops (AINAW)*, May 2007, pp. 754–760. [Online]. Available: http://dx.doi.org/10.1109/ainaw.2007.338

[227] R. Ajith, A. Tewari, D. Gupta, and S. Tallur, "Low-cost vibration sensor for condition-based monitoring manufactured from polyurethane foam," *IEEE Sensors Lett.*, vol. 1, no. 6, pp. 1–4, Dec. 2017. [Online]. Available: http://dx.doi.org/10.1109/LSENS.2017.2773652

[228] "Adxl362." Analog Devices. 2024. Accessed: Nov. 23, 2023. [Online]. Available: https://www.analog.com/en/products/adxl362.html

[229] T. Murakita, T. Ikeda, and H. Ishiguro, "Human tracking using floor sensors based on the Markov chain monte carlo method," in *Proc. 17th Int. Conf. Pattern Recognit. (ICPR)*, 2004, pp. 917–920. [Online]. Available: http://dx.doi.org/10.1109/ICPR.2004.1333922

[230] M. Mirshekari, S. Pan, J. Fagert, E. M. Schooler, P. Zhang, and H. Y. Noh, "Occupant localization using footstep-induced structural vibration," *Mech. Syst. Signal Process.*, vol. 112, pp. 77–97, Nov. 2018. [Online]. Available: http://dx.doi.org/10.1016/j.ymssp.2018.04.026

[231] S. Narayana, R. V. Prasad, V. S. Rao, T. V. Prabhakar, S. S. Kowshik, and M. S. Iyer, "PIR sensors: Characterization and novel localization technique," in *Proc. 14th Int. Conf. Inf. Process. Sensor Netw.*, Apr. 2015, pp. 142–153. [Online]. Available: http://dx.doi.org/10.1145/2737095.2742561

[232] "How HC-SR501 PIR sensor works & interface it with Arduino." ARDUINO. 2024. Accessed: Apr. 26, 2024. [Online]. Available: https://lastminuteengineers.com/pir-sensor-arduino-tutorial/

[233] M. Kastek, T. Sosnowski, and T. Piatkowski, "Passive infrared detector used for detection of very slowly moving of crawling people," *Opto-Electron. Rev.*, vol. 16, no. 3, pp. 328–335, Jan. 2008. [Online]. Available: http://dx.doi.org/10.2478/s11772-008-0022-3

[234] S. Narayana et al., "LOCI: Privacy-aware, device-free, low-power localization of multiple persons using IR sensors," in *Proc. 19th ACM/IEEE Int. Conf. Inf. Process. Sensor Netw. (IPSN)*, Apr. 2020, pp. 121–132. [Online]. Available: http://dx.doi.org/10.1109/IPSN48710.2020.00018

[235] N. Faulkner, F. Alam, M. Legg, and S. Demidenko, "Device-free localization using privacy-preserving infrared signatures acquired from thermopiles and machine learning," *IEEE Access*, vol. 9, pp. 81786–81797, 2021. [Online]. Available: http://dx.doi.org/10.1109/ACCESS.2021.3086431

[236] S. Zhang, K. Liu, Y. Zhang, and Y. Wang, "A coarse fingerprint-assisted multiple target indoor device-free localization with visible light sensing," *IEEE Sensors J.*, vol. 22, no. 2, pp. 1461–1473, Jan. 2022. [Online]. Available: http://dx.doi.org/10.1109/JSEN.2021.3130711

[237] C. Xu, B. Firner, Y. Zhang, and R. E. Howard, "The case for efficient and robust RF-based device-free localization," *IEEE Trans. Mobile Comput.*, vol. 15, no. 9, pp. 2362–2375, Sep. 2016. [Online]. Available: http://dx.doi.org/10.1109/TMC.2015.2493522

[238] J. Zhang, W. Xiao, and Y. Li, "Data and knowledge twin driven integration for large-scale device-free localization," *IEEE Internet Things J.*, vol. 8, no. 1, pp. 320–331, Jan. 2021. [Online]. Available: http://dx.doi.org/10.1109/JIOT.2020.3005939

[239] S. G. Conti, P. Roux, D. A. Demer, and J. de Rosny, "Measurements of the total scattering and absorption cross-sections of the human body," *J. Acoust. Soc. Am.*, vol. 114, p. 2357, Oct. 2003. [Online]. Available: http://dx.doi.org/10.1121/1.4776827

[240] K. Ngamakeur, S. Yongchareon, J. Yu, and S. U. Rehman, "A survey on device-free indoor Localization and tracking in the multi-resident environment," *ACM Comput. Surv.*, vol. 53, no. 4, pp. 1–29, Jul. 2020. [Online]. Available: http://dx.doi.org/10.1145/3396302

[241] Y.-K. Cheng and R. Y. Chang, "Device-free indoor people counting using Wi-Fi channel state information for Internet of Things," in *Proc. GLOBECOM IEEE Global Commun. Conf.*, Dec. 2017, pp. 1–6. [Online]. Available: http://dx.doi.org/10.1109/GLOCOM.2017.8254522

[242] L. Lubna et al., "Radio frequency sensing and its innovative applications in diverse sectors: A comprehensive study," *Front. Commun. Netw.*, vol. 3, Sep. 2022, Art. no. 1010228. [Online]. Available: http://dx.doi.org/10.3389/frcmn.2022.1010228

[243] M. Cheraghinia et al., "A comprehensive overview on UWB radar: Applications, standards, signal processing techniques, datasets, radio chips, trends and future research directions," *IEEE Commun. Surveys Tuts.*, early access, Oct. 30, 2024, doi: 10.1109/COMST.2024.3488173. [Online]. Available: http://dx.doi.org/10.1109/COMST.2024.3488173

[244] J. Zhang et al., "A survey of mmWave-based human sensing: Technology, platforms and applications," *IEEE Commun. Surveys Tuts.*, vol. 25, no. 4, pp. 2052–2087, 4th Quart., 2023.

[245] T. Li, X. Xiong, Y. Xie, G. Hito, X.-D. Yang, and X. Zhou, "Reconstructing hand poses using visible light," *Proc. ACM Interact., Mobile, Wearable Ubiquitous Technol.*, vol. 1, no. 3, pp. 1–20, Sep. 2017. [Online]. Available: http://dx.doi.org/10.1145/3130937

[246] M.-D. A. Kaholokula, "Reusing ambient light to recognize hand gestures," M.S. thesis, Dept. Comput. Sci., Dartmouth College, Hanover, NH, USA, 2016. [Online]. Available: https://digitalcommons.dartmouth.edu/senior_theses/105/

[247] C. An, T. Li, Z. Tian, A. T. Campbell, and X. Zhou, "Visible light knows who you are," in *Proc. 2nd Int. Workshop Visible Light Commun. Syst.*, Sep. 2015, pp. 39–44. [Online]. Available: http://dx.doi.org/10.1145/2801073.2801078

[248] S. Mahmood, R. H. Venkatnarayan, and M. Shahzad, "Recognizing human gestures using ambient light," in *Proc. IEEE Int. Conf. Depend., Autonom. Secure Comput., Int. Conf. Pervasive Intell. Comput., Int. Conf. Cloud Big Data Comput., Int. Conf. Cyber Sci. Technol. Congr. (DASC/PiCom/CBDCom/CyberSciTech)*, Aug. 2020, pp. 420–428. [Online]. Available: http://dx.doi.org/10.1109/DASC-PICom-CBDCom-CyberSciTech49142.2020.00081

[249] Q. Hu, Z. Yu, Z. Wang, B. Guo, and C. Chen, "ViHand: Gesture recognition with ambient light," in *Proc. IEEE SmartWorld, Ubiquitous Intell. Comput., Adv. Trusted Comput., Scalable Comput. Commun., Cloud Big Data Comput., Internet People Smart City Innov. (SmartWorld/SCALCOM/UIC/ATC/CBDCom/IOP/SCI)*, Aug. 2019, pp. 468–474. [Online]. Available: http://dx.doi.org/10.1109/SmartWorld-UIC-ATC-SCALCOM-IOP-SCI.2019.00122

[250] M. Huang, H. Duan, Y. Chen, Y. Yang, J. Hao, and L. Chen, "Demo abstract: FingerLite: Finger gesture recognition using ambient light," in *Proc. IEEE Conf. Comput. Commun. Workshops (INFOCOM WKSHPS)*, Jul. 2020, pp. 1268–1269. [Online]. Available: http://dx.doi.org/10.1109/INFOCOMWKSHPS50562.2020.9163016

[251] T. Hao, R. Zhou, and G. Xing, "COBRA: Color barcode streaming for smartphone systems," in *Proc. 10th Int. Conf. Mobile Syst., Appl., Services*, Jun. 2012, pp. 85–98. [Online]. Available: http://dx.doi.org/10.1145/2307636.2307645

[252] H.-T. Cheng, A. M. Chen, A. Razdan, and E. Buller, "Contactless gesture recognition system using proximity sensors," in *Proc. IEEE Int. Conf. Consum. Electron. (ICCE)*, Jan. 2011, pp. 149–150. [Online]. Available: http://dx.doi.org/10.1109/ICCE.2011.5722510

[253] J. Webber, A. Mehbodniya, A. Arafa, and A. Alwakeel, "Gesture recognition using machine learning for light communication systems," in *Proc. Int. Mobile Embed. Technol. Conf. (MECON)*, Mar. 2022, pp. 52–56. [Online]. Available: http://dx.doi.org/10.1109/MECON53876.2022.9752211

[254] J. Webber, A. Mehbodniya, R. Teng, A. Arafa, and A. Alwakeel, "Finger-gesture recognition for visible light communication systems using machine learning," *Appl. Sc.*, vol. 11, no. 24, Dec. 2021, Art. no. 11582. [Online]. Available: http://dx.doi.org/10.3390/app112411582

[255] J. Webber and A. Mehbodniya, "Recognition of hand gestures using visible light and a probabilistic-based neural network," in *Proc. 4th IEEE Middle East North Afr. Commun. Conf. (MENACOMM)*, 2022, pp. 54–58.

[256] Z. Liao et al., "SMART: Screen-based gesture recognition on commodity mobile devices," in *Proc. 27th Annu. Int. Conf. Mobile Comput. Netw.*, Oct. 2021, pp. 283–295. [Online]. Available: http://dx.doi.org/10.1145/3447993.3483243

[257] Q. Wang, D. Giustiniano, and D. Puccinelli, "OpenVLC: Software-defined visible light embedded networks," in *Proc. 1st ACM MobiCom Workshop Visible Light Commun. Syst.*, Sep. 2014, pp. 15–20. [Online]. Available: http://dx.doi.org/10.1145/2643164.2643167

[258] H. Liu, H. Ye, X. Zhang, J. Yang, and Q. Wang, "Fingertip air-writing with ambient light," in *Mobile and Ubiquitous Systems: Computing, Networking and Services*. Cham, Switzerland: Springer, 2024, pp. 179–191. [Online]. Available: http://dx.doi.org/10.1007/978-3-031-63992-0_11

[259] H. Liu, H. Ye, J. Yang, and Q. Wang, "Through-screen visible light sensing empowered by embedded deep learning," in *Proc. 19th ACM Conf. Embed. Netw. Sensor Syst.*, Nov. 2021, pp. 478–484. [Online]. Available: http://dx.doi.org/10.1145/3485730.3493454

[260] D. Ma et al., "Gesture recognition with transparent solar cells: A feasibility study," in *Proc. 12th Int. Workshop Wireless Netw. Testbeds, Exp. Eval. Characterization*, Oct. 2018, pp. 79–88. [Online]. Available: http://dx.doi.org/10.1145/3267204.3267209

[261] D. Ma et al., "Recognizing hand gestures using solar cells," *IEEE Trans. Mobile Comput.*, vol. 22, no. 7, pp. 4223–4235, Jul. 2023. [Online]. Available: http://dx.doi.org/10.1109/TMC.2022.3148143

[262] Y. Li, T. Li, R. A. Patel, X.-D. Yang, and X. Zhou, "Self-powered gesture recognition with ambient light," in *Proc. 31st Annu. ACM Symp. User Interface Softw. Technol.*, Oct. 2018, pp. 595–608. [Online]. Available: http://dx.doi.org/10.1145/3242587.3242635

[263] D. Ma, G. Lan, M. Hassan, W. Hu, and S. K. Das, "Sensing, computing, and communications for energy harvesting IoTs: A survey," *IEEE Commun. Surveys Tuts.*, vol. 22, no. 2, pp. 1222–1250, 2nd Quart., 2020. [Online]. Available: http://dx.doi.org/10.1109/COMST.2019.2962526

[264] A. Soleiman (Uppsala Univ., Uppsala, Sweden). *Battery-Free Visible Light Sensing*. 2018. [Online]. Available: https://uu.diva-portal.org/smash/record.jsf?pid=diva2

[265] B. Parida, S. Iniyan, and R. Goic, "A review of solar photovoltaic technologies," *Renew. Sustain. Energy Rev.*, vol. 15, no. 3, pp. 1625–1636, Apr. 2011. [Online]. Available: http://dx.doi.org/10.1016/j.rser.2010.11.032

[266] H. Zou, J. Yang, Y. Zhou, L. Xie, and C. J. Spanos, "Robust WiFi-enabled device-free gesture recognition via unsupervised adversarial domain adaptation," in *Proc. 27th Int. Conf. Comput. Commun. Netw. (ICCCN)*, Jul. 2018, pp. 1–8. [Online]. Available: http://dx.doi.org/10.1109/ICCCN.2018.8487345

[267] Y. Zou, J. Xiao, J. Han, K. Wu, Y. Li, and L. M. Ni, "GRfid: A device-free RFID-based gesture recognition system," *IEEE Trans. Mobile Comput.*, vol. 16, no. 2, pp. 381–393, Feb. 2017. [Online]. Available: http://dx.doi.org/10.1109/TMC.2016.2549518

[268] J. Wang, L. Zhang, C. Wang, X. Ma, Q. Gao, and B. Lin, "Device-free human gesture recognition with generative adversarial networks," *IEEE Internet Things J.*, vol. 7, no. 8, pp. 7678–7688, Aug. 2020. [Online]. Available: http://dx.doi.org/10.1109/JIOT.2020.2988291

[269] J. Park and S. H. Cho, "IR-UWB radar sensor for human gesture recognition by using machine learning," in *Proc. IEEE 18th Int. Conf. High Perform. Comput. Commun., 14th Int. Conf. Smart City, 2nd Int. Conf. Data Sci. Syst. (HPCC/SmartCity/DSS)*, Dec. 2016, pp. 1246–1249. [Online]. Available: http://dx.doi.org/10.1109/HPCC-SmartCity-DSS.2016.0176

[270] S. Sigg, M. Scholz, S. Shi, Y. Ji, and M. Beigl, "RF-sensing of activities from non-cooperative subjects in device-free recognition systems using ambient and local signals," *IEEE Trans. Mobile Comput.*, vol. 13, no. 4, pp. 907–920, Apr. 2014. [Online]. Available: http://dx.doi.org/10.1109/TMC.2013.28

[271] J. Xiong and K. Jamieson, "ArrayTrack: A fine-grained indoor location system," in *Proc. 10th USENIX Symp. Netw. Syst. Design Implement. (NSDI)*, Apr. 2013, pp. 71–84. [Online]. Available: https://www.usenix.org/conference/nsdi13/technical-sessions/presentation/xiong

[272] Q. Pu, S. Gupta, S. Gollakota, and S. Patel, "Whole-home gesture recognition using wireless signals," in *Proc. 19th Annu. Int. Conf. Mobile Comput. Netw.*, New York, NY, USA, 2013, pp. 27–38. [Online]. Available: https://doi.org/10.1145/2500423.2500436

[273] K. Chatterjee et al., "HaCk: Hand gesture classification using a convolutional neural network and generative adversarial network-based data generation model," *Information*, vol. 15, no. 2, p. 85, Feb. 2024. [Online]. Available: http://dx.doi.org/10.3390/info15020085

[274] A. Arabi, M. Straus, Z. Tang, Z. Ye, and Y. Wang, "Phone-based CSI hand gesture recognition with lightweight image-classification model," in *Proc. 24th Int. Symp. Theory, Algorithmic Found., Protocol Design Mobile Netw. Mobile Comput.*, Oct. 2023, pp. 412–417. [Online]. Available: http://dx.doi.org/10.1145/3565287.3617613

[275] D. G. León et al., "Video hand gestures recognition using depth camera and lightweight CNN," *IEEE Sensors J.*, vol. 22, no. 14, pp. 14610–14619, Jul. 2022. [Online]. Available: http://dx.doi.org/10.1109/JSEN.2022.3181518

[276] W. Wang, A. X. Liu, and K. Sun, "Device-free gesture tracking using acoustic signals," in *Proc. 22nd Annu. Int. Conf. Mobile Comput. Netw.*, Oct. 2016, pp. 82–94. [Online]. Available: http://dx.doi.org/10.1145/2973750.2973764

[277] Y. Qifan, T. Hao, Z. Xuebing, L. Yin, and Z. Sanfeng, "Dolphin: Ultrasonic-based gesture recognition on smartphone platform," in *Proc. IEEE 17th Int. Conf. Comput. Sci. Eng.*, Dec. 2014, pp. 1461–1468. [Online]. Available: http://dx.doi.org/10.1109/CSE.2014.273

[278] H. Watanabe, T. Terada, and M. Tsukamoto, "Ultrasound-based movement sensing, gesture-, and context-recognition," in *Proc. Int. Symp. Wearable Comput.*, Sep. 2013, pp. 57–64. [Online]. Available: http://dx.doi.org/10.1145/2493988.2494335

[279] L. Wang, Z. Cui, Y. Pi, C. Cao, and Z. Cao, "A Terahertz radar feature set for device-free gesture recognition," in *Proc. IEEE Radar Conf. (RadarConf21)*, May 2021, pp. 1–5. [Online]. Available: http://dx.doi.org/10.1109/RadarConf2147009.2021.9455229

[280] J. L. Raheja, S. Subramaniyam, and A. Chaudhary, "Real-time hand gesture recognition in FPGA," *Optik*, vol. 127, no. 20, pp. 9719–9726, Oct. 2016. [Online]. Available: http://dx.doi.org/10.1016/j.ijleo.2016.07.016

[281] T. Zhang, W. Zhou, X. Jiang, and Y. Liu, "FPGA-based implementation of hand gesture recognition using convolutional neural network," in *Proc. IEEE Int. Conf. Cyborg Bionic Syst. (CBS)*, Oct. 2018, pp. 133–138. [Online]. Available: http://dx.doi.org/10.1109/CBS.2018.8612238

[282] S. Hossain, P. Kamboj, A. Maity, T. Azuma, A. Banerjee, and S. Gupta, "EdGCon: Auto-assigner of iconicity ratings grounded by lexical properties to aid in generation of technical gestures," in *Proc. 38th ACM/SIGAPP Symp. Appl. Comput.*, Mar. 2023, pp. 3–10. [Online]. Available: http://dx.doi.org/10.1145/3555776.3577623

[283] W. Qi, Y. Xie, H. Zhang, J. Zhou, R. Zhang, and X. Jing, "An efficient cross-domain device-free gesture recognition method for ISAC with federated transfer learning," in *Proc. 1st ACM MobiCom Workshop Integr. Sens. Commun. Syst.*, Oct. 2022, pp. 67–71. [Online]. Available: http://dx.doi.org/10.1145/3556562.3558575

[284] H. Abuella and S. Ekin, "Non-contact vital signs monitoring through visible light sensing," *IEEE Sensors J.*, vol. 20, no. 7, pp. 3859–3870, Apr. 2020. [Online]. Available: http://dx.doi.org/10.1109/JSEN.2019.2960194

[285] H. Abuella and S. Ekin, "A new paradigm for non-contact vitals monitoring using visible light sensing," in *Proc. 16th Annu. IEEE Int. Conf. Sens., Commun., Netw. (SECON)*, Jun. 2019, pp. 1–2. [Online]. Available: http://dx.doi.org/10.1109/SAHCN.2019.8824819

[286] C. Massaroni, A. Nicolo, M. Sacchetti, and E. Schena, "Contactless methods for measuring respiratory rate: A review," *IEEE Sensors J.*, vol. 21, no. 11, pp. 12821–12839, Jun. 2021. [Online]. Available: http://dx.doi.org/10.1109/JSEN.2020.3023486

[287] H. Abuella, F. Miramirkhani, S. Ekin, M. Uysal, and S. Ahmed, "ViLDAR—Visible light sensing-based speed estimation using vehicle headlamps," *IEEE Trans. Veh. Technol.*, vol. 68, no. 11, pp. 10406–10417, Nov. 2019. [Online]. Available: http://dx.doi.org/10.1109/TVT.2019.2941705

[288] H. Abuella, S. Ekin, S. Ahmed, F. Miramirkhani, B. Kebapci, and M. Uysal, "Wireless sensing using vehicle headlamps for intelligent transportation systems: Proof of concept," in *Proc. MATEC Web Conf.*, 2019, p. 6004. [Online]. Available: http://dx.doi.org/10.1051/matecconf/201927106004

[289] H. Abuella, S. Ekin, and M. Uysal, "ViLDAR: A novel speed estimation system using visible light in vehicles," in *Proc. IEEE 38th Sarnoff Symp.*, Sep. 2017, pp. 1–6. [Online]. Available: http://dx.doi.org/10.1109/SARNOF.2017.8080383

[290] Z. Xu et al., "LiFall: Passive indoor fall detection system based on illumination and visible light communication networks," in *Proc. Photon. Electromag. Res. Symp. (PIERS)*, Apr. 2024, pp. 1–8. [Online]. Available: http://dx.doi.org/10.1109/PIERS62282.2024.10618192

[291] S. Nižetić, P. Šolić, D. López-de-Ipiña González-de Artaza, and L. Patrono, "Internet of Things (IoT): Opportunities, issues and challenges towards a smart and sustainable future," *J. Clean. Prod.*, vol. 274, Nov. 2020, Art. no. 122877. [Online]. Available: http://dx.doi.org/10.1016/j.jclepro.2020.122877

[292] K. Shaaban, M. A. Khan, H. Menouar, and R. Hamila, "Advanced mobility: Integrating visible light communication and sensing technologies," in *Proc. Intermount. Eng., Technol. Comput. (IETC)*, May 2024, pp. 335–340. [Online]. Available: http://dx.doi.org/10.1109/IETC61393.2024.10564224

[293] Z. Salem, C. Krutzler, C. Fragner, and A. P. Weiss, "Visible light technologies for the Industrial Internet of Things," in *Proc. 17th Int. Conf. Telecommun. (ConTEL)*, Jul. 2023, pp. 1–8. [Online]. Available: http://dx.doi.org/10.1109/ConTEL58387.2023.10199004

[294] W. Xue, S. Li, and Z. Xu, "Sunlight enabled vehicle detection by LED street lights," in *Proc. Asia Commun. Photon. Conf. (ACP)*, Oct. 2018, pp. 1–3. [Online]. Available: http://dx.doi.org/10.1109/ACP.2018.8596156

[295] D. Wu, W. Zhong, Z. Ghassemlooy, and C. Chen, "Short-range visible light ranging and detecting system using illumination light emitting diodes," *Inst. Eng. Technol. Optoelectron.*, vol. 10, no. 3, pp. 94–99, Jun. 2016. [Online]. Available: http://dx.doi.org/10.1049/iet-opt.2015.0066

[296] D. Wu, Z. Wende, and C. chen, "A noise cancellation approach for an illuminating LEDs based short-range visible light sensing system," *Procedia Eng.*, vol. 140, pp. 195–202, Jul. 2016. [Online]. Available: http://dx.doi.org/10.1016/j.proeng.2016.07.345

[297] D. Saint-Pierre, "Light interreflexions in ridged surfaces: Influence of surface structure, material and lighting on color," Ph.D. dissertation, Laboratoire Hubert-Curien (LHC), Université de Lyon, Lyon, France, 2020, Accessed: Apr. 19, 2024. [Online]. Available: https://theses.hal.science/tel-03215591

[298] B. A. Wandell, "Color constancy: Theory." 2020. Accessed: Apr. 19, 2024. [Online]. Available: https://foundationsofvision.stanford.edu/chapter-9-color/

[299] P. Kumar, "Spectral sensitivity: A quick guide to understanding the impact." 2023. Accessed: Apr. 19, 2024. [Online]. Available: https://www.e-consystems.com/blog/camera/technology/spectral-sensitivity-a-quick-guide-to-understanding-the-impact/

[300] J. Beck, "The perception of surface color," *Sci. Am.*, vol. 233, no. 2, pp. 62–77, 1975. [Online]. Available: http://www.jstor.org/stable/24949866

[301] Z. Ghassemlooy, W. Popoola, and S. Rajbhandari, *Optical Wireless Communications: System and Channel Modelling with MATLAB®*. Boca Raton, FL, USA: CRC Press, Apr. 2019. [Online]. Available: http://dx.doi.org/10.1201/9781315151724

[302] S. Dimitrov and H. Haas, *Principles of LED Light Communications: Towards Networked Li-Fi*. Cambridge, U.K.: Cambridge Univ. Press, Mar. 2015. [Online]. Available: http://dx.doi.org/10.1017/CBO9781107278929

[303] L. Rodrigues, M. Figueiredo, L. N. Alves, and Z. Ghassemlooy, "Visible light communication systems architectures for the Internet of Things," in *Proc. IEEE 9th World Forum Internet Things (WF-IoT)*, Oct. 2023, pp. 1–2. [Online]. Available: http://dx.doi.org/10.1109/WF-IoT58464.2023.10539390

[304] H. Haas and C. Chen, *Visible Light Communication in 5G*. Cambridge, U.K.: Cambridge Univ. Press, Jan. 2017, pp. 289–332. [Online]. Available: http://dx.doi.org/10.1017/9781316771655.015

[305] S. Rajagopal, R. Roberts, and S.-K. Lim, "IEEE 802.15.7 visible light communication: Modulation schemes and dimming support," *IEEE Commun. Mag.*, vol. 50, no. 3, pp. 72–82, Mar. 2012. [Online]. Available: http://dx.doi.org/10.1109/MCOM.2012.6163585

[306] H. Elgala, R. Mesleh, and H. Haas, "Indoor optical wireless communication: Potential and state-of-the-art," *IEEE Commun. Mag.*, vol. 49, no. 9, pp. 56–62, Sep. 2011. [Online]. Available: http://dx.doi.org/10.1109/MCOM.2011.6011734

[307] X. Yang, Y. Zhuang, M. Shi, X. Sun, X. Cao, and B. Zhou, "RatioVLP: Ambient light noise evaluation and suppression in the visible light positioning system," *IEEE Trans. Mobile Comput.*, vol. 23, no. 5, pp. 5755–5769, May 2024. [Online]. Available: http://dx.doi.org/10.1109/TMC.2023.3312550

[308] S. Liu et al., "Real-time implementation of hybrid visible light/infrared communications supporting full-range dynamic dimming control," *IEEE Photon. J.*, vol. 16, no. 1, pp. 1–14, Feb. 2024. [Online]. Available: http://dx.doi.org/10.1109/JPHOT.2024.3353776

[309] M. Haus et al., "Enhancing indoor IoT communication with visible light and ultrasound," in *Proc. IEEE Int. Conf. Commun. (ICC)*, May 2019, pp. 1–6. [Online]. Available: http://dx.doi.org/10.1109/ICC.2019.8762001

[310] M. S. Uddin, J. S. Cha, J. Y. Kim, and Y. M. Jang, "Mitigation technique for receiver performance variation of multi-color channels in visible light communication," *Sensors*, vol. 11, no. 6, pp. 6131–6144, Jun. 2011. [Online]. Available: http://dx.doi.org/10.3390/s110606131

[311] B. J. Hadwen, "Spectrally compensating a light sensor," U.S. Patent 20 110 043 503 A1, Feb. 24, 2011.

[312] S. Aboagye, A. R. Ndjiongue, T. M. N. Ngatched, O. A. Dobre, and H. V. Poor, "RIS-assisted visible light communication systems: A tutorial," *IEEE Commun. Surveys Tuts.*, vol. 25, no. 1, pp. 251–288, 4th Quart., 2023.

[313] A. M. Abdelhady, A. K. S. Salem, O. Amin, B. Shihada, and M.-S. Alouini, "Visible light communications via intelligent reflecting surfaces: Metasurfaces vs mirror arrays," *IEEE Open J. Commun. Soc.*, vol. 2, pp. 1–20, 2021. [Online]. Available: http://dx.doi.org/10.1109/OJCOMS.2020.3041930

[314] S. Sun, T. Wang, F. Yang, J. Song, and Z. Han, "Intelligent reflecting surface-aided visible light communications: Potentials and challenges," *IEEE Veh. Technol. Mag.*, vol. 17, no. 1, pp. 47–56, Mar. 2022. [Online]. Available: http://dx.doi.org/10.1109/MVT.2021.3127869

[315] B. Cao, M. Chen, Z. Yang, M. Zhang, J. Zhao, and M. Chen, "Reflecting the light: Energy efficient visible light communication with reconfigurable intelligent surface," in *Proc. IEEE 92nd Veh. Technol. Conf. (VTC)*. Nov. 2020, pp. 1–5. [Online]. Available: http://dx.doi.org/10.1109/VTC2020-Fall49728.2020.9348585

[316] S. Aboagye, A. R. Ndjiongue, T. M. N. Ngatched, and O. A. Dobre, "Design and optimization of liquid crystal RIS-based visible light communication receivers," *IEEE Photon. J.*, vol. 14, no. 6, pp. 1–7, Dec. 2022. [Online]. Available: http://dx.doi.org/10.1109/JPHOT.2022.3211730

[317] H. Hillmer et al., "Optical MEMS-based micromirror arrays for active light steering in smart windows," *Jpn. J. Appl. Phys.*, vol. 57, no. 8S2, Jul. 2018, Art. no. 8PA07. [Online]. Available: http://dx.doi.org/10.7567/JJAP.57.08PA07

[318] M. S. Amjad and F. Dressler, "Using visible light for joint communications and vibration sensing in industrial IoT applications," in *Proc. IEEE Int. Conf. Commun. (ICC)*, Jun. 2021, pp. 1–6. [Online]. Available: http://dx.doi.org/10.1109/ICC42927.2021.9500879

[319] I. Gokarn and A. Misra, "VibranSee: Enabling simultaneous visible light communication and sensing," in *Proc. 18th Annu. IEEE Int. Conf. Sens., Commun., Netw. (SECON)*, Jul. 2021, pp. 1–9. [Online]. Available: http://dx.doi.org/10.1109/SECON52354.2021.9491608

[320] "iPhone 16-technical specifications." Apple Inc. 2024. Accessed: Nov. 14, 2024. [Online]. Available: https://www.apple.com/iphone-16/specs/

[321] "Philips hue." Philips. 2024. Accessed: Sep. 17, 2024. [Online]. Available: https://www.philips-hue.com/en-us

Morteza Alijani received the M.Sc. degree in mechatronics engineering, specializing in robotics and electronics, from the University of Trento, Italy, in 2022. He is currently pursuing the Ph.D. degree in electrical engineering with Ghent University, Belgium. From December 2021 to September 2022, he worked as a Research Assistant with Centro Ricerche Fiat, Trento, Italy. In September 2022, he joined the imec-WAVES Research Group, Department of Information Technology, Ghent University. His research focuses on AI-driven solutions for visible light positioning and sensing, IoT localization in indoor and outdoor environments, and IoT sensing applications.

Cedric De Cock received the M.S. degree in electronics and ICT engineering technology from Ghent University in 2020. In 2020, he became a member of the imec-WAVES Group, Department of Information Technology, Ghent University. His research interests include IMU-enabled indoor positioning and Bayesian filtering algorithms.

Wout Joseph (Senior Member, IEEE) was born in Ostend, Belgium, in 21 October 1977. He received the M.Sc. degree in electrical engineering from Ghent University, Belgium, in July 2000, and the Ph.D. degree in March 2005; this work dealt with measuring and modeling of electromagnetic fields around base stations for mobile communications related to the health effects of the exposure to electromagnetic radiation. He was a Postdoctoral Fellow with the FWO-V (Research Foundation—Flanders) from 2007 to 2012. Since October 2009, he has been a Professor in the domain of "Experimental Characterization of Wireless Communication Systems" with Ghent University. He has been a IMEC PI since 2017. His professional interests are electromagnetic field exposure assessment, propagation for wireless communication systems, antennas, and calibration. Furthermore, he specializes in wireless performance analysis and quality of experience.

David Plets (Member, IEEE) has been a member of the imec-WAVES Group, Department of Information Technology, Ghent University, since 2006, where he has also been a Professor since 2016. His current research interests include localization techniques and the IoT, for both industry- and health-related applications. He is also involved in the optimization of wireless communication and broadcast networks, with a focus on coverage, exposure, and interference.